Danilo Eugênio de França Laurindo Flôres

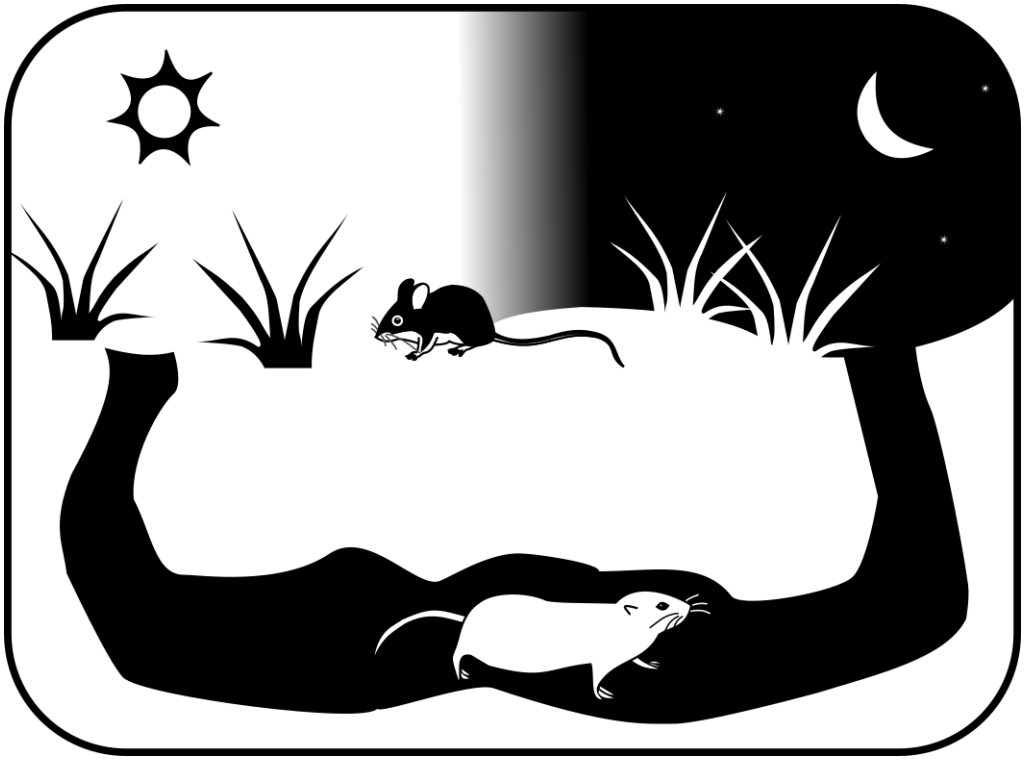

Photic and non-photic synchronization of the circadian rhythms in subterranean rodents (*Ctenomys* aff. *knighti*) and laboratory model rodents (*Mus musculus*)

Sincronização fótica e não fótica dos ritmos circadianos em roedores subterrâneos (*Ctenomys* aff. *knighti*) e roedores modelo de laboratório (*Mus musculus*)

São Paulo

July 2016

Danilo Eugênio de França Laurindo Flôres

Photic and non-photic synchronization of the circadian rhythms in subterranean rodents (*Ctenomys* aff. *knighti*) and laboratory model rodents (*Mus musculus*)

Sincronização fótica e não fótica dos ritmos circadianos em roedores subterrâneos (*Ctenomys* aff. *knighti*) e roedores modelo de laboratório (*Mus musculus*)

Tese apresentada ao Instituto de Biociências da Universidade de São Paulo, para a obtenção de Título de "Doutor em Ciências", no Programa: Ciências (Fisiologia Geral), Área de concentração: Fisiologia Geral.

Orientador(a): Gisele Akemi Oda

Co-orientadora: Verónica Sandra Valentinuzzi

Esta é a versão corrigida da tese, que inclui as sugestões da banca avaliadora. O original encontra-se disponível no Instituto de Biociências da USP.

São Paulo

July 2016

Ficha catalográfica

Flôres, Danilo Eugênio de França Laurindo.

Sincronização fótica e não fótica dos ritmos circadianos em roedores subterrâneos (*Ctenomys* aff. *Knighti*) e roedores modelo de laboratório (*Mus musculus*) / Danilo Eugênio de França Laurindo Flôres ; orientadora Gisele Akemi Oda -- São Paulo, 2016.

126 f.

Tese (Doutorado) – Instituto de Biociências da Universidade de São Paulo. Departamento de Fisiologia Geral.

1. Campo e laboratório. 2. *Light logger*. 3. Restrição alimentar. 4. Recompensa. 5. Gene *Period*. I. Oda, Gisele Akemi. II. Universidade de São Paulo. Instituto de Biociências. Departamento de Fisiologia Geral. III. Título.

Comissão Julgadora:

Prof(a). Dr(a).

Prof(a). Dr(a).

Prof(a). Dr(a).

Prof(a). Dr(a).
Orientador(a)

Acknowledgements

- ✓ At first, I would like to thank my parents Rosângela Maria Eugênio de França Flôres and Antonio Laurindo Flores, who supported me at all times during these years of graduate school. I also thank my sister Lílian Eugênio de França Flôres Melim, my nephew Théo Eugênio Flôres Melim, my niece Nina Eugênio Flôres Melin and my dear friend/brother Marcos Correa de Carvalho Flôres Melim.

- ✓ I wish to thank Dr. Gisele Akemi Oda and Dr. Verónica Valentinuzzi, my Brazilian and Argentinian supervisors, respectively. They gave me a place in their laboratories and held my hand through the path of my academic life. Besides introducing to me the amazing world of science, these two great researchers helped me acquire many skills, such as leadership, ethics, communication, initiative and independence. Words are not enough to express my gratitude for their emotional, professional, scientific and financial support.

- ✓ Dr. Shin Yamazaki was an invaluable advisor during my year at the University of Texas Southwestern Medical Center, in Dallas. A man of great values, vast knowledge and unique methodological rigor, with whom I learned to ask the right questions, use the right protocols and present my results in an attractive fashion.

- ✓ I cannot thank enough Patricia Tachinardi, André Yamachi, Vinicius Dokkedal Silva, Barbara Mizumo Tomotani, Milene Gomes Janetti, Tamiris Yassumoto, Giovane Carreira Improta and Jefferson Silva. They were more than my labmates. We have been through some happy and some not so happy moments in the long-lasting travels to Anillaco, helping one another in our experiments. In the paper discussions, together with our supervisors, we ventured into the wilderness of abstract concepts.

- ✓ I could not forget to thank Dr. Mirian Marques, to whom I owe my life as a biologist. Alongside Dr. Oda, Dr. Marques introduced me to Chronobiology and taught me the meaning of science and evolution.

- ✓ José Paliza and Eugenio Sanchez (Charly) built the equipment, facilities and the field enclosures that were used in all my experiments. Thanks to them, our ideas could reach the material world.

- ✓ Cintia Etsuko Yamachita, Jéssica Camargo and Ivan Salles Santos shared our lab space and contributed fruitful arguments to our paper discussions. Food and science were the main topics of our conversations. I hope that I have impacted their lives as much as they have impacted mine.

- ✓ I wish to thank the coordinators of the Graduate Program in Physiology. A special thank you is reserved to Roseli Silva Santos, the secretary of the program, who patiently helped me with the bureaucracy of the thesis, qualification exam, entrance test, etc. She was also a very pleasant partner in the social events of our Department.

- ✓ My colleagues in the laboratory at CRILAR Lucia Krapovikas, Juan Pablo Amaya, Pablo Martín Lopez, Tatiana Sanches and Carina Colque were important in many occasions of my graduate work and helped me find my way in Anillaco.

- ✓ Dr. Loren Buck, our collaborator from the Northern Arizona University, gave some essential inputs into my graduate work. Together with Barbara Tomotani, he presented to us the light logger devices used in the field recordings. Dr. Buck was an invaluable source of motivation; he believed in my potential when I myself did not.

- ✓ My time in Anillaco was marked with the joy and sympathy of its inhabitants, especially the researchers and employees of CRILAR. Thanks to them, my travels were rather pleasant experiences.

- ✓ A special thanks is reserved to the students, teachers and employees of Department of Physiology in the Institute of Biosciences, University of São Paulo. Thank you for the enlightening discussions on Physiology and the contributions in aspects of my academic career that went well beyond the laboratory bench work. In particular, I wish to thank all the colleagues with whom I organized the *Curso de Inverno* –

Tópicos em Fisiologia Comparativa, in the years of 2012, 2013 and 2016, as well as the *Semana de Integração da Fisiologia* in 2015.

- ✓ Dr. Joseph Takahashi provided the infrastructure for the behavioral experiments at UT Southwestern.

- ✓ I would like to thank as well my labmates at UT Southwestern, Crystal Bettilyon, Lori Jia and Nicola Ludin, who helped me with the experiments, taught me new techniques and shared the hard work. I could not forget to thank as well the help and company from the members of the Takahashi lab.

- ✓ Diego Golombeck and his team at the University of Quilmes, in Buenos Aires, received me and my colleagues in their laboratory and answered all our questions on the Simonetta System.

- ✓ Otto von Friesen developed the Neurodynamix software and kindly helped us several times with doubts and software maintenance.

- ✓ The research presented here benefitted from frequent discussions with Brazilian and international researchers in the Chronobiology conferences to which I had the chance to go.

- ✓ I also thank the furry tuco-tucos and mice that took part in all the experiments.

- ✓ My personal friends helped me maintain a social life and a healthy mind throughout these graduate years. I love you guys!

- ✓ Maykon Merlin Rodrigues dos Santos, my partner and confident, was beside me during important times in my personal and professional life. He was always there for me, even with the long distance during the year I spent in Dallas.

- ✓ Mauricio Sebastian Fernandez, my roommate in the USA, made the life in Dallas a wonderful experience. We shared amazing moments in bars, restaurants, flee markets and sports games.

✓ At last, I thank the funding agencies that provided my scholarships: **CNPq** process 161438/2011-3 (*Doutorado*) and **FAPESP** process 2011/24120-0 (*Doutorado*) and 2013/24740-3 (*Bolsa de Estágio de Pesquisa no Exterior* - BEPE). I also thank the agencies that funded the equipment, travels and maintenance of the projects: **FAPESP** (2014/20671-0, 2013/50482-1, 2012/15767-2) in Brazil, **FONCyT** (PICT2013-2753 and PICT 2011/1979) and **CONICET** (PIP-11420090100252 and PIP-11220120100415) in Argentina. The agency **CAPES** also contributed with the scholarship in my master's study, when we began the studies on photic synchronization.

Abstract

Our research group studies circadian rhythms in a subterranean rodent from the genus *Ctenomys*, the tuco-tuco. In this thesis, I will present data on photic and non-photic synchronization of circadian rhythms in tuco-tucos, as well as a study on non-photic synchronization in the laboratory mouse. Natural photic synchronization in tuco-tucos was verified with field and laboratory approaches. We initially measured the natural light/dark cycle experienced by tuco-tucos in semi natural field enclosures, by means of automatic light logger devices that continuously recorded the daily temporal pattern of light exposure. Next, a model of this light exposure pattern was applied to tuco-tucos in the laboratory, to test its potential as a photic synchronizer of the circadian rhythms. The model consisted of single light pulses applied once a day at varying random times. Despite the minimal timing information, this light regimen was a successful synchronizer in many instances, as predicted from previous computer simulations of a mathematical oscillator. These results revealed that the synchronization of circadian oscillators is even more robust than previously thought. Our second set of experiments evaluated the non-photic synchronization in the herbivorous tuco-tucos, by exposing animals to daily cycles of food availability. Similar to other rodent species, tuco-tucos in this protocol developed a circadian food anticipatory activity (FAA) right before the daily feeding time. However, there was great interindividual variability in FAA expression, likely related to differences in the metabolic responses to time-restricted feeding. The final work was a collaboration with Dr. Shin Yamazaki from the University of Texas Southwestern Medical Center, regarding non-photic synchronization in wildtype and mutant mice with genetic disruption of the circadian clock. Daily cycles of palatable food and wheel running induced self-sustaining rhythmicity in arrhythmic mutant mice, which do not express the *Period* genes, key components of the molecular machinery responsible for circadian rhythm generation within the cells. These results suggest the existence of novel circadian oscillators responsive to daily rewarding signals. While model laboratory species such as the mouse can bring valuable information on physiological mechanisms, wild species like the tuco-tuco can give us insights into the ecological meaning of circadian phenomena.

Keywords

Field and laboratory, light logger, entrainment, restricted feeding, reward, *Period* gene

Resumo

Nosso grupo de pesquisa estuda ritmos circadianos em um roedor subterrâneo do gênero *Ctenomys*, o tuco-tuco. Nesta tese, apresentarei dados sobre sincronização fótica e não-fótica dos ritmos circadianos em tuco-tucos, e sobre sincronização não-fótica em camundongos. Investigamos a sincronização fótica em tuco-tucos por meio de uma abordagem conjunta de campo e laboratório. Inicialmente medimos o ciclo claro/escuro natural percebido por animais mantidos em áreas cercadas em campo, utilizando aparelhos *light loggers* que registraram continuamente o padrão temporal diário da exposição à luz. Em seguida, foi aplicado um modelo desse padrão de exposição à luz em laboratório, para testar o seu potencial como um sincronizador fótico dos ritmos circadianos dos tuco-tucos. O modelo consistiu em pulsos de luz aplicados uma vez por dia em diferentes momentos aleatórios. Apesar de carregar o mínimo de informação temporal, esse regime luminoso foi um sincronizador eficiente em muitos casos, tal como previsto anteriormente a partir de simulações computacionais de um oscilador matemático. Os resultados revelam que a sincronização de osciladores circadianos é ainda mais robusta do que se imaginava. Nosso segundo conjunto de experimentos avaliou a sincronização não-fótica em tuco-tucos, os quais são herbívoros, expostos a ciclos diários de disponibilidade de alimentos. Semelhante a outras espécies de roedores, tuco-tucos desenvolveram uma atividade antecipatória ao alimento, expressa diariamente antes da alimentação. Houve, no entanto, grande variabilidade inter-individual na expressão da atividade antecipatória, provavelmente relacionada com diferenças nas respostas metabólicas à restrição temporal do alimento. O trabalho final foi uma colaboração com o Dr. Shin Yamazaki, sobre sincronização não-fótica em camundongos do tipo selvagem e camundongos mutantes com ablação genética do relógio circadiano. Ciclos diários de alimentos palatáveis e de corrida em roda induziram ritmicidade autossustentada em camundongos mutantes arrítmicos, que não expressavam os genes *Period*, componentes importantes da maquinaria molecular que gera os ritmos circadianos nas células. Estes resultados sugerem a existência de novos osciladores circadianos que respondem a sinais diários de recompensa. Enquanto espécies modelo de laboratório, tais como o camundongo, podem trazer informações valiosas sobre os mecanismos fisiológicos, as espécies selvagens como o tuco-tuco podem nos dar pistas sobre o significado ecológico dos fenômenos circadianos.

Palavras-chave

Campo e laboratório, *light logger*, arrastamento, restrição alimentar, recompensa, gene *Period*

Table of Contents

Chapter 1. General Introduction

Abstract

Endogenous circadian rhythms in behavior and physiology are expressed in most organisms studied to date. These rhythms are adjusted to the 24 hours of the environment by means of two different synchronization processes: entrainment and masking. The study of circadian rhythms is particularly interesting in animal species that inhabit extreme photic environments, where the light/dark cycle is partially compromised. This is the case of subterranean rodents that spend most of the day inside dark underground tunnels. Our research focuses on the tuco-tuco, a subterranean rodent from Argentina, which presents functional circadian rhythms. The present thesis will explore photic and non-photic synchronization, by means of field and laboratory studies in this wild species. Non-photic synchronization was also explored in a side project with wild-type and mutant mice.

Rhythms and the circadian system

In an ever-changing world, living beings evolved physiological strategies to anticipate recurrent events in their environments. For instance, in anticipation to the changes that happen between the light hours of the day and the dark hours of the night every 24 hours, most organisms express daily changes in behavioral and physiological variables. These regular changes are described as **daily biological rhythms**.

To facilitate the presentation and discussion of data on daily rhythms, I will first define some parameters that describe a generic rhythm. Let us imagine a biological variable that goes up and down day after day (Figure 1.1). Any instant point of that variable within one cycle of the rhythm is referred to as a **phase**. We might also refer to the phase as a portion of the cycle, not as a single point; for example, within the daily activity-rest rhythm of an animal, the whole time when the animal is active is referred to as the activity phase. The time interval between two peaks, or between two troughs, or between any two equivalent

phases in subsequent cycles is denominated **period**. The period is, therefore, the duration of a complete cycle within the rhythm. Finally, here we call **amplitude** the difference between the peak and the trough values of the rhythmic variable.

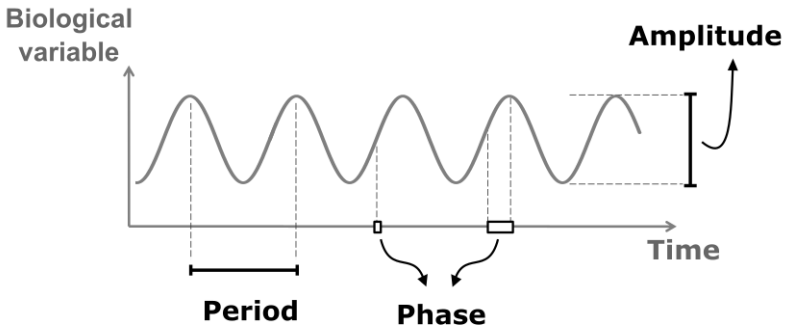

Figure 1.1. Parameters of a generic biological rhythm. A biological variable goes up and down through time, in a regular daily rhythm, with particular rhythmic parameters: period, amplitude and phases.

These daily rhythms are, in many cases, not a mere reaction to stimuli that cycle throughout day and night. They are, in fact, generated by endogenous biological clocks that keep ticking even if an organism is maintained in an artificially constant environment, without daytime references. This phenomenon is illustrated, for instance, when the activity of a rodent is measured in the laboratory, initially in a daily changing environment and later in constant conditions (Figure 1.2). In most of the organisms studied so far endogenous daily rhythms persist in constant conditions usually with periods close to, but different from, 24 hours; they are, therefore, named **circadian rhythms** (from the latin "circa" = close to, "dien" = 24 hours). Accordingly, the physiological entities that generate these endogenous rhythms within the body are called **circadian clocks** or **circadian oscillators**. Even though an organism could simply react to environmental stimuli of day and night, the presence of an endogenous clock can bring selective advantages (DeCoursey, 2014; Spoelstra et al., 2016).

Of note, rhythms of other periodicities also occur within the biology of many living beings (Moore-Ede et al., 1982). For instance, many female mammals present oscillations in reproductive state with periods lasting several days and several organisms express variations in their physiology and morphology following the seasons of the year. These

rhythms with periods greater than 24 hours are named **infradian**. Likewise, biological variables may also oscillate with periods much shorter than a day, such as the heart rate, breathing rate and the pulsatile movement of the sperm cell. These short-period rhythms are called **ultradian**. Each of these rhythms may differ on their endogenous nature and on whether they have a correspondent environmental cycle of similar period.

Back to circadian rhythms, one of their important features is the compensation of the endogenous period to variations in ambient temperature. The endogenous period (speed) of a circadian clock is fairly conserved under different temperatures, which contrasts to other chemical and biological processes (Pittendrigh, 1954). This is of great value in natural environments, where the average daily temperature may change by 10-20ºC between weeks or months. If the speed of the clock was dependent on temperature, the internal day of the organism would be too fast or too slow to adjust to the 24-hour environment.

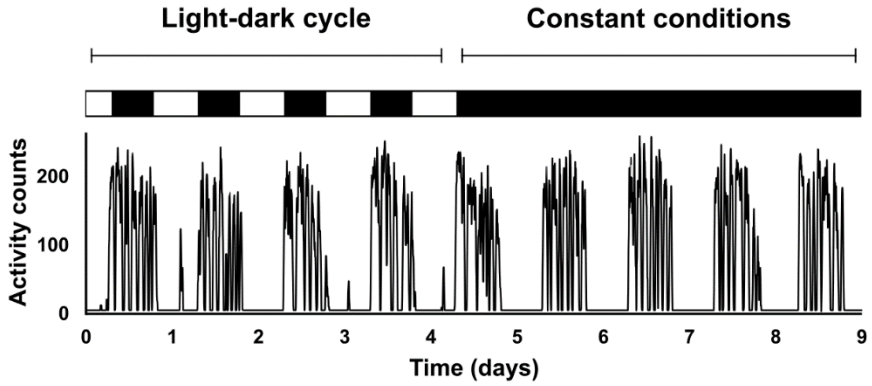

Figure 1.2. Activity record of a rodent (*Ctenomys* sp.) under controlled conditions in the laboratory. The animal was kept individually in a running-wheel cage and its activity was continuously recorded. White and black bars on top of the graph show the moments of lights-on and lights-off in the laboratory, respectively. During the first 4 days, lights were turned on and off every day in a regular light/dark cycle. The animal's activity concentrated in the dark hours, resulting in a daily activity-rest rhythm. From day 5 onwards, the animal was kept in constant darkness and the activity-rest rhythm persisted, suggesting that the rhythm was generated by an endogenous clock. Modified from (Valentinuzzi et al., 2009).

A conceptual model was formulated to explain how circadian rhythms are generated within the body (Figure 1.3). When an animal is maintained in a 24-hour environment, its circadian oscillator is synchronized by daily environmental cycles (for instance, the

light/dark cycle) perceived through afferent pathways. This synchronized oscillator then regulates the timing of the rest of the body through efferent pathways, resulting in 24-hour rhythms in biological variables. If the animal is placed in an artificially constant environment, without environmental cycles, the circadian oscillator still expresses a rhythm, however with its own endogenous period, different from 24 hours. The **free-running** oscillator then regulates endogenous free-running biological rhythms within the body. The circadian oscillator, together with its afferent and efferent pathways compose the **circadian system** (Dibner et al., 2010).

In mammalian animals, a central circadian oscillator is located in the suprachiasmatic nuclei (SCN) of the hypothalamus, which coordinate circadian rhythms among the different organs and tissues in the organism (Moore and Eichler, 1972; Ralph et al., 1990; Stephan and Zucker, 1972; Yoo et al., 2004). The SCN endogenous rhythm is synchronized to the daily light/dark cycle of the environment. This is achieved by means of cyclic photic input that is transduced in the retina, in intrinsically photosensitive retinal ganglion cells expressing melanopsin (Hannibal et al., 2002; Hattar et al., 2002; Panda et al., 2003). These retinal cells transmit the cyclic signal to the SCN through the retinohypothalamic tract (Berson et al., 2002). Rhythmic signals from the SCN are then sent to the whole body via neuronal and humoral signals (Bartness et al., 2001; Silver et al., 1996) as well as via the daily body temperature and feeding rhythms (Buhr et al., 2010; Damiola et al., 2000; Stokkan et al., 2001).

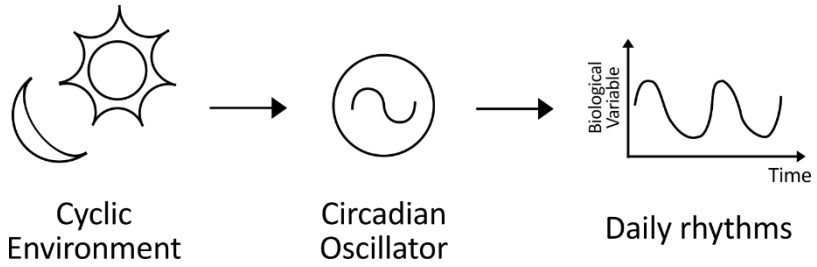

Figure 1.3. Conceptual model of the circadian system. A self-sustaining circadian oscillator generates daily rhythms, which are transmitted to behavior and physiology. In a regular cyclic environment, this oscillator is adjusted to local time, thus keeping the organisms' physiology at an appropriate timing. When the cyclic variation of the environment is removed, the oscillator keeps ticking with a circa-24-hour periodicity and persisting circadian rhythms are observed in several biological variables.

Activity rhythms and indirect assessment of the circadian oscillator

Since circadian rhythms reflect the motion of the endogenous oscillator, the properties of the oscillator can in many instances be studied indirectly, by assessing the properties of the output rhythms (Pittendrigh and Daan, 1976a). Usually, the phase and period of a rhythm in constant conditions are taken to represent the phase and period of the oscillator. The amplitude of the rhythm is usually less representative of the oscillator, since the peak and trough values of a physiological variable are more dependent on the state of the effector organ or tissue that expresses the overt rhythm (Takahashi et al., 2008).

The circadian rhythm of activity and rest is commonly used as a marker of the circadian oscillator (Pittendrigh and Daan, 1976a). Especially in rodents, the rhythm of activity in the running-wheel is widely used, because many rodents express sharp wheel-running rhythms, with marked activity and rest phases (Figure 1.2), thus favoring the assessment of the rhythm's parameters and, indirectly, the oscillator's parameters. A usual way of presenting activity-rest rhythms is in the form of an **actogram** graph, in which successive days are plotted below each other, so that the day-to-day variations in the rhythm's phase and period can be easily followed (Figure 1.4).

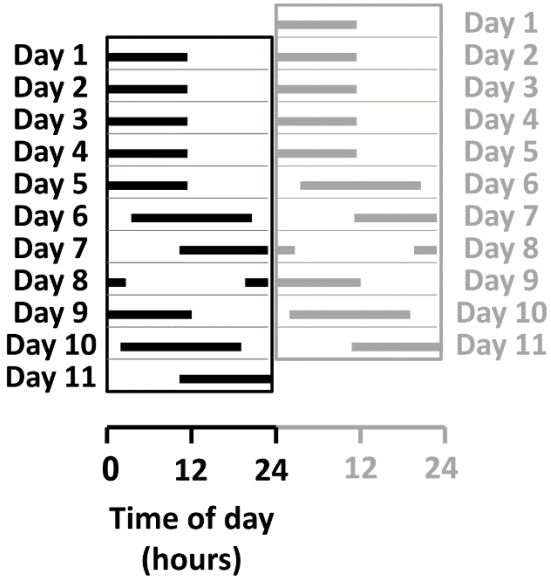

Figure 1.4. Actogram representation of a hypothetical activity-rest rhythm. Each day of data is represented in a line of the graph (along the x axis) and successive days are plotted below each other (along the y axis). Black horizontal marks indicate the time of activity on each day. Data is double-plotted, i.e. the graph is duplicated and copied on the right side, displaced 1 day upwards.

Thus, each line presents 48-hours of data: first line, days 1 and 2; second line, days 2 and 3; and so forth. From days 1 to 5, the rhythm is synchronized to a 24-hour period, indicated by the maintenance of the activity band at the same time day after day. From day 6 onwards, the activity-rest rhythm free-runs with a period greater than 24 hours, as seen by the activity band that starts later and later each new day. Double plotting makes it easier to follow free-running rhythms in constant conditions, with periods different from 24 hours. Modified from (Flôres, 2011).

Mechanism of synchronization: entrainment

When a rhythm is synchronized by an environmental cycle, both its phase and its period are adjusted to the cyclic environment. Let us consider a hypothetical nocturnal animal initially in constant conditions. It would express an endogenous activity-rest rhythm that would free-run with a period different from 24 hours. If we exposed this animal to a 24-hour light/dark cycle, the rhythm would eventually assume a period of 24 hours and the activity phase would be fixed to the dark phase of the synchronizing cycle. Two processes could generate the observed synchronization: masking of the rhythmic biological variable or entrainment of an underlying oscillator (Figure 1.5).

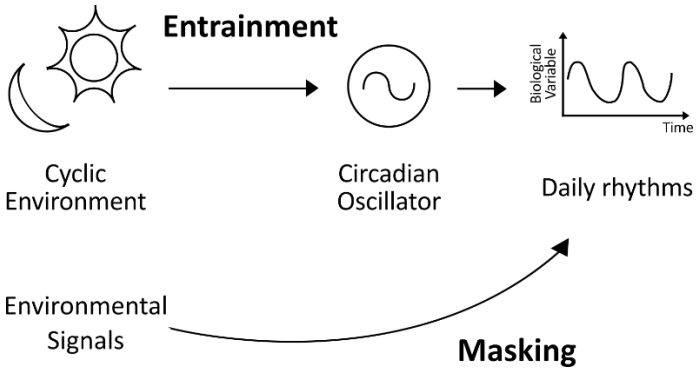

Figure 1.5. Two mechanisms for synchronization to the cyclic environment. An environmental cycle can promote synchronized rhythms either by adjusting the phase and period of an underlying circadian oscillator (entrainment), or by cyclic inhibition and induction of a biological process (masking).

On the one hand, synchronization can be achieved when the cyclic environment adjusts the period and phase of an underlying biological clock, which in turn leads to a synchronized rhythmic output in the regulated biological variable, as pointed above. This process that depends on a biological clock is denominated **entrainment** (Moore-Ede et

al., 1982). Environmental signals that entrain the biological clocks are termed **zeitgebers**, from the German "time givers". Alternatively, environmental signals can acutely enhance or inhibit the amplitude of biological variables. Thus, a synchronized rhythm can be expressed from the cyclic inhibition and induction of a biological process every 24 hours, without the participation of the biological clock. In the study of circadian rhythms, this direct action on the biological variable is called **masking** (Mrosovsky, 1994).

It is a common practice in circadian rhythm research to release the studied organism in constant conditions after observing synchronized rhythms. This methodological step is important when we want check if a rhythm was generated by masking or by entrainment of a circadian clock. If the rhythm is abolished in constant conditions, it is most likely generated by masking and not by an endogenous circadian clock. However, if it persists, with a period different from 24 hours, we can be sure that there is an underlying circadian oscillator. However, even when persistence is verified, there is still a chance that the environmental cycle(s) was overriding the circadian clock and generating a synchronized rhythm irrespective of a free-running endogenous signal. This is what happens, for instance, with flying squirrels exposed to daily ambient temperature cycles (DeCoursey, 1960). To clearly separate entrainment from synchronization by masking, one definitive protocol requires that a rhythm is followed through three successive conditions: free-running, synchronization and free-running again. We can verify whether synchronization results from entrainment if, in the final constant conditions, the initial phase of free-running is predicted from the phase of synchronization, not from the phase of the previous free-run (Moore-Ede et al., 1982) (Figure 1.6).

Another strategy to verify whether an environmental variable may constitute a zeitgeber is to present a pulse stimulus in constant conditions. For instance, the light/dark cycle is known to be a zeitgeber for many species; if we keep one of these organisms in constant darkness (free-running) and give it a short pulse of light, we will observe a change in the phase of its circadian rhythms, i.e., a phase-shift. This is an evidence that the phase of the endogenous circadian clock was affected by light and that daily variations in light level have the potential to entrain the clock. The observed phase-shift can be either an advance or a delay, depending on the phase when this stimulus is given. If the experiment is repeated at different phases until the whole day is covered, we can have a picture of the phase-dependent responses of the circadian clock to the zeitgeber; by convention, this is plotted in a graph, the Phase Response Curve (PRC) (Johnson, 1999).

When the rhythms of an organism are entrained to the light/dark cycle they assume a fixed phase-relationship to the zeitgeber: the phase of activity onset in a nocturnal animal, for example, usually coincides with the phase of lights off. By convention, a relative time-scale is used to describe the time of a particular event or treatment applied to an organism under a light/dark cycle. The scale is named **Zeitgeber time (ZT)** and starts at the beginning of the light phase (ZT0). An interference made at ZT4 means that it was performed 4 hours after lights on.

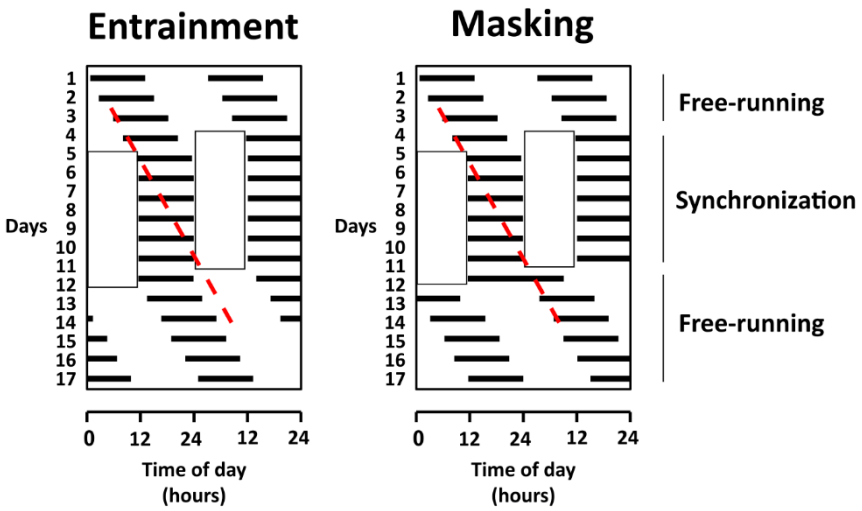

Figure 1.6. Synchronization by entrainment or by masking verified in two hypothetical datasets presented in actograms. Left – Synchronization by entrainment. Initially in constant conditions, the activity-rest rhythm free-runs with a period greater than 24 hours: the activity phase starts later each new day. An environmental light/dark cycle is applied, starting on day 5 (lights-on = white rectangles), and the period of the rhythm is adjusted to 24 hours (activity phase at the same time every day). After release in constant conditions, the rhythm free-runs again, with a period greater than 24 hours. The phase of the free-running rhythm is predicted from the phase it had during synchronization, indicating that the endogenous circadian clock was adjusted (entrained) by the environmental cycle. Right – Synchronization by masking. The data follows the same pattern, except for the final free-run. The phase of the rhythm in the final constant conditions is predicted from the phase of the previous free-run (dashed red line), not from the phase of synchronization. This suggests that the endogenous circadian clock was not affected by the synchronizing cycle and that the rhythm was generated by inhibition of activity in the light phase (masking).

Photic and non-photic entrainment

Among the environmental cycles that act as zeitgebers, the light/dark cycle is surely the most studied (Pittendrigh and Daan, 1976b). As pointed above, in mammals the photic information comes directly to the circadian oscillator by means of a monosynaptic pathway coming from a single (and rather expected) anatomical locus, the retina (Moore, 1983). The relative simplicity of the photic entrainment system makes it more amenable to exploration.

However, non-photic stimuli can also synchronize the circadian rhythms of mammals (Mrosovsky, 1988; Mrosovsky et al., 1989). Interestingly, the pathways for non-photic entrainment of the circadian clock are different from the photic ones: signals from at least two brain regions (intergeniculate leaflet and raphe) seem to mediate non-photic inputs to the SCN (Mistlberger and Antle, 2011). Non-photic stimuli that have been shown to act as zeitgebers include ambient temperature cycles (Refinetti, 2010), social interaction cycles (Davidson and Menaker, 2003) and food availability cycles (Mistlberger, 1994; Stephan, 2002).

Two modes of entrainment

Two conceptual models have been proposed to explain how entrainment works: parametric (continuous) and non-parametric (discrete) modes (Beersma et al., 1999; Daan, 2000; Pittendrigh and Daan, 1976a; Roenneberg et al., 2003). Most of the knowledge behind these two concepts comes from studies on photic entrainment.

Non-parametric explanations derive from the fact that circadian clocks can entrain to a 24-hour environmental cycle, composed of a short daily pulse at the same time every day. This means that a light/dark cycle with only a few hours or less of light per day can mimic the effects of a complete light/dark cycle with 12 hours of light (DeCoursey, 1972; Pittendrigh and Daan, 1976b). Moreover, when the effect of a short light stimulus is assayed at different phases of the circadian clock, a rhythm of responsiveness is evidenced: at specific phases the stimulus advances the clock and at others the stimulus delays the clock (Daan and Pittendrigh, 1976a; Johnson, 1999). Non-parametric entrainment then proposes that the clock is entrained to 24 hours by periodic delays or advances that end up adjusting the free-running period of the clock (Chandrashekaran et

al., 1973). For instance, a clock that free-runs with a period of 25 hours could be entrained to a 24-hour cycle by advancing its phase in 1 hour every day, if a single daily stimulus was applied at the right time.

On the other hand, parametric entrainment implicates a continuous adjustment of the clock. The basis for a parametric mechanism are the effects of constant light on the period of the circadian clock. For instance, when a rhythm is recorded in constant light, its free-running period is dependent on the intensity of the continuous background illumination (Aschoff, 1979). It is then proposed that in a light/dark cycle, with varying light intensities, the clock is continuously speeded-up and slowed-down to different degrees along the day, resulting in a net adjustment of the clock's period to 24 hours.

The two conceptual modes of entrainment are probably complementary and the predominance of one or the other may depend on the natural photic environment of each organism (Daan, 2000).

Circadian rhythms in subterranean rodents

Some ecological contexts give rise to extreme photic environments, in which there is not a regular light/dark transition between day and night. For instance, animals that live near the Earth poles experience continuous days during summer and continuous nights in the winter (van Oort et al., 2005; Stokkan et al., 1986; Williams et al., 2012a), although changes in light spectrum still occur. Animals that live in subterranean tunnels also experience long time intervals of constant darkness and some even present reduction in visual structures (Nemec et al., 2007; Nevo, 1979). These ecological conditions have intrigued chronobiologists as to whether the residing species present rhythms and whether and how these rhythms synchronize to the daily environment.

Subterranean rodents have evolved from different branches of the Rodentia clade and they present varying degrees of adaptations to the underground environment (Lacey et al., 2000). Circadian rhythms have been studied in the mole-rats of Europe, Africa and Asia (Ben-Shlomo et al., 1995; Oosthuizen et al., 2003; Riccio and Goldman, 2000) and in the coruros of Chile (Begall et al., 2002). In most of the cases, they do present circadian rhythms, but there is great variability in the expression of rhythms and synchronization to the light/dark cycle.

The genus *Ctenomys* is the single genus of the family Ctenomyidae, with more than 50 species of subterranean rodents, the tuco-tucos, that distribute through different environments in the south of South America (Lacey et al., 2000). We studied the species *Ctenomys* aff *knighti* (Figure 1.7), which inhabits the Monte desert of Argentina, a region of semi-arid environment, with variable annual precipitation concentrated in the summer months (Abraham et al., 2009). The area includes the town of Anillaco, where our laboratory is located, in the research institute CRILAR (*Centro Regional de Investigaciones Cinetíficas y Transferencia Tecnológica*). The institute location allows for laboratory and field studies very close to the natural habitats of the animals.

In this arid environment, tuco-tucos live in self-built underground tunnel systems, consisting of a long central tunnel and shorter lateral tunnels, dug in the dry soil of the desert. According to our few excavations, we verified that the burrow systems lack a nest and that tunnels go as deep as 60-70cm. Soil temperatures were measured at one of our study sites from April 2014 until March 2015. In the coldest moth of 2014 (July), the average temperature on the soil surface varied between 12.97ºC during the day and 6.44ºC at night, while the temperature at 60cm depth was more stable, ranging from 13.20ºC during the day and 13.13ºC at night. The highest average temperature was observed six months later, in January 2015, going from 25.55ºC in the day and 21.49ºC at night on the surface and from 28.26ºC (day) to 28.21ºC (night) at 60cm depth.

Our initial laboratory studies with this tuco-tuco species revealed marked daily rhythms of activity in the running wheel (Figure 1.2), with wheel revolutions concentrated in the dark phase (Valentinuzzi et al., 2009). The rhythm persisted in constant lighting conditions and was synchronized to artificial daily light/dark cycles. During my master's study (Flôres et al., 2013), we have demonstrated that the tuco-tuco's circadian oscillator present a circadian rhythm of responsiveness to light, a Phase Response Curve (PRC), which is yet another indication of their preserved circadian system.

Even though we demonstrated that the rhythms of tuco-tucos can synchronize to daily light/dark cycles in the laboratory, we still did not know whether this was true in the natural environment. In the laboratory, synchronization was tested with artificial light/dark (LD) cycles composed of alternating 12 hours of light and 12 hours of dark (**LD 12:12**). In the field, however, tuco-tucos spend most of their time inside dark underground tunnels and they only see light when visiting the surface, in the moments of foraging and/or tunnel maintenance. What is the daily light exposure temporal pattern of tuco-tucos? Does the natural light/dark regimen have the potential to synchronize the

circadian rhythms of these animals? What about the participation of natural non-photic cycles in the synchronization?

Figure 1.7. Pictures of tuco-tucos (*Ctenomys* aff. *knighti*). Animals were studied in the laboratory (left) and in the field (right).

During my master's dissertation, our group has verified the temporal light exposure pattern of tuco-tucos in the field, by means of visual observations of behavior in semi-natural field enclosures. We saw that animals leave their burrows and expose to light during the day, but at varying times day after day (Tomotani et al., 2012). We could not predict whether this irregular light exposure pattern would synchronize the circadian rhythms of tuco-tucos. Computer simulations of a mathematical oscillator were used to simulate simplified models of the recorded light exposure (Flôres et al., 2013). These simulations predicted that light exposure episodes, distributed randomly along the light phase, can still synchronize the rhythms in the field. Experimental tests were needed to confirm this prediction.

Main objectives

In the present thesis, we describe the follow-up studies on photic synchronization of tuco-tucos, as well as initial studies of non-photic synchronization in tuco-tucos and in laboratory mice. Below is a summary of the objectives divided by chapter:

- Chapter 2 - At first, we wanted to confirm the light exposure pattern of tuco-tucos in the field, by means of automatic recordings with light loggers. A simplified version of this light exposure pattern was applied to animals in the laboratory, to test the predictions of the computer simulations and to verify the potential of this signal as a zeitgeber.

- Chapter 3 – We tested whether the circadian rhythm of tuco-tucos could synchronize to non-photic environmental cycles, by exposing tuco-tucos to daily food availability cycles in the laboratory.

- Chapter 4 – During the year of 2014, I visited the laboratory of Dr. Shin Yamazaki at the University of Texas Southwestern Medical center. We verified the synchronization to periodic non-photic stimuli (food and rewarding signals) in wild-type mice and in mice with genetic disruption of the circadian clock.

Chapter 2. Entrainment of circadian rhythms to irregular light/dark cycles: a subterranean perspective

2.1. BACKGROUND

In this second chapter, we will explore the photic synchronization of circadian rhythms in the tuco-tuco, by means of field measurements, laboratory experiments and computer simulations. Results are presented in the form a manuscript, which has been submitted for publication. Before presenting the data, I will first punctuate some background information to contextualize our findings.

Light exposure records

Depending on an animal's spatial and temporal niches, it will sample the light/dark cycle at different times and receive a particular light information along the 24 hours of the day (Roenneberg and Foster, 1997). The particularities of its natural light exposure profile will dictate whether and how the circadian rhythms are synchronized by the light-dark cycle in nature.

We had previously obtained data for the temporal light exposure pattern of tuco-tucos, by means of visual observations (Tomotani et al., 2012). In those earlier stages, we managed to register episodes of light exposure by observing three animals in one semi-natural field enclosure, during the light phase, and recording the times when they presented aboveground activity. Besides the preliminary light exposure data, this methodology gave us fruitful insights into the natural behaviors of tuco-tucos: animals exposed to light while foraging for plants and removing earth out of their burrows (Tomotani et al., 2012). Nevertheless, the data collection was limited by our attention and visual acuity at lower light levels and by the necessity of shift-work among many lab members.

In parallel, since 2008, we have tried different light-logger devices to measure light exposure automatically (Figure 2.1.1). An initial device (Insight Equipamentos, Pesquisa e Ensino; Ribeirão Preto, SP, Brazil) (Figure 2.1.1A) was built to measure both activity and light exposure continuously, but there was a crosstalk between the two measurements and the size of the device was an issue (Flôres, 2011). The second and third devices (Ecotone; Gdynia, Poland) (Figure 2.1.1B, C) were fairly smaller and the third device was thoroughly tested in the laboratory and once in the field. Yet, it did not fit well to the animals and the material was too fragile for fieldwork, in addition to having a problem with time measurements. The report in Attachment 1 of this thesis illustrates the typical problems that we met. Besides, this device required that a heat-sensitive LiPo battery was soldered at each time of use.

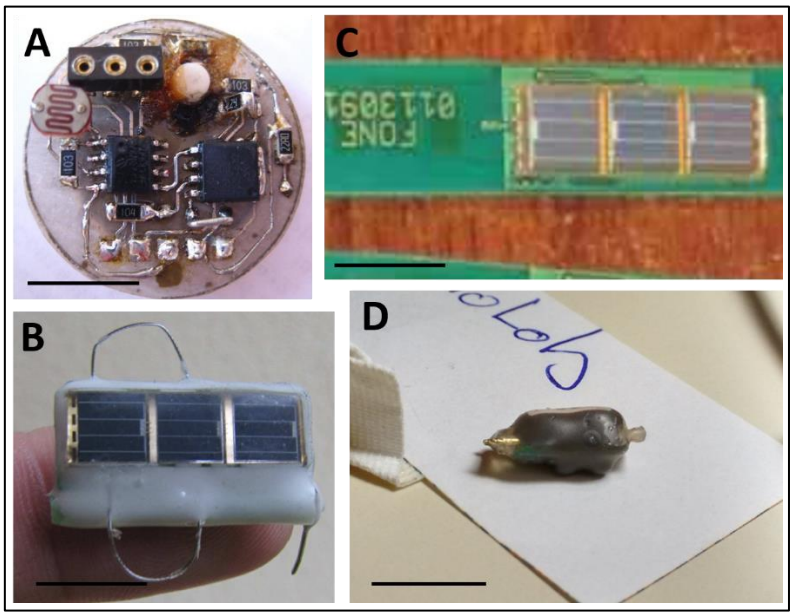

Figure 2.1.1. Light logger devices tested for light exposure recordings. Models are organized in the chronological order in which they were tested along the years. **A**: First model, developed by the company Insight, tested from 2008 to 2010. **B** and **C**: Second and third models, from the company Ecotone, tested in 2011 and 2012. D: Final model, from Migrate Technology, tested since 2013. Scale bar on the lower left of each figure: 1 cm.

We finally arrived at a nice and small light-logger (Figure 2.1.1D, 2) (Migrate Technology; Cambrigde, UK), kindly indicated by Dr. Loren Buck, from the Northern Arizona University, and by Barbara Tomotani. Dr. Buck tested devices from different

companies in his own work on free-living mammals (Williams et al., 2012a). Apart from being small (Figure 2.1.2) and sensitive to a wide range of light intensities, it also has a long-lasting battery, ideal for long-term recordings in the field.

Two new field enclosures were built between the years of 2013 and 2015 (Figure 2.1.2) to allow for recordings of multiple animals at once. With the proper light logger device and the new field enclosures, we managed to obtain the first automated light exposure data from tuco-tucos, as described in the manuscript.

Figure 2.1.2. Field recordings setup. **Left**: Lateral view of the two new semi-natural field enclosures. Enclosures are surrounded by wire-mesh walls aboveground and concrete-block walls underground. **Right**: Light-logger used for light exposure recordings in the field. Each device (arrow) was attached to a custom collar, made of zip ties and silicone tubing.

Testing entrainment to a model light exposure

There is indirect evidence that tuco-tucos are synchronized to the daily environment in their natural habitat. Freshly captured animals express rhythms in constant conditions, with periods very close to 24 hours, which strongly indicate aftereffects of a previous entrainment (Tomotani et al., 2012). We have also confirmed that the tuco-tucos' circadian rhythms can be synchronized in the laboratory by artificial light/dark cycles, via entrainment of a circadian oscillator (Valentinuzzi et al., 2009). However, the participation of light information for entrainment in the field remained to be confirmed.

We began to answer this question during my master's work, using computer simulations of a mathematical circadian oscillator of the limit-cycle type, subjected to

different virtual light regimens (Flôres, 2011; Flôres et al., 2013). As a common approach to mathematical modelling studies, we devised a simplified version of light exposure that would capture the critical aspects of the particular light regimen experienced by tuco-tucos in the field.

Light/dark regimens consisting of a single short light pulse at the same time every day are denominated "single pulse T-cycles" (Figure 2.1.3A). It is well stablished in the literature that such regimens can synchronize the circadian rhythms of different organisms, even though the lights are only turned on for some minutes or seconds every day (DeCoursey, 1972; Pittendrigh and Daan, 1976b). This phenomenon can be simulated with mathematical oscillators, which are prone to entrainment by periodic discrete pulses (Abraham et al., 2010; Granada et al., 2011).

Our preliminary data on the light exposure pattern of tuco-tucos indicated that the times of exposure would change from day to day (Flôres et al., 2013). Thus, our simplified model of this pattern was a variation of the single pulse T-cycle, in which the phase of the single daily pulses would change randomly from day to day (Figure 2.1.3B, C). We applied to the mathematical oscillator a single 1-hour light pulse per day, with fixed intensity (amplitude), administered at random phases distributed uniformly within a time window/interval ("I") of predetermined duration.

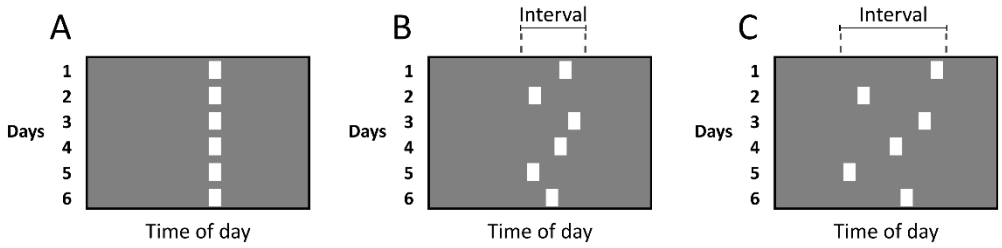

Figure 2.1.3. Variations of our light exposure model. In previous computer simulations (Flôres et al., 2013), we tested different versions of this simplified model of light exposure. **A**: Simulated light exposure pattern with a single exposure episode per day (white rectangles) occurring at a fixed time. **B** and **C**: daily light exposure episodes distributed randomly within time intervals of different durations.

We predicted that this model regimen would only entrain the mathematical oscillator to a 24-hour period if the phases of the daily pulses happened within narrow time interval, similar to the single-pulse T-cycle (Figure 2.1.3A). As the phase distribution interval was widened (Figure 2.1.3B, C), the great variability in the phases of the pulses would

presumably fail to keep the mathematical oscillator in synchrony with the 24-hour day. We would then include more complexity into the model light regimen, bringing it closer to the real data collected with light loggers, as an attempt to increase the strength of the synchronizing signal. This complexity would involve: (i) more than one pulse per day, (ii) pulses with a biased distribution concentrated in the middle of the distribution interval, (iii) varying pulses intensities associated to the natural variation in light intensity along the day. Contrary to our expectations, however, the mathematical oscillator was in fact entrained to a 24-hour period in response to the minimal model of light exposure (Figure 2.1.3C), with distribution intervals I as wide as 14 hours. This finding was replicated with three different parameter configurations of the mathematical oscillator (Flôres, 2011).

In the following manuscript, we tested the prediction of the mathematical model experimentally, with tuco-tucos maintained in our laboratory setup, to explore the potential of these model light regimens as synchronizing agents in the real world.

2.2. MANUSCRIPT

Entrainment of circadian rhythms to irregular light/dark cycles: a subterranean perspective

Published in Scientific Reports (Flôres et al., 2016a).

Authors: Danilo E. F. L. Flôres[1], Milene G. Jannetti[1], Veronica S. Valentinuzzi[2], Gisele A. Oda[1,*]

Affiliations:

1. Institute of Biosciences, Department of Physiology, University of São Paulo; São Paulo, São Paulo, 05508-900; Brazil.

2. Centro Regional de Investigaciones Científicas y Transferencia Tecnológica de La Rioja (CRILAR), Provincia de La Rioja, UNLaR, SEGEMAR, UNCa, CONICET. Entre Ríos y Mendoza s/n, (5301) Anillaco, La Rioja, Argentina.

Abstract

Synchronization of biological rhythms to the 24-hour day/night has long been studied with model organisms, under artificial light/dark cycles in the laboratory. The commonly used rectangular light/dark cycles, comprising hours of continuous light and darkness, may not be representative of the natural light exposure for most species, including humans. Subterranean rodents live in dark underground tunnels and offer a unique opportunity to investigate extreme mechanisms of photic entrainment in the wild. Here, we show automated field recordings of the daily light exposure patterns in a South American subterranean rodent, the tuco-tuco (*Ctenomys* aff. *knighti*). In the laboratory, we exposed tuco-tucos to a simplified version of this natural light exposure pattern, to determine the minimum light timing information that is necessary for synchronization. As predicted from our previous studies using mathematical modeling, the activity rhythm of tuco-tucos synchronized to this mostly simplified light/dark regimen consisting of a single light pulse per day, occurring at randomly scattered times within a day length interval. Our integrated semi-natural, lab and computer simulation findings indicate that

photic entrainment of circadian oscillators is robust, even in face of artificially reduced exposure and increased phase instability of the synchronizing stimuli.

Introduction

Synchronization of circadian rhythms to the 24-hour day/night has long been studied with model organisms under laboratory conditions, using artificially controlled light/dark (LD) cycles (Golombek and Rosenstein, 2010; Pittendrigh and Daan, 1976b). In mammals, this synchronization is mediated by a neuronal retino-hypothalamic pathway that transduces the light information and entrains the master circadian oscillator in the suprachiasmatic nuclei of the hypothalamus (Moore, 1983). In most cases, patterns of photic entrainment are studied under "rectangular" LD cycles comprising hours of continuous light and darkness. Although this procedure has offered great insights into synchronization mechanisms, it has often been criticized because, under natural conditions, most organisms, including humans, are not continuously exposed to light during the day (DeCoursey and DeCoursey, 1964; Hut et al., 1999; de la Iglesia et al., 2015; Moreno et al., 2015; Okudaira et al., 1983; Wright et al., 2013).

An insightful approach to evaluate how much artificial LD cycles can reliably represent natural light/dark cycles has been the study of entrainment patterns under discrete and continuous, cyclic light regimens. This distinction led to the development of two conceptual models of photic entrainment, namely the "parametric" (continuous) and "non-parametric" (discrete) mechanisms, which have greatly helped to coordinate our understanding of photic synchronization (Comas et al., 2008; Daan and Pittendrigh, 1976b; Pittendrigh and Daan, 1976b; Taylor et al., 2010).

Subterranean rodents offer a unique opportunity to investigate natural photic entrainment mechanisms. On one hand, they live mostly underground in the extreme photic environment of constant darkness. On the other hand, they do expose themselves to light at least while removing earth out of their burrows; and this is true even for those species that are considered "strictly" subterranean (Jarvis et al., 1994). Cumulative evidence reveals that they possess functional circadian oscillators and intact neuronal pathways for photic entrainment (Ben-Shlomo et al., 1995; Oosthuizen et al., 2003; Rado et al., 1993). Furthermore, our group reported a Phase Response Curve (PRC) (Johnson, 1999) to light pulses for a subterranean rodent, revealing similar photic entrainment

properties to those of non-subterranean rodent species (Flôres et al., 2013). The frequency of exposure to the external light should vary among subterranean rodent species but there is still little knowledge on how often and when they perform this typical behavior.

We present the first automated recording data of daily light exposure patterns in a subterranean rodent species of Argentina, the tuco-tucos (*Ctenomys* aff. *knighti*) (Cook and Lessa, 1998), carrying light sensing loggers (Williams et al., 2012b) in their natural habitat. Together with behavioral observations of these solitary animals (Tomotani et al., 2012) the current data confirm that tuco-tucos are exposed to light at irregular times, in brief episodes of foraging and earth removal. This exposure pattern should however sustain entrainment, because individuals that were transferred directly to constant conditions upon capture from the wild displayed 24-hour period "aftereffects" of entrainment (Tomotani et al., 2012).

We have previously simulated photic entrainment using a mathematical model of circadian oscillator that displayed a qualitatively similar PRC of the tuco-tucos (Flôres et al., 2013). The oscillator was given simulated daily light pulses, scattered randomly within a daytime window, to grossly model the natural daily light exposure of tuco-tucos. We manipulated the length of the daytime window and verified the limits of entrainment to this simplified model. For short time windows, entrainment was expected, as the light schedules would resemble a single-pulse T-cycle with period equal to 24 hours. As the window was widened to longer durations, the oscillator might either free-run or become arrhythmic. Our computer simulations unexpectedly predicted that entrainment to a 24-hour period might be achieved even if the light regimen were composed of one single light pulse per day, occurring at random times scattered at a broad (up to 14-hour) range along the days (Flôres et al., 2013).

In the present work, we tested the predictions experimentally with tuco-tucos in the laboratory, using wheel-running circadian rhythms as markers of their circadian oscillator motion. The confirmed synchronization under this peculiar light regimen reveals that photic entrainment is achieved by the contribution of both "parametric" and "non-parametric" effects and this is based on integrated field, laboratory and computer simulation approaches.

Results

Light exposure patterns during winter in semi-natural enclosures

We recorded the daily light exposure patterns from 8 tuco-tucos maintained in field enclosures in the winters of 2014 and 2015 (Figure 2.2.1). All animals exposed themselves to light at least once a day, in brief episodes. Within each individual record, the timing of these episodes changed from day to day. Values greater than 1.2 lux were never detected beyond the limits of civil twilight, indicating no exposure to natural or artificial light at night. Maximum recorded light levels were always close to the higher limits of detection (19,000 lux or 74,000 lux depending on the logger). It is noteworthy that even though light exposure episodes were scattered throughout the day, the overall exposure during winter was distributed in a unimodal pattern, concentrated in the middle of the day (Figure 2.2.1).

Entrainment under pulse regimens of increasing dispersion

The light exposure pattern recorded in the field inspired a laboratory model that captures some essential properties of the natural light/dark regimen of tuco-tucos. The model is a simplification that explores an extreme scenario with minimal timing information provided by the light/dark cycle. The protocol consists of a single light pulse of 1 hour (1,000 lux) applied once a day, at random times within a pre-defined time window "**I**". Computer simulations of a mathematical oscillator have predicted the synchronizing potential of this simplified light exposure (Flôres et al., 2013).

Figure 2.2.2 illustrates the overall features of the protocol in comparison to the natural light exposure of tuco-tucos. In the example (Figure 2.2.2 right panel), the single 1-hour light pulse was administered every day at a different time within an 8-hour interval (I=8h). Data from a representative animal illustrate that, despite the irregular light/dark timing, the activity rhythm remained stably adjusted to a 24-hour period. We describe below further results with these randomly distributed light pulses.

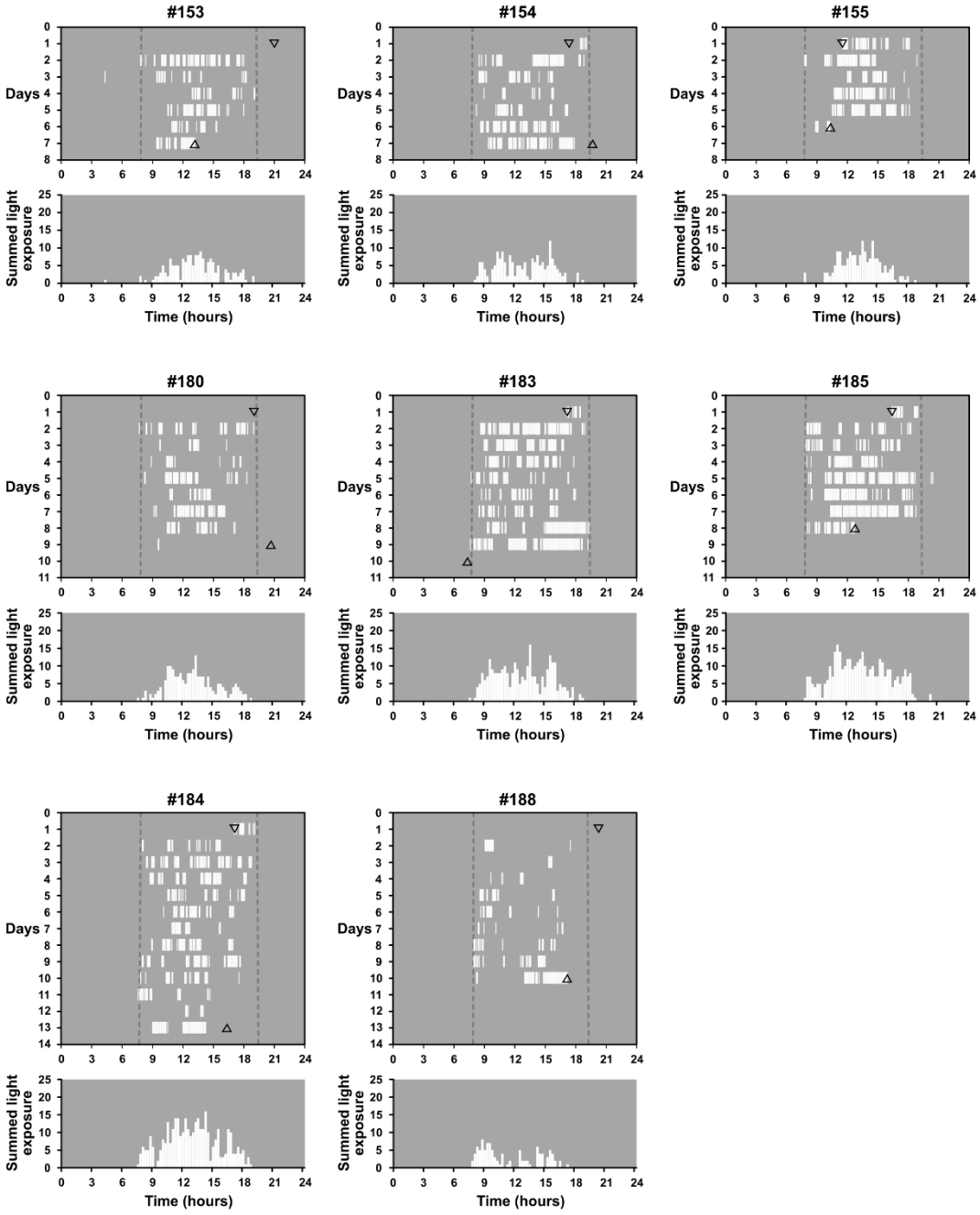

Figure 2.2.1. Daily temporal pattern of light exposure from 8 tuco-tucos , during the 2014 (July) and 2015 (July and August) south hemisphere winters. For each animal an actogram and a histogram illustrate its light exposure pattern. Actograms (**upper graphs**) show times of daily light exposure episodes (white vertical bars against a gray background) and consecutive days are shown below each other. Civil twilight times are demarked with vertical dashed lines. Downward and upward pointing triangles indicate the times of release and recapture from the enclosure, respectively. Histograms (**lower graphs**) show the summed light exposure of all days in the field enclosure for each animal, throughout the 24 hours of the day. Animals #153-155 were recorded in July 2014 and #180-188 in July 2015.

In the first experiment, we verified the limits to which the interval "**I"** could be widened and still promote 24-hour synchronization (Figure 2.2.3). Tuco-tucos (N=9, 6 males, 3 females) were initially left in constant darkness and their running-wheel activity rhythms free-ran with periods different from 24 hours, as illustrated by two representative animals (Figure 2.2.3, DD). We then applied the sequence of single daily light pulses represented on the left panel of Figure 2.2.3 (Pulses); each light pulse treatment lasted from 29 to 54 days.

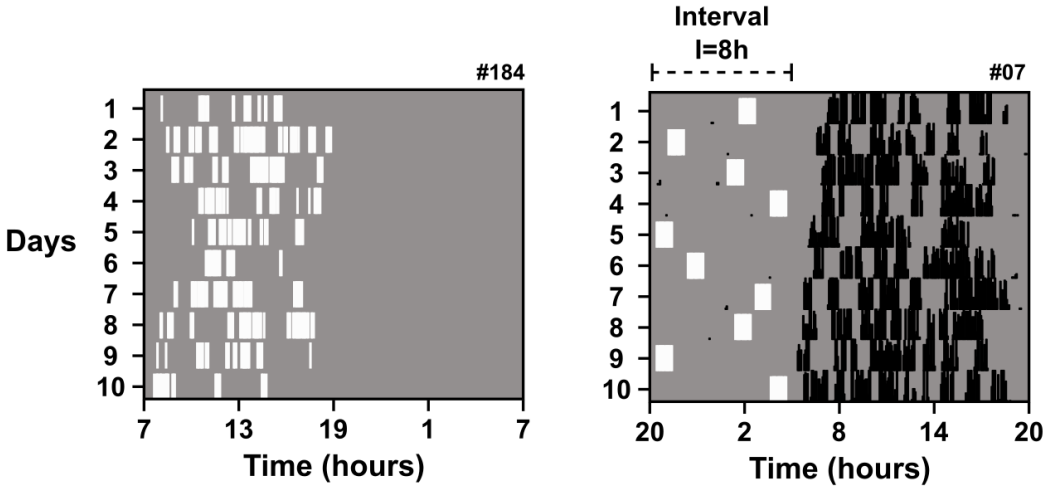

Figure 2.2.2. A simplified model of the tuco-tuco's light exposure pattern. **Left:** Temporal pattern of light exposure in the field, measured by light sensors. **Right:** Light exposure model and its effect on the rhythm of a representative animal in the laboratory. The figure depicts the random dispersion of the daily light pulses (1 hour; 1,000 lux) along a fixed interval I. In both graphs, light exposure is marked in white over the darkness (gray) background. The running-wheel activity of the tuco-tuco is represented by black marks. The number on the upper right of the actogram indicates the custom lab ID of the animal.

In response to daily pulses at the same time every day, the rhythms assumed periods closer to 24 hours, after some transient cycles (Figure 2.2.3, LD1:23). Next, the timing of the single daily light-pulses was randomized within an 8-hour time-window (Figure 2.2.3, **I**=8h). Some transients were observed, but the rhythms attained synchronization to a 24-hour period. To confirm that the observed synchronization was due to photic entrainment and not to some uncontrolled environmental cycle, we delayed the pulse interval by 6 hours. The activity band was delayed accordingly, indicating that the pulses actively entrained the underlying circadian oscillator (Figure 2.2.3, **I**=8h (shifted)). Period

quantification of the rhythms from all animals confirms the maintenance of periods close to 24 hours upon exposure to the randomly timed light pulses within an 8-hour interval (Supplementary Fig. S2.2.2).

After an increase in the time window of pulses to 15 hours, the rhythms still sustained a 24-hour periodicity (Figure 2.2.3, **I**=15h, Supplementary Fig. S2.2.2). When the pulse interval **I** was finally widened to 20 hours, the two representative animals presented different responses (Figure 2.2.3, **I**=20h). Animal #72 expressed a rhythm with period greater than 24 hours, while animal #76 sustained the 24-hour rhythmicity. Numerical data from all individuals show a great increase in the variability of periods and an overall deviation from 24 hours (Supplementary Fig. S2.2.2). Of the 9 animals, 3 presented rhythms with periods far from 24 hours, 2 became arrhythmic and 4 remained with a 24-hour rhythmicity in this last regimen.

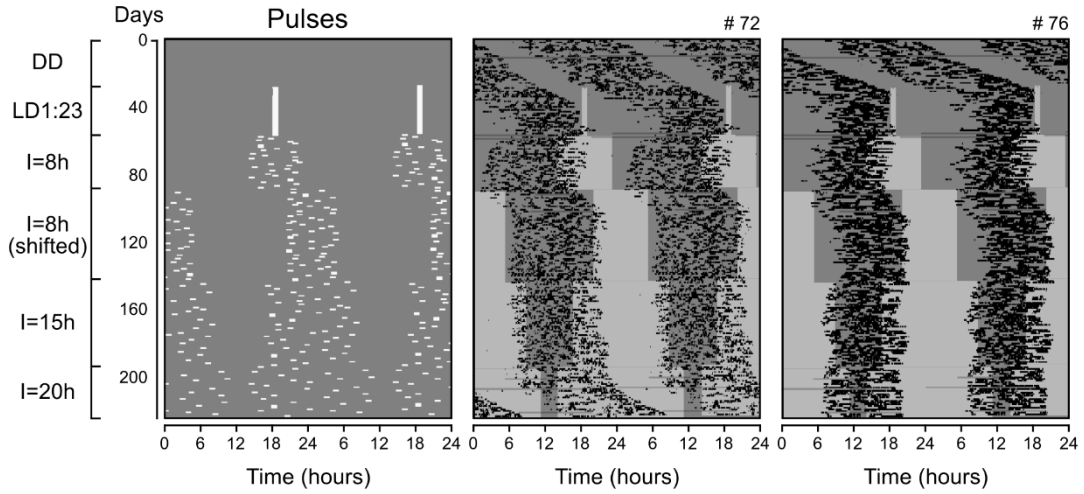

Figure 2.2.3. Synchronization of tuco-tucos' circadian activity rhythms to regimens of 1 light pulse per day distributed at random times. **Left graph**: protocol indicating timing of the daily single 1-hour light pulses of intensity L=1,000 lux (white marks), against the darkness (gray) background. The dispersion of pulses was progressively increased from the first to the last light regimen, as described on the left of the actogram. **Middle and right graphs**: actograms of the rhythms from two representative animals. Light-gray areas on the background represent the time interval "I" to which the single daily pulses were restricted. Activity times are marked in black. Actograms from all individuals are shown in Supplementary Fig. S2.2.1.

Our previous computer simulations predicted that, even though the circadian oscillator should remain entrained to 24 hours in regimens with large **I** (Flôres et al., 2013), the day-

to-day phase variability should be increased as the light pulse times became more disperse. In our current experiment with tuco-tucos, however, we found no obvious tendency for higher phase variability in regimens of greater "**I**", regardless whether using activity onsets, activity offsets or center of gravity as phase markers (Supplementary Fig. S2.2.3). Finally, periodogram analysis from rhythms associated with increased **I** did not show side-band periods (Granada et al., 2011) that indicate gradual loss of entrainment (Supplementary Fig. S2.2.4).

Entrainment under pulse regimens of decreasing dispersion

We next tested whether the synchronization by randomly distributed light stimuli was dependent on the order of the light pulse regimens. In this sense, we repeated the last three light pulse regimens shown in Figure 2.2.3, however, in the converse order, with 6 animals (3 males and 3 females). Three of the animals (#07, 60, 80) were reused from the first experiment, which finished 8 months earlier. Data from two representative animals are shown in Figure 2.2.4. Both presented circadian rhythms in constant darkness (Figure 2.2.4, DD). In the **I**=20h regimen, the rhythms of most individuals attained periods different from 24 hours (Figure 2.2.4, **I**=20h) and only 1 presented stable 24-hour rhythmicity (Supplementary Fig. S2.2.2).

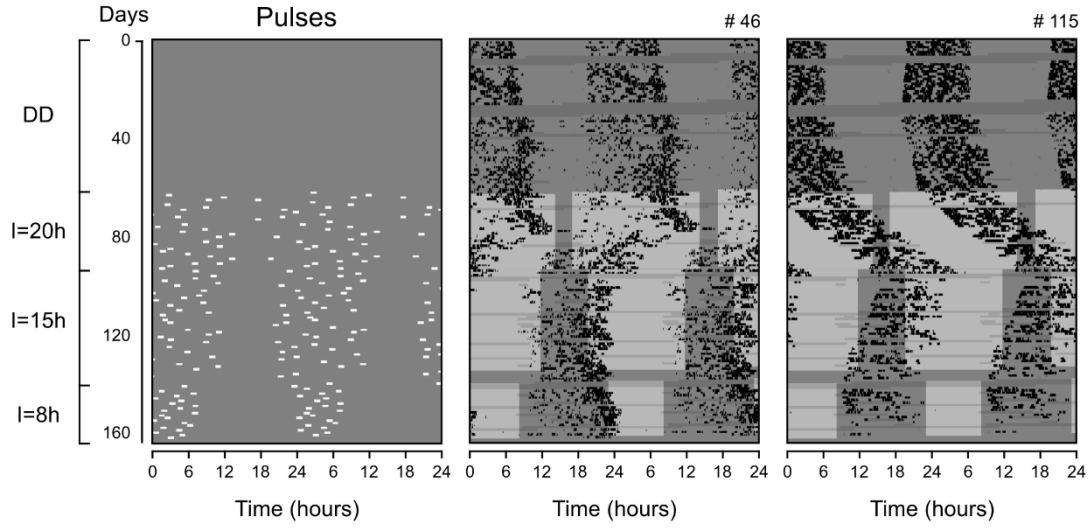

Figure 2.2.4. Effects of light-pulse regimens applied on tuco-tucos in a converse order relative to the first experiment. Light pulses were applied at an intensity L=1,000 lux. For other specifications, see Figure 2.2.3. Actograms from all individuals are shown in Supplementary Fig. S2.2.5.

Upon transfer to the **I**=15h regimen, the rhythm from animal #46 was apparently adjusted to 24 hours, with signs of relative coordination (Figure 2.2.4, **I**=15h). Animal #115 was either not prone to synchronization or was still in transients and would require more days to synchronize to the **I**=15h regimen. Quantification (n=3) returned periods closer to 24 hours upon transfer from **I**=20h to **I**=15h, confirming a tendency for synchronization (Supplementary Fig. S2.2.2). Three animals could not be followed in the transition to **I**=15h due to data loss (#07, 60) or arrhythmicity (#80) (Supplementary Fig. S2.2.5), therefore, conclusions should be taken with caution.

In the **I**=8h regimen, both representative animals had their rhythms adjusted to 24 hours with activity concentrated during the hours of "darkness", when no light-pulse was presented (Figure 2.2.4, **I**=8h). Quantification of the rhythms from the whole group confirmed periods close to 24 hours in all the measurable individuals (Supplementary Fig. S2.2.2); two animals could not be analyzed at this regimen due to data loss.

Entrainment under pulse regimens of different light intensity

Finally we asked how the strength of the light pulses (light intensity **L**) would influence the synchronization to our simplified light exposure model. Following the previous experiment, animals were immediately transferred to DD to start the new experiment; female #115 was not used in the analyses because of great data loss. They were thereafter exposed to pulses distributed at I=15h with L=100 lux and then to pulses at I=15h with L=1,000 lux.

Figure 2.2.5 shows the light pulses and the activity records from two representative individuals. In the **I**=15h (**L**=100 lux) regimen, neither of the representative animals was stably synchronized by this pulse regimen; animal #07 presented period shorter than 24 hour, while animal #46 was in relative coordination (Figure 2.2.5, **I**=15h **L**=100 lux). Quantifications confirm that only 1 animal presented a 24-hour rhythm in this regimen (Supplementary Fig. S2.2.2).

Upon increasing light intensity to **L**=1,000 lux (same intensity used in the previous experiments), the rhythms of both animals displayed periods very close to 24 hours (Figure 2.2.5, **I**=15h **L**=1,000 lux). The quantified periods of all individuals confirm the tendency: 4 out of 5 lied within the 24-hour range in **L**=1,000 lux (Supplementary Fig. S2.2.2). Upon release into DD, periods remained in the range of 24-hours, indicating period aftereffects of entrainment from the last pulse regimen (Figure 2.2.5, DD;

Supplementary Fig. S2.2.2). The distinct transient patterns shown in **I**=15h (**L**=1,000 lux) were replicated in computer simulations, using different light intensities for the simulated pulses (Supplementary Fig. S2.2.7, Supplementary simulations).

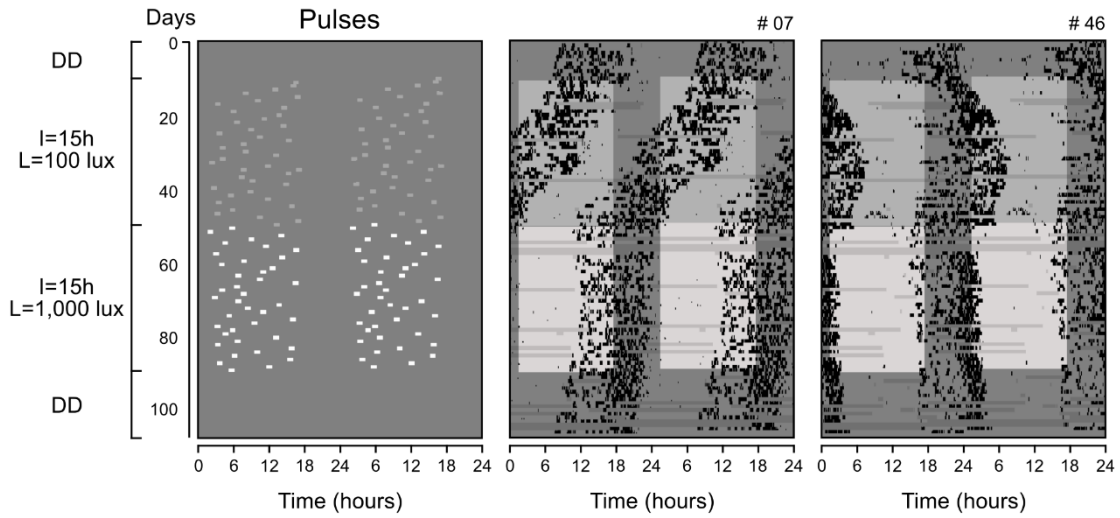

Figure 2.2.5. Effect of light intensity in synchronization to the random daily single light-pulse regimen. Two gray tonalities are used to represent the weak- (darker) and strong- (brighter) pulse regimens. For other specifications, see Figure 2.2.3. Actograms from all individuals are shown in Supplementary Fig. S2.2.6.

Discussion

Our field and laboratory data reveal a simple and non-intuitive way of photic entrainment that, to our knowledge, has not been explored before experimentally. The results confirm and extend the predictions from computer simulations (Flôres et al., 2013) and strongly suggest that the process of entrainment is even more robust than previously known.

Synchronization is achieved when the light/dark cycle of the Earth forces a circadian oscillator to a 24-hour period. Two parallel conceptual models of photic entrainment have long coordinated our understanding of the mechanism behind this period-forcing process (Supplementary Fig. S2.2.8). The "parametric" (continuous) model proposes that the circadian oscillator is continuously driven by the light/dark cycle to achieve a 24-hour period. The "non-parametric" (discrete) model, on the other hand, proposes that the timing of the oscillator is reset by abrupt phase shifts, just like we kick a swing in discrete,

periodic drives. In this model, light would not affect the oscillator throughout the entire duration of the light phase but especially during the transitions that occur at twilight times (Chandrashekaran et al., 1973).

The physical basis of these two modes has been simulated by limit-cycle oscillators driven either by continuous, harmonic forces (Tomita et al., 1977) or by impulsive, kicking forces (Campbell et al., 1989). The latter model relies on the time-dependent phase responses of circadian oscillators to light pulses, which are provided by species-specific Phase Response Curves (PRCs) (Daan and Pittendrigh, 1976a; Johnson, 1999; Roenneberg et al., 2003; Taylor et al., 2010). It was not evident, however, how these theoretical constructions could account for entrainment in the "real world", where each species in its habitat displays specific light exposure patterns.

It has been proposed that non-parametric mechanisms could reliably model the natural photic entrainment of nocturnal animals (DeCoursey and DeCoursey, 1964; Twente, 1955; Voute et al., 1974), that presumably expose themselves to light briefly during dawn and/or dusk hours (Pittendrigh and Daan, 1976c). This proposition was supported by DeCoursey (DeCoursey, 1986) in her pioneering approaches to natural entrainment with flying squirrels in simulated laboratory burrows. The flying squirrels were allowed the opportunity to retreat to their burrows and expose themselves voluntarily to light and, indeed, they achieved entrainment by sporadic phase resetting of the circadian oscillator, at times of self light exposure.

Could a similar mechanism explain entrainment in diurnal organisms? Daytime activity presumably implies exposure to light during most of the activity phase; thus, an initial, non-parametric approach conceived symmetric phase resetting occurring at dawn and dusk (Boulos and Rusak, 1982). However, the first field study on natural entrainment, using diurnal ground squirrels carrying light sensors, showed that these animals are not exposed at all to light during twilights (Hut et al., 1999), favoring a more parametric-like approach for diurnal entrainment (Beersma et al., 1999).

One non-intuitive prediction of the non-parametric model is that few minutes or even a single second of light per day is sufficient for photic entrainment (DeCoursey, 1972; Pittendrigh and Daan, 1976a). This has been successfully tested experimentally with single pulse T-cycle experiments, in which single light pulses are administered at a fixed phase within a cycle (in the same time of day, for 24-hour cycles) (Elliot, 1976; Pittendrigh and Daan, 1976a) The phenomenon can also be simulated by physical

oscillators of the limit-cycle type, which are synchronizable by periodically-kicking forces (Campbell et al., 1989).

Our computer model of photic entrainment (Flôres et al., 2013) provided an unexpected and even less intuitive prediction than the T-cycle regimens: entrainment could be sustained by a single daily light pulse administered at randomly changing times within a daytime interval. Computer simulations also predicted that, for our light pulse duration and intensity, synchronization would prevail even if this daytime interval achieved surprisingly wide lengths such as 14 hours.

The present experimental tests inspired by our in silico mathematical model confirmed that the simplified light regimen is sufficient to sustain entrainment also in vivo. In nature the studied *Ctenomys* species in Anillaco, Argentina, never experiences photophases greater than 14 h 53 min (civil twilight times available at <http://www.arachnoid.com/lutusp/sunrise>, accessed on March 14th, 2016), which is less than the 15 hours that successfully sustained entrainment in the lab. This situation is a simplification of light exposure patterns in the field for a subterranean animal and in particular for tuco-tucos, which are definitely exposed to light at several random times per day, according to our current light-logger data. Therefore, simulations, laboratory and field data indicate that photic entrainment is a strong component of field entrainment in subterranean tuco-tucos.

It has long been suggested that parametric and non-parametric models should be integrated for a complete understanding of photic entrainment (Johnson et al., 2003). Peterson (Peterson, 1980) posed this question while observing the "sluggish" behavior of the *Drosophila* circadian oscillator when released from constant light to darkness or the reverse way. This concept of sluggish dynamics was better formalized in Abraham et al. (Abraham et al., 2010), where the "relaxation rate" was brought to light as a parameter that determines how fast a limit-cycle's amplitude is recovered after exposure to light stimuli (Indic et al., 2005). This concept challenges and complements the instantly recovering oscillations presumed by the non-parametric model.

We propose that the slow relaxation rate of circadian oscillators underlies their ability to recognize a 24-hour period out of randomly distributed light pulse times. Each day the light stimulus impinges a phase-shift on the oscillator, but the shift occurs only after transient slow changes in amplitude (Abraham et al., 2010; Casiraghi et al., 2012; Granada et al., 2011; Peterson, 1980). If the amplitude were instantly recovered our random pulse regimens would presumably cause equally random back and forth changes

in the phase of the circadian oscillator, possibly failing to keep the phase stable within a 24-hour day. This effect was not displayed in our entrainment patterns – as shown by the equal phase dispersion of activity under different regimens (Supplementary Fig. S2.2.3).

Instead, the transient phase shifts that occur at each new light pulse result in the overall sluggish process that resembles a parametric, continuous adjustment, even though there is no continuous light. Thus, although our studies of synchronization under this peculiar, random light regimen were not meant to discern parametric from non-parametric models, they reveal that photic entrainment is achieved by the contribution of both components. The key to this integration lies in the fact that there is no "pure" non-parametric synchronization, because circadian limit-cycle oscillators (Indic et al., 2005) seem to display non-instant recovery of their amplitude.

It has been shown that entrainment of a free-running circadian oscillator occurs only for a specific range of period and light intensity combinations of the light/dark cycle which set the "range of entrainment" (Abraham et al., 2010; Casiraghi et al., 2012; Granada et al., 2011). In our "random pulse" paradigm, we have fixed the period of the desired entrainment to 24 hours and have instead manipulated the dispersion length **I** (Figures 2.2.3, 2.2.4) or the intensity **L** of light pulses (Figure 2.2.5). We then proceeded to see if the concept of range of entrainment could also be established for these particular parameters, **I** and **L**.

For a fixed light intensity **L** of 1,000 lux, entrainment was lost after **I** was gradually increased to 20 hours, as predicted by our computer simulations (Flôres et al., 2013). We then converted the direction of **I** change, from a gradual increase to a decrease, to assure that the 24-hour period synchronization at each new **I** step of the protocol was not dependent on the period aftereffects of previous entrainment (Aton et al., 2004; Pittendrigh and Daan, 1976a). Indeed, entrainment was similar (Figure 2.2.3, 2.2.4, S2.2.2), regardless of the direction of the change in **I**, with most periods farther from 24 hours in **I**=20h and closer to 24 hours in **I**=15h. In **I**=8h, all animals remained within the 24-hour range.

On the other hand, for a fixed **I**, random pulse regimens that sustained entrainment for the first light intensity lost this ability when this parameter **L** was weakened, both in our experiments (Figure 2.2.5) and in computer simulations (Supplementary Fig. S2.2.7, Supplementary simulations). As it occurs with the period in the range of entrainment, our data suggests that the "threshold **I** for entrainment" was modified with **L**. The regimen

I=15h was within the range of entrainment when **L** was higher, however, outside this limit for weaker intensities.

Granada et al. (Granada et al., 2011) have shown that close to the border of the range of entrainment, mathematical oscillators tend to assume a zig-zag-like pattern in the actograms, which are quantified by side-band periods in the periodograms. Similarly, in our computer studies with randomly distributed light pulse regimens (Flôres et al., 2013), mathematical oscillators close to the "threshold **I** for entrainment" also acquired a zig-zag pattern, with great phase-variability along consecutive days and side-band periods in the periodograms. In the experimental work with tuco-tucos, we did not detect side-band periods, most probably because unlike in those simulations, what we observe here is the overt activity rhythm, not the state variable of the oscillator (Yamazaki et al., 2000) and this may make detection of these side bands more difficult.

Finally, it would be interesting to see how a system of weakly or strongly coupled oscillators (Yamaguchi et al., 2013) would differ in their responses to a random pulse regimen. This is a complex and intriguing question, since coupling force changes both the range of entrainment and the relaxation rate of the emergent oscillatory system (Abraham et al., 2010).

Photic entrainment studies are usually based on model species and laboratory experiments. Field information from unconventional, wild species can add to these studies, because each species presents a particular temporal pattern of light exposure, revealing extreme photic conditions that may inspire refinements or reelaborations of theoretical entrainment models (DeCoursey, 1986; Pratt and Goldman, 1986; Roenneberg and Foster, 1997). In this context, here we present a new, random pulse paradigm that provides less periodic timing information, than the single pulse T-cycle, and which was inspired by our natural measurements of daily light exposure patterns in a subterranean rodent. Previous computer simulations of this paradigm had predicted an unexpected robustness of entrainment to daily light stimuli at irregular phases and we successfully tested these predictions experimentally. Furthermore, we suggest that this paradigm presents a route for integrating "parametric" and "non-parametric" components of photic entrainment. Our field, laboratory and computer simulation approaches come together to uncover new properties of circadian oscillators.

Methods

Ethics statement

Trapping and laboratory protocols were approved and authorized by the Legal and Technical board (*Oficina de Técnica Legal*) of the Environmental Department of La Rioja (*Secretaria de Ambiente, Ministerio de Producción y Desarrollo Local*), permit number 062-08. They were also approved by the CEUA from the Institute of Biosciences, University of São Paulo (Protocol 152/2012) and by the CICUAL (Comité Institucional para el Cuidado y Uso de Animales de Laboratorio) from the *Facultad de Ciencias Veterinarias, Universidad de La Plata* (Protocol 29-01-12). Every procedure in this study followed the guidelines of the American Society of Mammalogists for animal care and handling (Sikes and Gannon, 2011).

Animal trapping

Tuco-tucos were obtained from a natural population, in the Monte Desert (Abraham et al., 2009), east of the town of Anillaco, La Rioja, Argentina (28º48'S; 66º56'W; 1,350 m). Animals were captured with PVC live-traps similar to the ones described in (Sargeant, 1966), placed at freshly tapped burrow entrances and checked every 2 hours.

Semi-Natural Enclosures and Light Exposure Recordings

Three outdoor enclosures were built in an area that is naturally occupied by wild tuco-tucos. Two enclosures measuring 12m x 6m were protected by wire mesh 1.5m aboveground and 1m underground, and a horizontal 20cm barrier in the inner perimeter at the bottom. The third enclosure measured 10m x 5m and was protected with wire mesh on top and sides (1.2m above-ground and 1m underground). The size of the enclosures was based both on the home-range determined for *C. talarum* (Cutrera et al., 2006) and on our telemetry-based estimation of the summer home range of the *Ctenomys* species found in Anillaco.

A meteorological station (Onset Computer Corporation, Bourne, MA) located at the site of the enclosures allowed constant recording of ambient temperature. Underground temperature was also continuously measured at a fixed 60-cm underground location inside the burrow using HOBO data loggers U10/003 (Onset Computer Corporation, Bourne, MA). Average temperatures were similar in the two years of recording – July 2014 max/min ambient temperatures: 18.9 ± 5.6ºC /4.7 ± 3.8ºC; max/min underground

temperatures: 13.8 ± 1.2ºC/ 13.4 ± 1.1ºC; July 2015: max/min ambient temperatures: 19.4 ± 5.4ºC/ 5.2 ± 5.1ºC max/min underground temperatures: 14.6 ± 1.1ºC/ 13.6 ± 3.6ºC.

A total of 11 tuco-tucos were released in the field enclosures, one at a time, in the two consecutive years. Of those, we were able to recover the records of light exposure from 8 individuals (4 males and 4 females, average weight 175 ± 44g). Before field recordings, animals were maintained in the laboratory, next to an open window, exposed to the natural light/dark cycle. Due to other experiments, they had implanted i-button temperature sensors and had remained in the lab for 1 to 5 months, before release into the enclosures. They were fed daily, at random times, with various items such as carrots, sweet potatoes, rabbit chow, sunflower seeds, oatmeal and lettuce.

On the day of release, individuals were anesthetized with isoflurane (1-1.5min, 3.5-4%, 4 L.min-1 O_2) and received light loggers affixed to neck collars (package weight < 5g; Intigeo loggers C65, W50, W65; Migrate Technology, Cambridge, UK). The collars were made of zip ties covered by silicone tubing. Light-loggers were set to detect illuminance every minute in the range of 0.3 to 19,000 lux (animals #153, 154, 155, 180, 184, 188) or 1 to 74,000 lux (animals #183, 185). Recorded data consist of a sequence of the highest values within each 5-minute interval.

Three animals were released at a time, one in each enclosure, in the winters of 2014 (July) and 2015 (July and August). Upon release, each animal readily excavated its own burrow system. No extra food was provided besides the natural vegetation. After 5 to 12 days in the enclosures, recapture was achieved using the same PVC tube traps described above and collars were removed immediately in the laboratory.

Laboratory Housing and Experiments

For the laboratory experiments, 12 tuco-tucos in total (7 males and 5 females, average weight of 178 ± 32g) were captured, as described above, and transferred to individual cages (length x width x height = 53 x 29 x 27cm) with running wheels (diameter 23 cm, width 10 cm, distance between bars 10 cm). They were kept in an isolated room with controlled light and temperature (T= 24 ± 1ºC) and were fed daily, as explained above. Cages were cleaned weekly. Running wheel turns for each animal were counted at 5-minute intervals by the Simonetta System (Universidad Nacional de Quilmes, Buenos Aires), to continuously record the animal's activity/rest rhythm.

Red incandescent light bulbs remained turned on continuously, at low illuminance (<5 lux) to allow proper cleaning and feeding during darkness conditions. White fluorescent

bulbs were used to define the conditions of "light" and "dark", superimposed to the background red light. The fluorescent light was regulated with a field light meter (TMI-201, Tenmars Electronics CO., Taiwan) to provide the two different illuminance levels, at the height of cage lids (**L**=100 or 1,000 lux). Light schedules in each experiment were programmed weekly into digital timers DNI-6610 (Dani Condutores Elétricos Ltda., São Paulo), which automatically promoted the light/dark changes.

Experimental light/dark schedules

Light pulses were applied once a day at random times, restricted to a distribution interval **I** of 8, 15 or 20 hours, as indicated in each experiment. The random pulse times were generated in Microsoft Excel (2007) with the function RANDBETWEEN. Each light pulse consisted of turning the fluorescent lights on for 1 hour at the specified light intensity. In the LD1:23 regimen, the 1-hour light pulses were delivered at the same time every day. During constant darkness (DD) only the dim background red light was left on.

Entrainment under random pulses with increasing dispersion

9 tuco-tucos (6 males, 3 females) were exposed to daily light pulses in the following sequence of treatments: constant darkness (DD); light/dark cycle with 1 hour of light and 23 hours of darkness per day (LD1:23); daily light pulses within an 8-hour interval (**I**=8h); daily light pulses within 8 hours, but delayed in 6 hours relative to the previous regimen (I=8h (shifted)); daily light pulses within a 15-hour interval (**I**=15h); daily light pulses within a 20-hour interval (**I**=20h). Each light pulse consisted of turning the lights on for 1 hour at **L**=1,000 lux.

Entrainment under random pulses with decreasing dispersion

6 animals (3 males, 3 females) previously free-running in DD were exposed to the sequence **I**=20h, **I**=15h and **I**=8h. Light pulses consisted of 1 hour of lights on at **L**=1,000 lux.

Entrainment under random pulses with different light intensities

5 animals (3 males, 2 females) were exposed to two pulse regimens with the same distribution window "**I**", but with different light intensities, in the following sequence of treatments: DD, **I**=15h (1-hour pulses of **L**=100 lux) and **I**=15h (1-hour pulses of **L**=1,000 lux).

Data analysis

Actograms and histograms for field light exposure data were built in Microsoft Excel. To build each actograms, we considered that a light exposure episode happened whenever the light level exceeded the basal (lowest) value of each individual record. For histograms, the light exposure episodes were summed in 15-minute intervals, to reveal the overall distribution of light exposure throughout the day, excluding the days of release and recapture.

Laboratory data was visually analyzed in actograms made with the software El Temps (A. Díez-Noguera, Universitat de Barcelona, 1999). Statistical quantification of the rhythms' periods was done using the chi-square periodogram with 0.05 significance level and 5-minute period precision (Sokolove and Bushell, 1978), in the software Clocklab (Actimetrics, Wilmette, USA). For each experimental regimen, data from the last 15 days were used for period determination. The rhythm was considered synchronized when its period lied within the 24 h ± 10 min interval. Phase was determined through activity onsets, offsets and "center of gravity" (CoG) (Kenagy, 1980) from the last 15 days of each experiment. Phase dispersion was calculated from the standard deviation of these reference phases, only when synchronization to 24 hours was achieved.

Acknowledgements

We would like to thank Dr. Loren Buck and Barbara Tomotani for indicating the Migrate Company UK that manufactured the light loggers; James Fox from this company for his kind assistance and interest; José D Paliza for technical assistance; Patricia Tachinardi and Jefferson Silva for their active participation in the field and laboratory recordings; Dr. Otto Friesen and Dr. Mirian Marques for their lessons; the funding agencies FAPESP (Fundação de Amparo à Pesquisa do Estado de São Paulo, grants 2014/20671-0, 2013/50482-1, 2012/15767-2), CONICET (*Consejo Nacional de Investigaciones Científicas y Técnicas*; grants PIP-11420090100252 and PIP-11220120100415) and Agencia Nacional de Promoción Científica y Tecnológica (grant PICT 2011/1979 and PICT2013-2753). DEFLF received Phd scholarships from FAPESP (grant 2011/24120-0) and CNPq (Conselho Nacional de Desenvolvimento Científico e

Tecnológico, grant 161438/2011-3). MGJ received scholarship from FAPESP (grant 2014/09324-6) and CAPES.

Author contributions

G.A.O., V.S.V. and D.E.F.L.F. conceived and designed the experiments; D.E.F.L.F., M.G.J and V.S.V. performed the experiments; D.E.F.L.F. and G.A.O. analyzed the results; M.G.J performed the computer simulations; G.A.O and D.E.F.L.F. wrote the manuscript; all authors revised the manuscript.

Competing financial interests

Authors declare no competing financial interests

Supplementary information

Supplementary simulations

To help the interpretation of the distinct patterns observed in Figure 2.2.5, computer simulations were performed, using a model limit-cycle oscillator developed by Pavlidis and Pittendrigh (Pittendrigh et al., 1991), which is defined by the following equations:

$$\frac{dR}{dt} = R - cS - bS^2 + d - L + K$$

$$\frac{dS}{dt} = R - aS$$

In these equations, R and S are state variables and letters a, b, c and d are four parameters that determine the oscillator configurations. We used a standard configuration (a=0.85, b=0.3, c=0.8, d=0.5), already employed in Flôres et al. (2013). K is a small nonlinear term (K = 1/[1 + 100R2]) formulated by W.T. Kyner, to prevent the variable R from achieving negative values. Simulated locomotor activity occurred every time the S variable rose above a threshold value, which we set to two thirds of the maximum amplitude of this variable. L represents the light level: a 1,000 lux light pulse, for instance, is mimicked by square-wave changes of L from baseline 0 to amplitude 1.1 (arbitrary unit) for the duration of the pulse. Simulations were performed using the *NeuroDynamix* software (www.neurodynamix.net).

We verified synchronization patterns of the model oscillator when exposed to daily 1-hour light pulses, whose daily timing changed randomly within a fixed interval **I**=15h. The times of light pulses were the same used in the experiment reported in Figure 2.2.5.

To check the response to weak or strong pulses on the long term, we first exposed the model oscillator to pulses with fixed amplitude throughout the whole simulation (Supplementary Fig. S2.2.7A, B, C). When subjected to weaker pulses, the oscillator was either not synchronized to 24 hours during the 80 days of pulses (Supplementary Fig. S2.2.7A) or it took several cycles (>60) to finally reach synchronization (Supplementary Fig. S2.2.7B). On the other hand, exposure to strong pulses readily synchronized the oscillator to 24 hours, within 30 days (Supplementary Fig. S2.2.7C).

At last, we repeated the protocol from the experiment reported in Figure 2.2.5, with two different pulse intensities in sequence (Supplementary Fig. S2.2.7D). The light pulses of the first 40 days had a lower light intensity (arbitrary value 0.13) while the light pulses

of the last 40 days had the highest light intensity (arbitrary value 1.1). As can be seen from the figure, stable entrainment was only achieved by the stronger light pulse regimen.

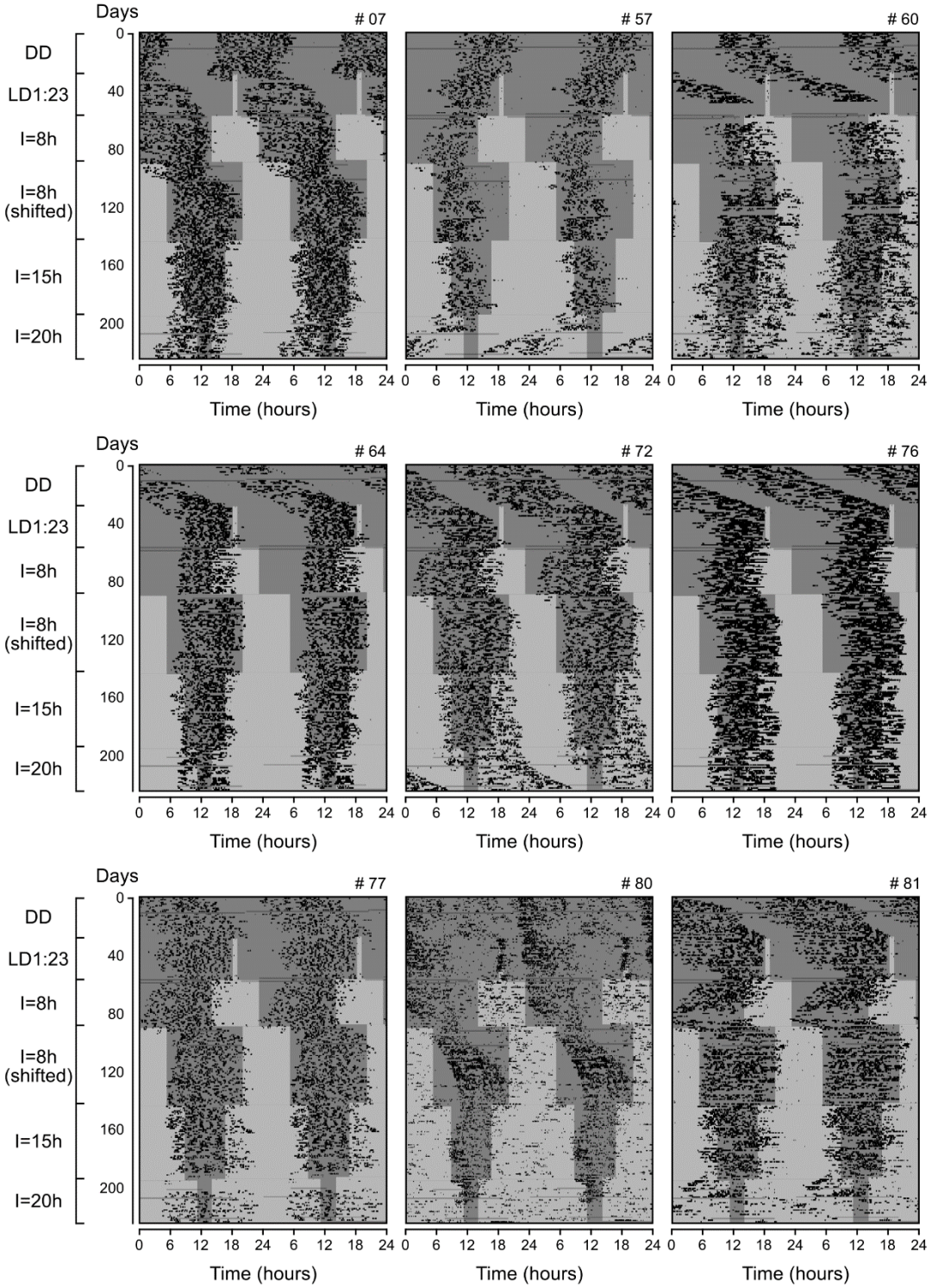

Figure S2.2.1. All actograms from the experiment with pulse regimens of increasing dispersion (Figure 2.2.3).

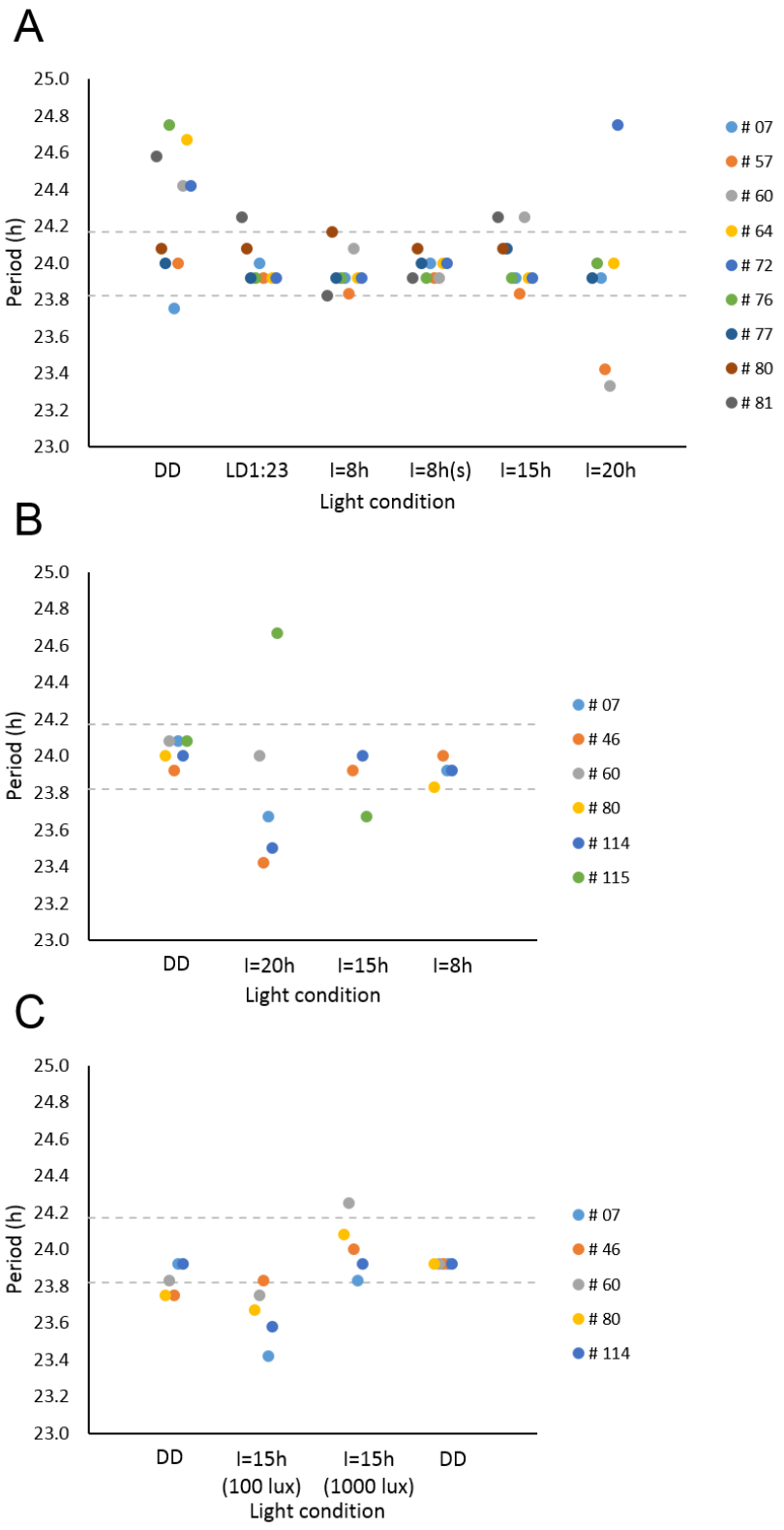

Figure S2.2.2. Period quantifications for each light regimen applied in the laboratory. **A**: Pulse regimens of increasing dispersion (Figure 2.2.3). **B**: Pulse regimens of decreasing dispersion (Figure 2.2.4). **C**: pulse regimens of different light intensity (Figure 2.2.5). Horizontal dashed lines indicate the 24 hour ± 10 minute interval.

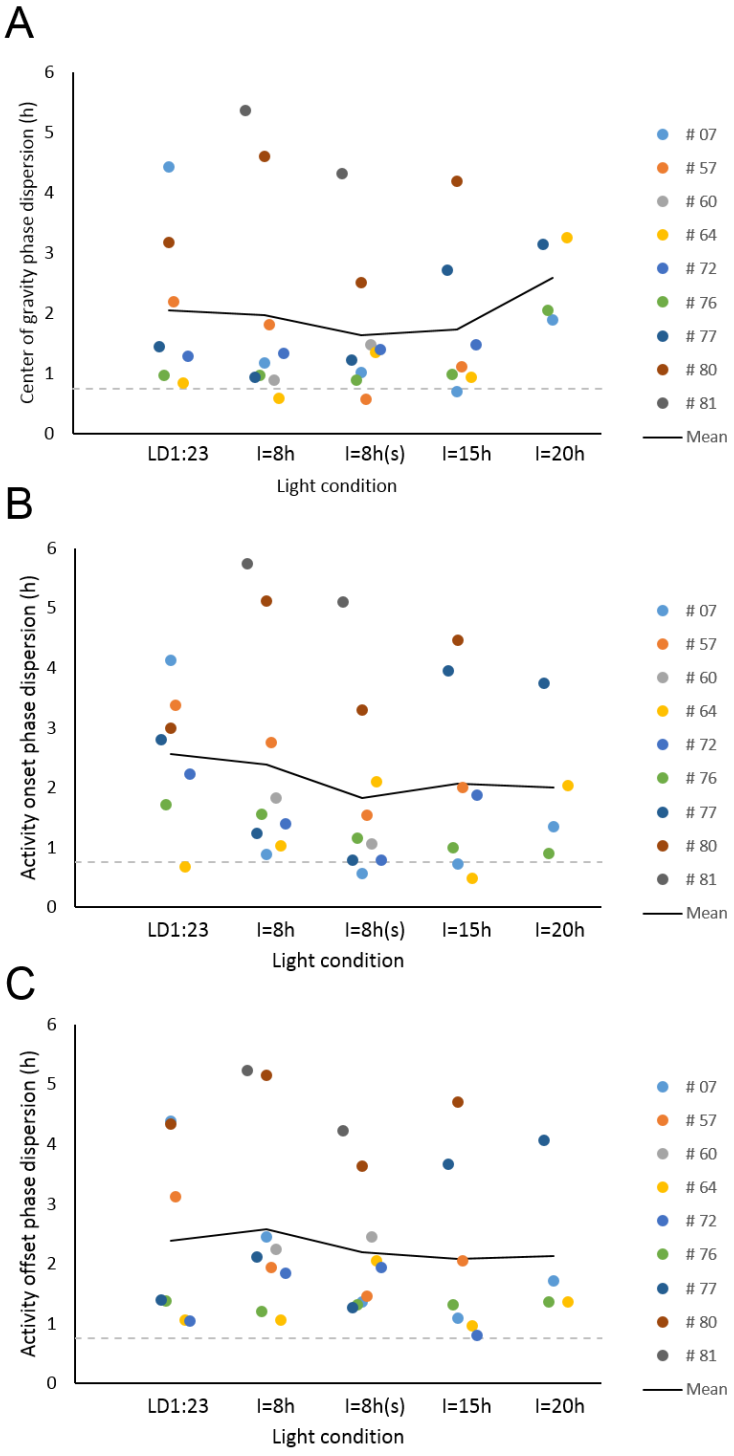

Figure S2.2.3. Phase variability of activity rhythm in the experiment with pulse regimens of increasing dispersion (Figure 2.2.3). The phase variability was based on different reference phase markers: (**A**) center of gravity (CoG), (**B**) activity onsets, (**C**) activity offsets. A dashed horizontal line indicates the maximal inherent phase dispersion that is unavoidable for rhythms with periods that deviate (± 10 minute) from 24 hours. In each graph, a solid line connects the average phase dispersion at the different light conditions.

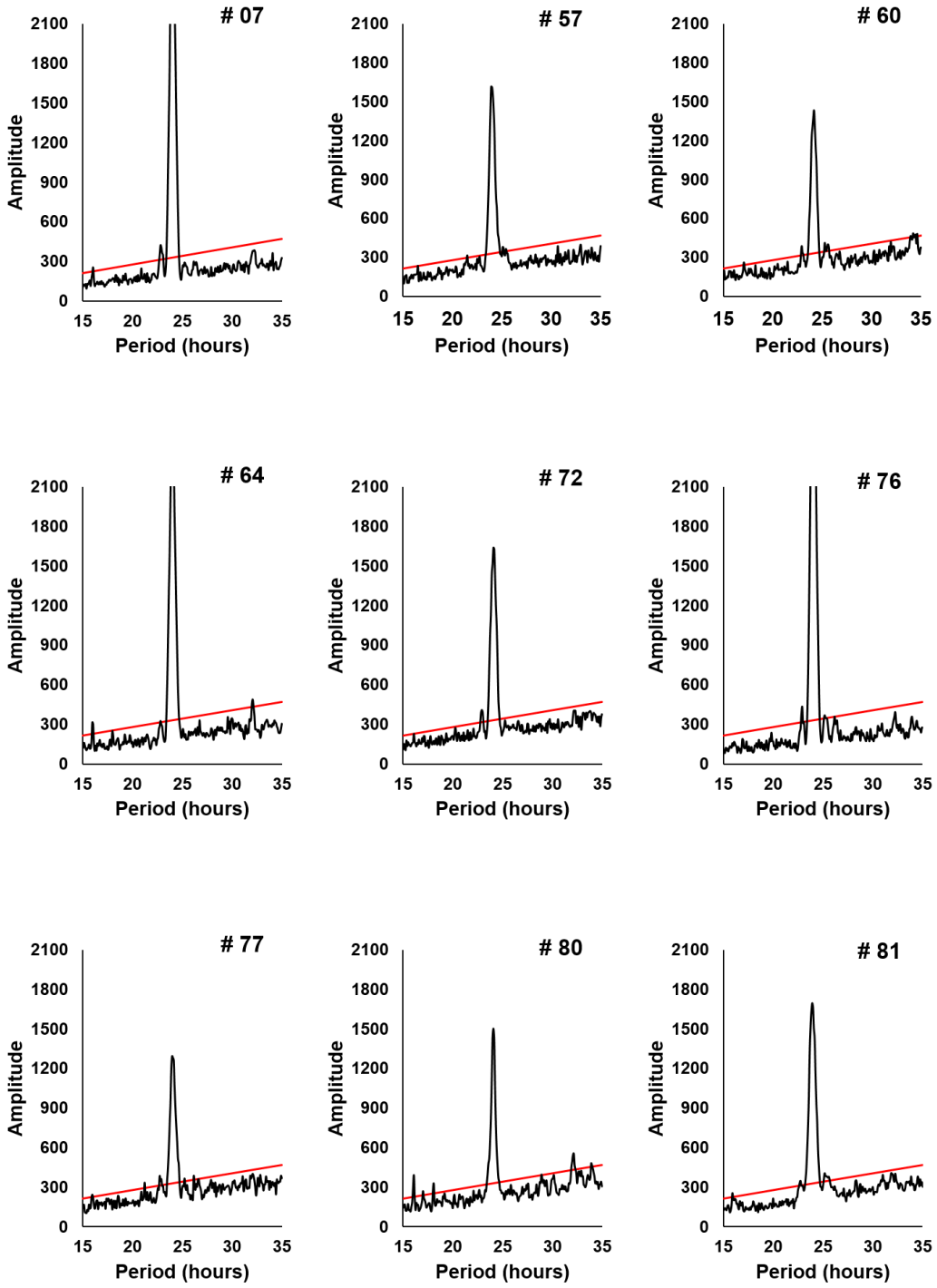

Figure S2.2.4. Period analysis of the rhythms from Figures 2.2.3 and S1, in the regimen I=15h. Each periodogram graph depicts the amplitude (significance) of the tested periods within the chosen range (15-35 hours), revealing the most probable (higher amplitude) period in the data, as well as potential side-band periods.

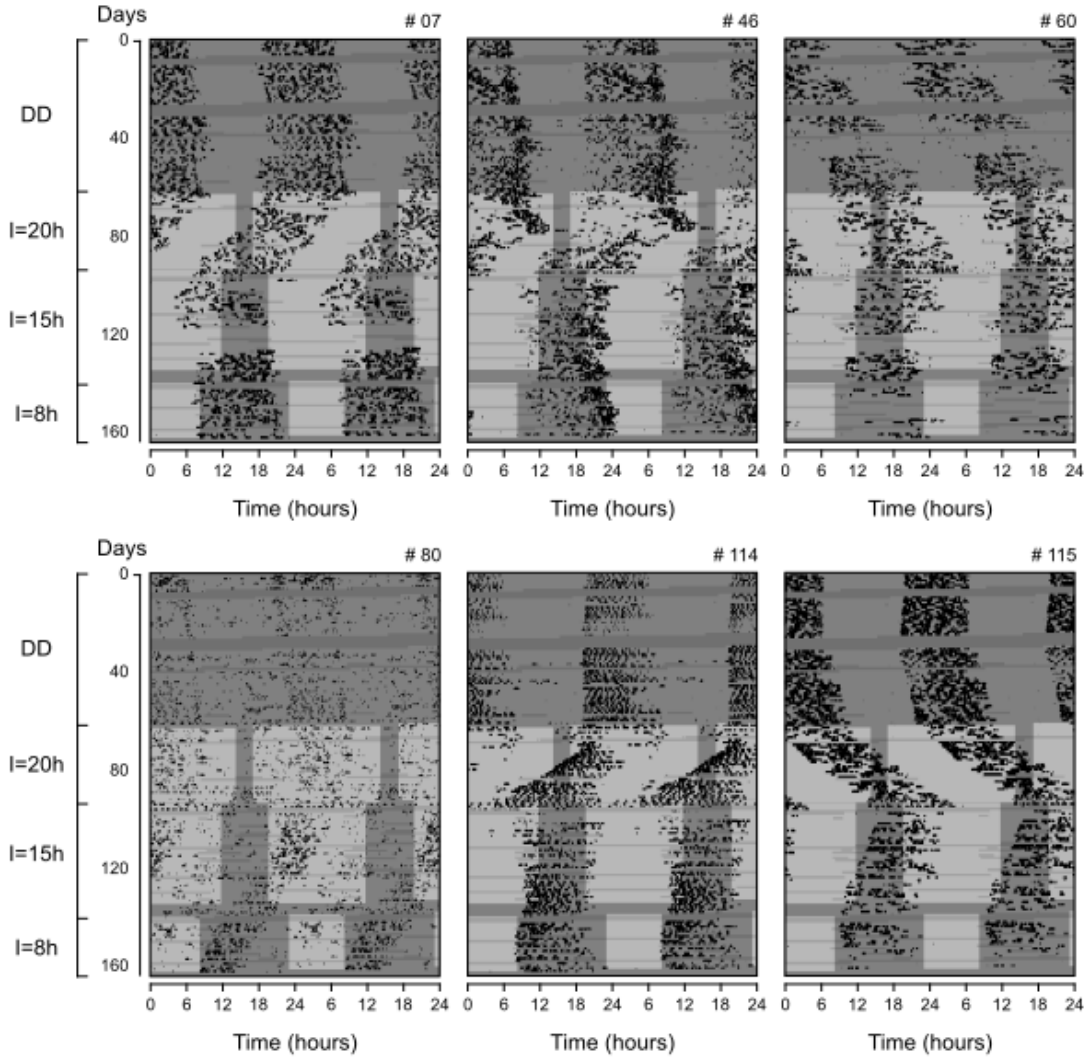

Figure S2.2.5. All actograms from the experiment with pulse regimens of decreasing dispersion (Figure 2.2.4).

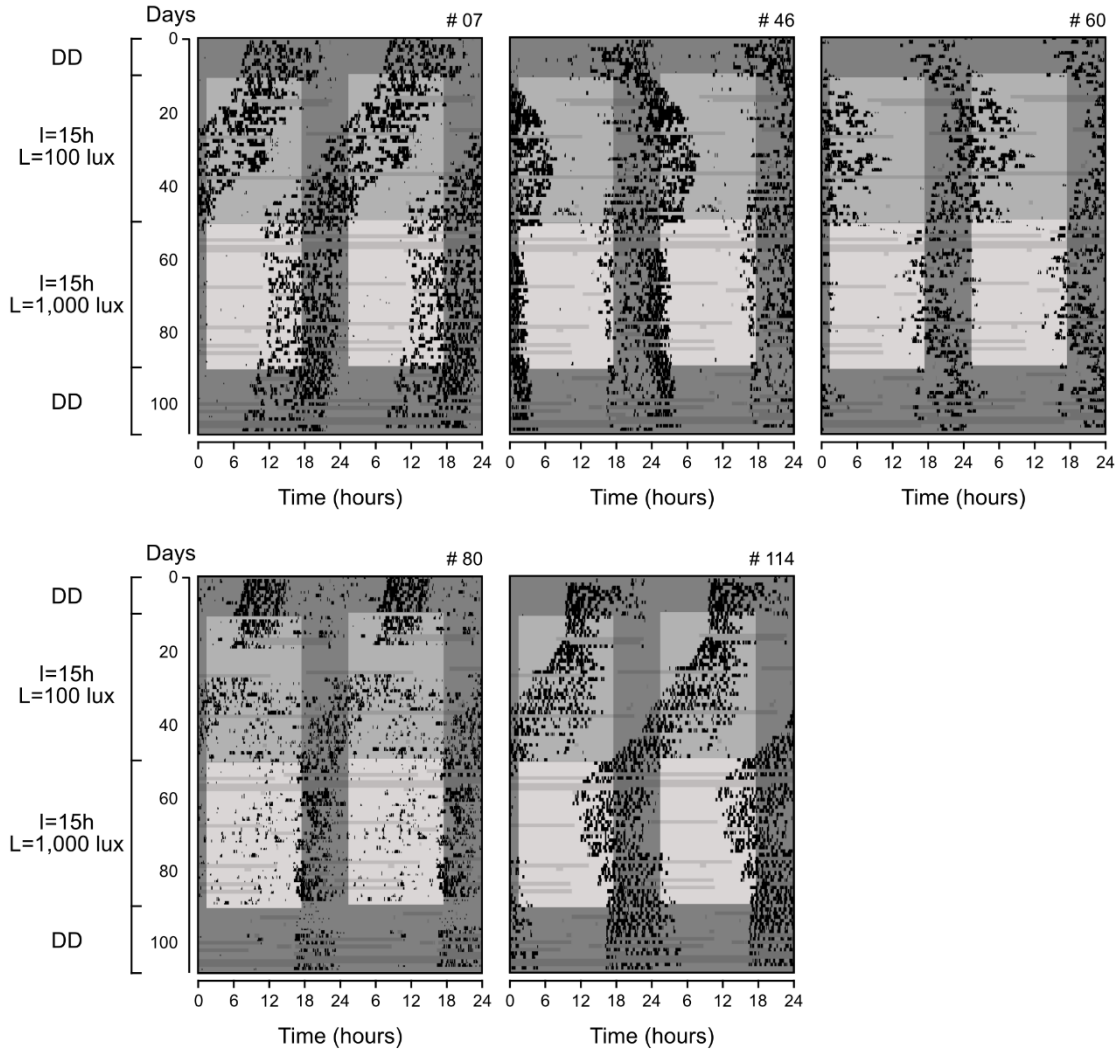

Figure S2.2.6. All actograms from the experiment with pulse regimens of different light intensities (Figure 2.2.5).

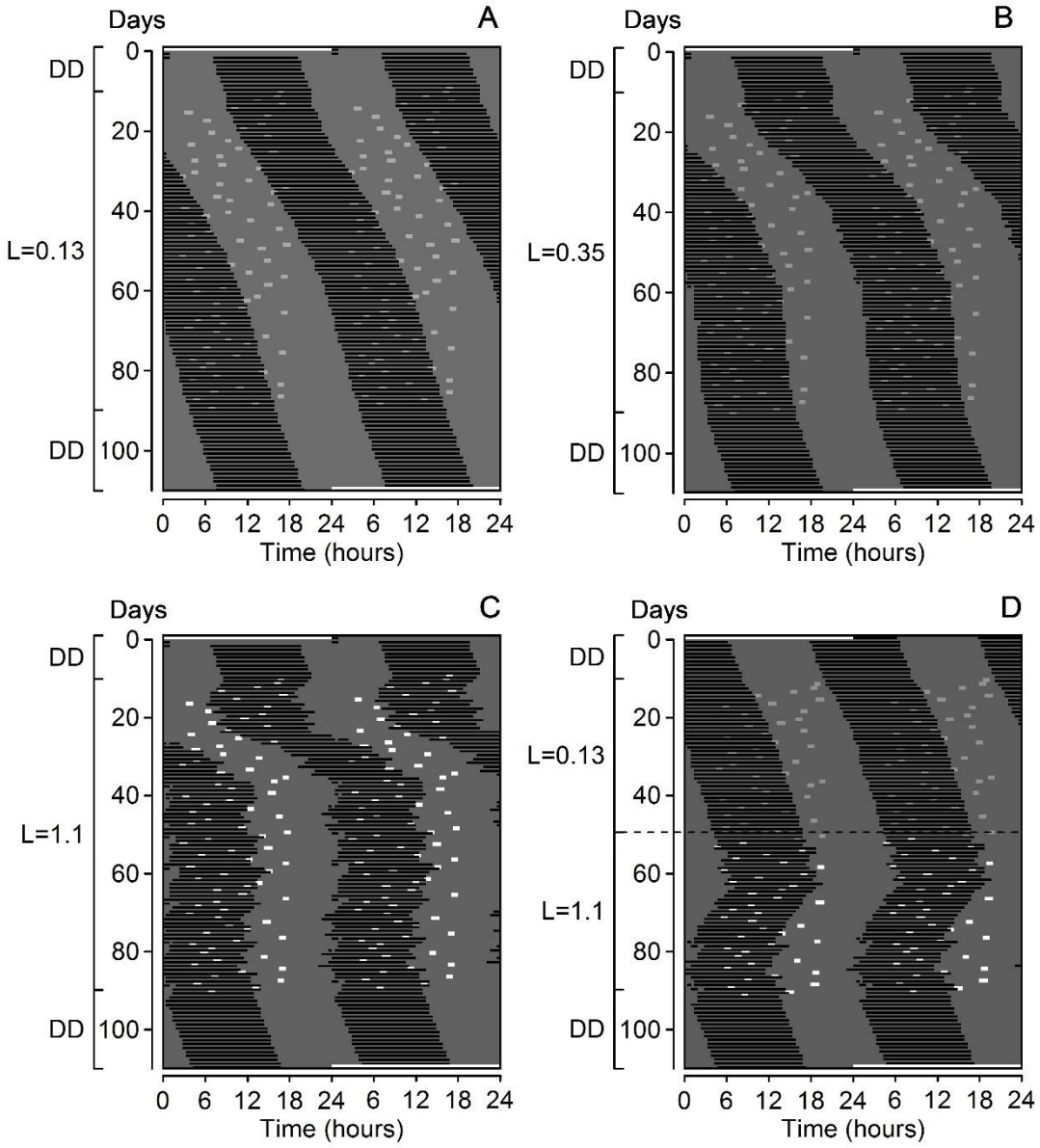

Figure S2.2.7. Computer simulations of a limit-cycle oscillator under the random pulse regimens of 1 light pulse per day and fixed interval I=15h. **A**) Weak light intensity (L=0.13); **B**) Intermediate light intensity (L=0.35); **C**) Strong light intensity (L=1.1); **D**) Combination of 40 days under weak (L=0.13) followed by 40 days under strong (L=1.1) light intensities, as in Figure 2.2.5. Light intensities are defined in arbitrary units. White and Black bars indicate light pulse and activity times, respectively. Oscillator parameters: a=0.85, b=0.3, c=0.8, d=0.5.

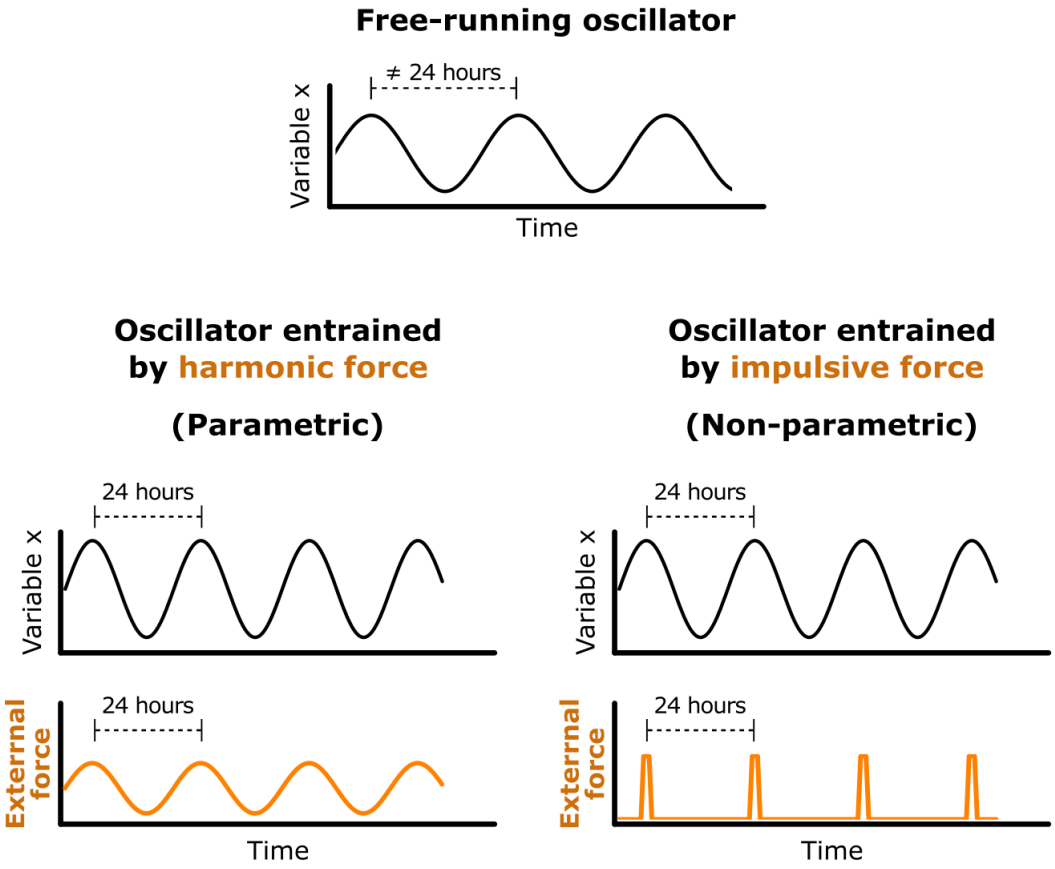

Figure S2.2.8. Two modes of entrainment. A free-running circadian oscillator (**upper figure**) has an inherent period that is different from 24 hours. Conceptually the oscillator period can be entrained to the 24 hours of the environment either by a harmonic, continuous force (**lower left**), or by an impulsive, discrete force (**lower right**). These two models are used to explain the parametric and non-parametric entrainment, respectively.

Chapter 3. Food anticipatory activity in the herbivorous tuco-tuco

Authors: Danilo E. F. L. Flôres, Gisele A. Oda, Veronica S. Valentinuzzi

Abstract

In addition to light, non-photic stimuli can also synchronize the circadian rhythms of mammals. Of special interest has been the role of daily feeding cycles as circadian zeitgebers. When food is restricted to a few hours per day, the resulting feeding cycle induces the expression of a food anticipatory activity (FAA) that has characteristics of a circadian rhythm. Evidences in the literature suggest the existence of a secondary food-entrainable oscillator, which regulates FAA independently of the suprachiasmatic nuclei. Few studies have explored food entrainment in herbivorous species, like the tuco-tuco, which may not face natural food availability cycles in nature. Here, we show that tuco-tucos can develop FAA when exposed to 9 hours of feeding per day, restricted to the light (rest) phase of the light/dark cycle. However, tuco-tucos present great variability among individuals in the expression of FAA, which may reflect the state of their circadian oscillatory system.

Introduction

In the previous chapter, we have focused on the photic entrainment of the circadian oscillator in tuco-tucos, but other non-photic stimuli can also act as daily zeitgebers in mammals. As we mentioned in chapter 1, daily ambient temperature cycles (Refinetti, 2010), food availability cycles (Stephan, 2002) and cycles of social interactions (Davidson and Menaker, 2003) have been shown to synchronize circadian rhythms in different mammalian species.

Of special interest has been the study of synchronization by feeding-fasting schedules. When rats (Boulos et al., 1980) and mice (Abe et al., 1989) in constant conditions are exposed to a daily feeding schedule, with food restricted to a few hours per day, some individuals synchronize their free-running rhythms to the restricted feeding cycle. Different from other non-photic cycles, the synchronization to feeding cycles depends on a novel oscillatory mechanism, independent from the SCN. Rats and mice with SCN lesions normally express no activity rhythm in constant conditions, nevertheless, when exposed to a daily feeding schedule, they develop a daily activity component in anticipation to the daily feeding time (Boulos et al., 1980; Marchant and Mistlberger, 1997; Phillips and Mikulka, 1979; Stephan et al., 1979), which is denominated **food anticipatory activity (FAA)** (Mistlberger, 1994).

Interestingly, when the period of the imposed feeding cycle is far from 24 hours, FAA fails to appear (Bolles and Lorge, 1962; Boulos et al., 1980; Petersen et al., 2014; Stephan, 1981). It is proposed that FAA is regulated by a self-sustaining circadian oscillator or oscillators outside the SCN (Figure 3.1), the **food entrainable oscillator(s) (FEO)** (Mistlberger, 1994; Stephan, 2002).

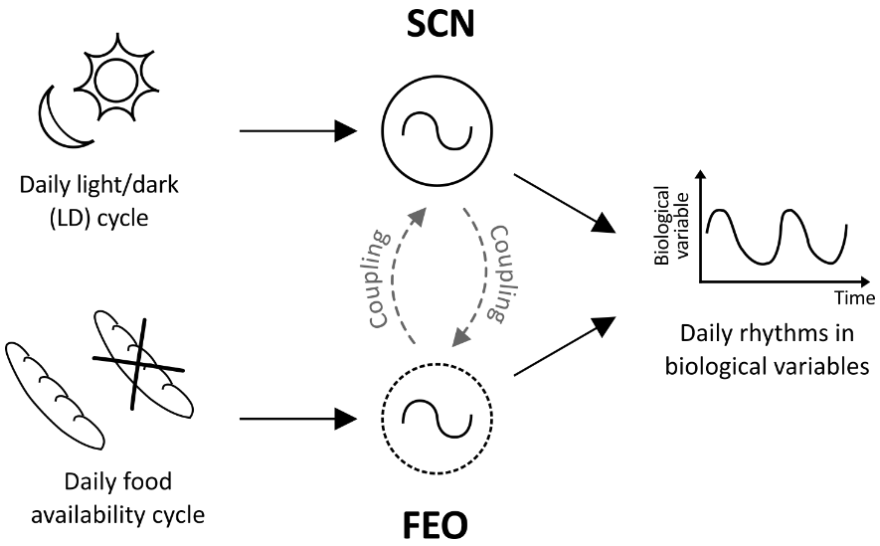

Figure 3.1. Conceptual model of the circadian system with two separate oscillators. The oscillator in the SCN is entrained by light/dark cycles and another oscillator (FEO) is entrained by cycles of food-availability. Evidences indicate that the FEO is coupled to the SCN and that both oscillators promote rhythms in the biological variables of rodents.

Despite the great number of studies on different central and peripheral structures, the anatomical locus of the FEO is still unknown (reviewed in Davidson, 2009; Mistlberger, 2011; Patton and Mistlberger, 2013). Food-restricted rats present a food anticipatory rise in corticosterone alongside the development of FAA, however, adrenalectomy does no abolish FAA. Likewise, lesions in central areas in the hypothalamus, related to feeding, satiety and arousal, fail to eliminate FAA. These areas include the paraventricular nucleus, lateral hypothalamus, ventromedial hypothalamus, arcuate nucleus (ARC) and dorsomedial hypothalamus. Not surprisingly, feeding-related hormones (ghrelin and leptin) that act on these areas are also dispensable for FAA expression, as are dispensable the neuropeptide Y and the receptors of the melanocortin system in the ARC. In addition, evidence has not been found for the participation of neither insulin nor glucagon in FAA. Back to the brain, many extra-hypothalamic areas are nonessential for FAA: neocortex, hypoccampus, amygdala, nucleus accumbens, bed nucleus of the stria terminalis, preoptic area, thalamic paraventricular nucleus, intergeniculate leaflet, nucleus of the solitary tract, area postrema and parabrachial nuclei. Hypophysectomy and lesions in the infralimbic cortex attenuate a food anticipatory temperature rise, but do not eliminate FAA. Finally, pharmacological studies indicate the participation of dopamine-related brain regions in FAA modulation, but D1 and D2 receptor KO mice still express FAA (Gallardo et al., 2014; Michalik et al., 2015). Failure to identify a single structure indicate that the FEO may be a network of widespread oscillators that together mediate food entrainment.

Although the FEO and the SCN are separate oscillators, they do communicate to each other, i.e., they are coupled (Figure 3.1). In intact animals changes in the LD cycle or in the feeding cycle can eventually reach both oscillator systems (Pendergast and Yamazaki, 2014; Stephan, 1986a, 1986b). To study the properties of the FEO as separately as possible from the SCN in intact animals, feeding cycles can be applied under the influence of the LD cycle, so that the SCN remains entrained with a fixed phase. In the case of nocturnal animals, when in LD and with *ad libitum* food, they concentrate both their activity and their feeding in the dark phase. To study FAA/FEO in these animals food availability can be restricted to the middle of the light phase (rest phase). As a result, the FEO-regulated component (FAA) and the SCN-regulated component (dark-phase activity) can be separated from each other (Figure 3.2), enabling experimental assessment and manipulation of the FAA.

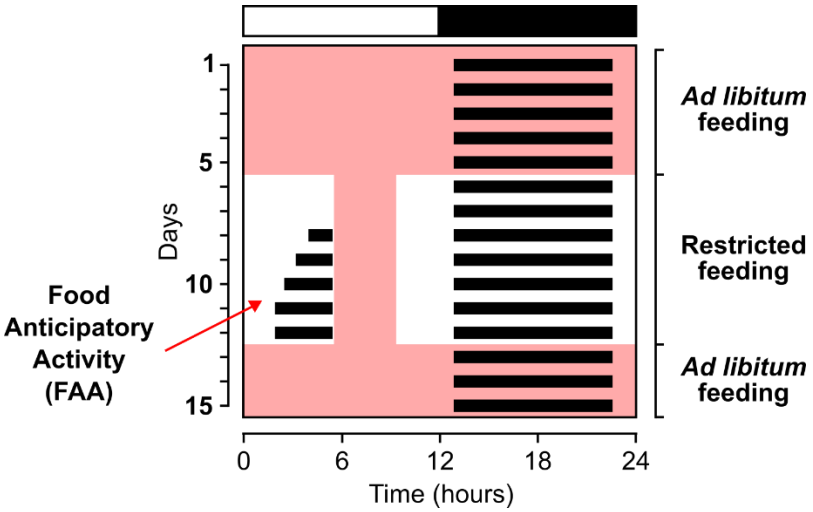

Figure 3.2. Schematic representation of the activity-rest rhythm from a hypothetical nocturnal animal exposed to a daily light/dark cycle and time-restricted feeding. Black marks on each line/day express the activity time for the hypothetical dark-active animal. The pink background indicates the time of food availability. During time-restricted feeding in the light phase, the nocturnal animal expresses a clear FAA, right before the expected feeding time window. The white and black bars on top of the graph indicate the light and dark phases, respectively.

The ecological meaning of FAA is still under debate. Most of the studies on FAA and on the properties of FEO have been performed with model laboratory rodents, mainly with rats. These species are opportunistic feeders and it is proposed that the expression of FAA would be an adjustment to eventual temporary food resources, available at a regular time of the day in nature. That justification is not easily applicable to herbivorous animals, since plants are normally available at all times throughout the 24 hours of the day. Therefore, it is not intuitive whether herbivores express FAA and whether they have a functional FEO (Piccione et al., 2010; Reierth and Stokkan, 1998).

Studies on the feeding habits of *Ctenomys* spp. have reported that tuco-tucos are herbivores and that they feed mostly on the aerial portions of the plants available in their habitats (Comparatore et al., 1995; Rosi et al., 2003). Thus our objectives in the present work were to: i) verify the timing of *ad libitum* feeding in tuco-tucos in the laboratory, ii) test whether this herbivorous species can develop FAA in response to daily time-restricted feeding.

Material and methods

Ethics statement

All procedures described here were approved by the CEUA (*Comissão de Ética no Uso de Animais*) from the Institute of Biosciences, University of São Paulo, Brazil (Protocol 152/2012), and by the CICUAL (*Comité Institucional para el Cuidado y Uso de Animales de Laboratório*) from the *Facultad de Ciencias Veterinarias*, University of La Plata, Argentina (Protocol 29-1-12). Experiments were devised following the guidelines of the American Society of Mammalogists (Sikes and Gannon, 2011).

Animal trapping, maintenance and activity recordings

Twelve tuco-tucos (5 males, 7 females) were trapped as described in chapter 2. Experiments were conducted in the same facility, using the same individual running-wheel cages and recording system as in chapter 2. The number of running-wheel turns was continuously recorded in 5-minute bins to register each animal's daily rest-activity rhythm. Two restricted feeding pilot studies were conducted in light-tight ventilated boxes within the facility.

Fluorescent white bulbs (1000 lux) were timed to provide a 12-hour light (L) and 12-hour dark (D) LD cycle, with lights on at 7:00. Dim red incandescent lights remained turned on continuously to allow handling and maintenance in the dark moments of the LD cycle. Ambient temperature was maintained within a range of 3ºC each day, but the daily average varied from 25ºC in the beginning of the experiment to 22ºC at the end.

In the *ad libitum* regimens, tuco-tucos were offered pieces of carrot and sweet potato, lettuce, sunflower seeds, oat meal and rabbit chow. Food was renewed manually every day at random times. On the days of *ad libitum* feeding quantification, a finer control of the feeding was necessary, thus, animals only received pieces of carrots and sweet potatoes, which were renewed every 12 hours in the light/dark and dark/light transitions. Likewise, on the restricted feeding days only carrots and sweet potatoes were offered.

Feeding schedules

We verified the expression of FAA in 7 animals (2 males and 5 females) exposed to the restricted feeding protocol. Based on two pilot studies with a 3-hour feeding window and a 9-hour feeding window (Supplemental material), we chose to offer 9 hours of food per day during restricted feeding. Animals were initially fed *ad libitum* for 16-26 days.

On the last day of *ad libitum* feeding, food was removed at 19:00. On the subsequent 76-86 days, a restricted feeding protocol was applied, with food available in excess in the 9-hour feeding window, from 10:00 to 19:00. Finally, animals were then given *ad libitum* food for 28 days, starting at 10:00 on the first day (Figure 3.3).

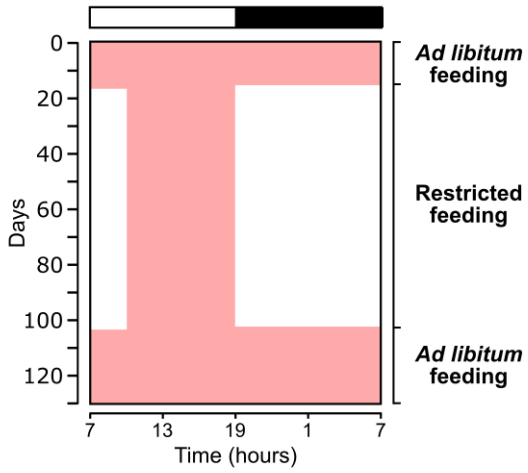

Figure 3.3. Protocol applied to verify the expression of FAA in tuco-tucos. The pink background indicates the time of food availability and the white/black bars on top of the graph indicate the phase of the light/dark cycle. In this example, time-restricted feeding with a daily feeding window of 9 hours (10:00 – 19:00) was applied on days 17 to 103.

Food consumption measurements

Food consumption was measured every 3 hours for 4 days in *ad libitum* feeding. In the first 24 days of restricted feeding, consumption was measured for the whole 9-hour feeding window.

The amount of food consumed in each interval was monitored by calculating the difference in the weight of the food before and after it was offered to the animals. Because fresh vegetables lose weight naturally, due to dehydration, we left control food pieces outside the cages, simultaneously to the offering of food to the animals, to help account for water weight loss. Further control pieces were obtained from food that was untouched inside the cages, without signs of eating.

Body Mass measurements

We followed the body mass of the tuco-tucos for 2 to 3 days during *ad libitum* feeding before restricted feeding and also every 3-7 days during the time-restricted feeding

protocol, to make sure that animals remained healthy along the experiment. In the weighing days, each animal was introduced individually into a weighing bag and placed on top of a scale. From the results of pilot studies (Supplemental material), we established a critical body mass of 80% of the average *ad libitum* value. Whenever an animal approximated this minimal threshold, the feeding window was extended for another 3 hours per day until the animal seemed recovered. Parallel to the eventual body mass loss, other responses to food shortage have been checked, such as reduced activity, reduced food consumption and reduced reaction to touch.

Data analysis

Activity data was plotted in actograms for visual analysis, in the software ElTemps (A. Díez-Noguera, Universitat de Barcelona, 1999, version 1.292). Food consumption measurements that happened in intervals shorter than 24 hours in *ad libitum* feeding were summed for the complete day to calculate the daily food intake. During *ad libitum* feeding, the average food consumption in the light was compared to the average consumption in the dark phase by means of a two-tailed Mann-Whitney test, with significance level 0.05. Proportional values of body mass and food consumption for each animal were calculated by dividing the average restricted feeding value by the average *ad libitum* feeding value.

Results

Food anticipatory activity

The activity-rest rhythms of all individuals throughout the protocol are shown in Figure 3.5. During *ad libitum* feeding conditions, as expected, tuco-tucos concentrated their wheel-running in the dark phase. When food was later restricted to 9 hours per day in the light phase, starting on day 17 (day 20 #99, day 27 #46) animals presented different responses.

Animal #7 developed a novel activity bout around day 30, 1-2 hours prior to the daily offering of food. This FAA was sustained until the last day of restricted feeding. Similarly, animal #46 started expressing FAA around day 55, but it was finished prematurely, before the end of the restricted feeding protocol, together with a reduction in the nocturnal activity. Animal #99 developed FAA around day 30, which disappeared

temporarily from days 60 to 80; FAA was also finished prematurely. The remaining 4 animals expressed no clear sign of FAA during the 86 days in restricted feeding.

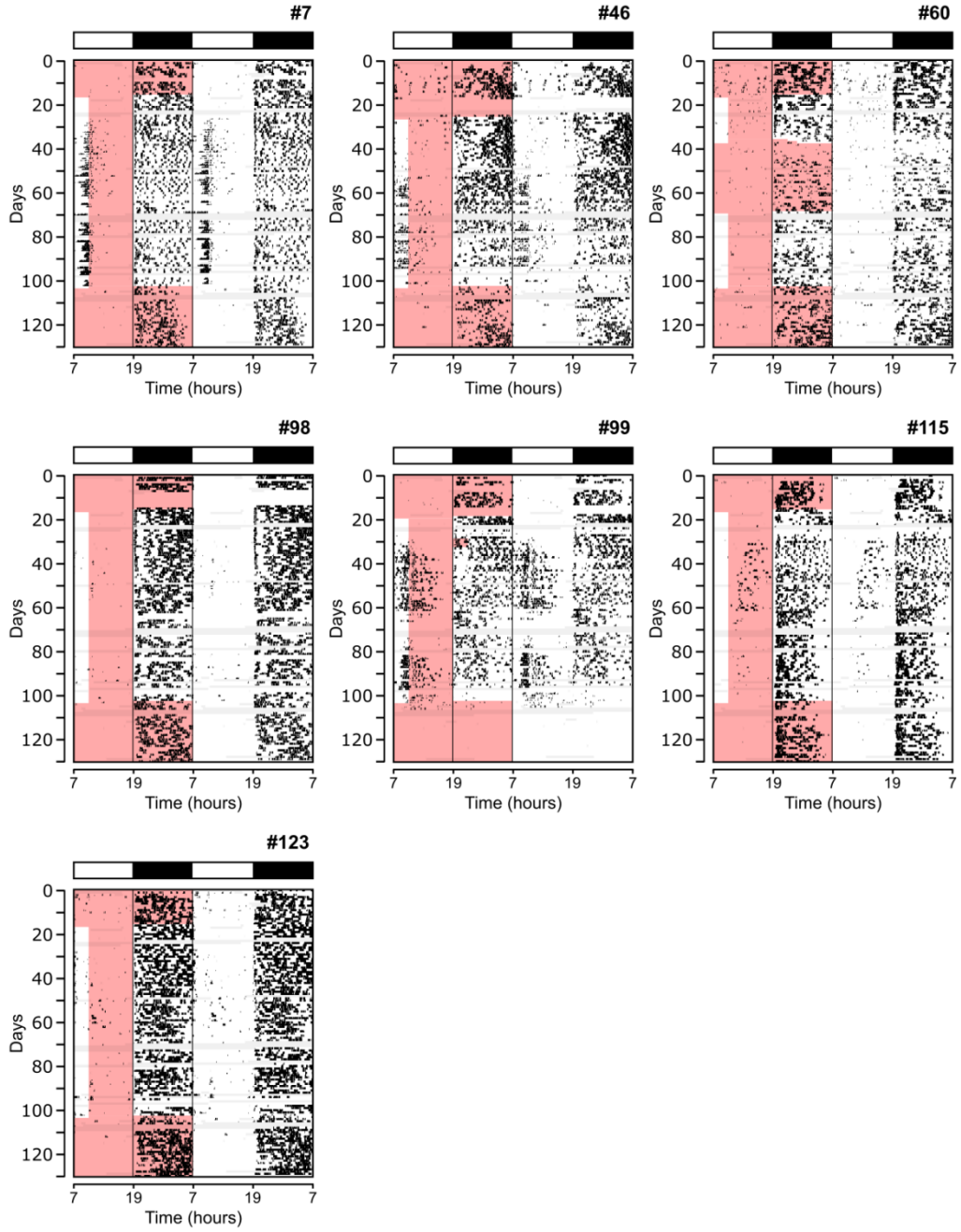

Figure 3.5. Activity records of tuco-tucos exposed to the time-restricted feeding protocol. Data is double-plotted: the graph is duplicated horizontally and, on the right half, displaced 1 day upwards, so that each line represents 48 hours of data. The feeding schedule is represented only on the left half and the pink background indicates the times of food availability. Black/white bars on top of the graphs indicate the light/dark cycle. Black marks on each day/line represent the times of wheel-running activity. Animal lab codes are marked on the upper right of each actogram. As indicated in the text, animal #60 broke its teeth and was left out of the time-restricted feeding protocol for a month.

Food consumption and body mass

To calculate food consumption based on the difference of the food weight before and after offering, we had to account for the expected food weight loss due to dehydration. The predicted weight loss was obtained for carrots and sweet potatoes, initially based on the control pieces of food left outside the cages (Table 3.1, "outside cage"). Unexpectedly, some pieces offered to the animals in the cage had no signs of consumption and those pieces were used as better controls, since the water loss was lower inside the microenvironment of the cages (Table 3.1, "inside cage"). Thus, we decided instead to use the "inside cage" control (untouched food) to account for the expected water weight loss. The final food consumption was calculated as the initial food weight before offering, minus the final food weight after offering, minus the expected proportional weight loss due to food dehydration "inside cage". Whenever this formula returned a negative value, food consumption was considered null.

Table 3.1. Proportional weight loss of the control food pieces due to dehydration. Values are expressed as mean ± standard deviation.

	Weight loss (%)			
	Carrots		Sweet Potatoes	
Elapsed time (h)	Outside cage	Inside cage	Outside cage	Inside cage
3	3.56 ± 1.15	**2.32 ± 0.70**	2.14 ± 1.09	**1.17 ± 0.48**
6	7.42 ± 2.20	**4.76 ± 0.86**	4.32 ± 2.28	**2.46 ± 0.79**
9	10.13 ± 3.71	**6.22 ± 1.92**	6.81 ± 2.72	**3.71 ± 1.03**
12	12.31 ± 3.37	**10.25 ± 2.32**	8.29 ± 3.06	**7.40 ± 1.78**

We then evaluated the preferred feeding phase of the tuco-tucos. On the days of *ad libitum* feeding before restricted feeding, food consumption occurred both during the light and dark phases. Of the 6 animals recorded, 2 ate more during the dark phase and 4 presented no difference in food consumption between the light and the dark phases (Table 3.2). We also verified the relationship between the expression of FAA in restricted feeding and the preferred feeding phase when *ad libitum* food was available. Of the six animals in which we analyzed the preferred feeding phase (Table 3.2), 3 expressed FAA

and 3 did not (Figure 3.5); both the FAA and the no-FAA group presented a 1/3 of dark-phase feeders. There was thus no difference between the two groups.

Table 3.2. *Ad libitum* food consumption during the two phases of the LD cycle. Values are expressed as mean ± standard deviation. Asterisks indicate statistical difference between the light and dark phases.

	Food consumption (g)		
Animal ID	Light phase	Dark phase	p-value
#7	18.05 ± 4.18	12.34 ± 4.02	0.10
#46	27.39 ± 7.12	8.84 ± 3.68	0.03 *
#60	20.90 ± 11.99	10.06 ± 6.63	0.11
#99	17.68 ± 4.20	15.74 ± 5.75	0.47
#115	15.81 ± 2.63	15.17 ± 2.37	0.89
#123	22.43 ± 5.93	5.01 ± 3.57	0.03 *

After the initial *ad libitum* feeding days, animals were offered 9 hours of food per day, restricted to the light phase, and this was enough to sustain food consumption and body mass close to the *ad libitum* feeding levels (Figure 3.4). The restricted feeding schedule was successfully maintained for up to 86 days. One large female (#46) had a body mass greater than usual for females, before the restricted feeding protocol. This animal did not present signs of weakness, anorexia or reduced reactivity during restricted feeding and was, thus, kept in the standard protocol despite the loss in body mass. One animal (#99) had an acute body mass loss at the end of the experiment and died on the first days of *ad libitum* feeding after restricted feeding.

On the days of restricted feeding, animals clearly changed their behavior and showed signs of alertness or annoyance at the time of feeding. Animal #60 broke its teeth after escaping the cage; it was left out of the feeding schedule for a month, until its teeth grew back and it was able to eat solid food again.

We checked if the variability in the expression of FAA had any relationship to the body mass and food consumption. Interestingly, the 3 animals that expressed FAA were the ones with lower body mass and lower food consumption in restricted feeding, proportionally to their *ad libitum* levels (Table 3.3).

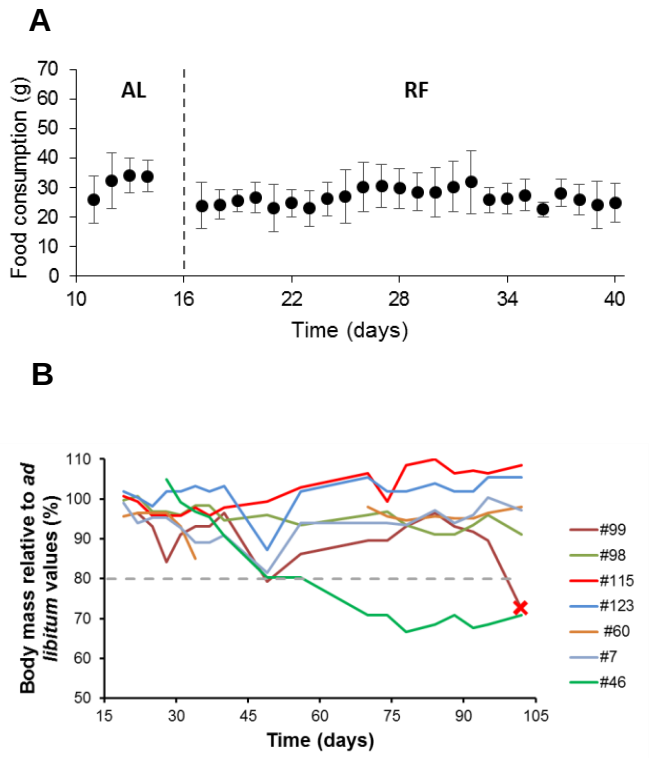

Figure 3.4. Food consumption and body mass variation during *ad libitum* and restricted feeding. **A**: average food consumption of the 7 tuco-tucos exposed to the experimental protocol, during 4 days of *ad libitum* feeding (AL) and in the first 24 days in restricted feeding (RF). Filled circles indicate the mean ± standard deviation for all the animals. A vertical dashed line is drawn on the last day of *ad libitum* feeding. **B**: Individual percentage body mass during restricted feeding, relative to the mass in *ad libitum* feeding. A critical proportional body mass of 80% (dashed gray line) was used to verify animal health.

Table 3.3. Individual food consumption and body mass in restricted feeding, as a percentage relative to the *ad libitum* values**.** FAA-expressing animals are marked in bold. Values are expressed as mean ± standard deviation.

		% relative to *ad libitum* feeding levels	
Animal ID	FAA	Food consumption	Body mass
#7	**Yes**	**75.19**	**93.73**
#46	**Yes**	**57.51**	**80.18**
#60	No	99.59	95.14
#98	No	NA	95.56
#99	**Yes**	**71.16**	**89.94**
#115	No	78.12	101.85
#123	No	104.43	101.62

Discussion

We have shown that herbivorous tuco-tucos can express food anticipatory activity (FAA) in response to time-restricted feeding in the light phase. In one case, FAA was expressed as a clear separate activity component. There was however an important variability, since only 3 of the 7 animals presented FAA. Moreover, these 3 animals were the ones mostly impacted by restricted feeding, in terms of food consumption and body mass.

Variability was also found in the preferred phase of feeding, with 2 animals eating more in the dark phase while others had no preference between light and dark. This result was based on a protocol that involved disturbances every 3 hours; we recognize that this might have affected our feeding phase assessment. A less invasive measurement of feeding time (e.g. video recording) might reveal a greater proportion of rhythmic feeding animals.

A few other herbivorous animals have been studied for their response to time-restricted feeding. When exposed to feeding cycles in the active phase, Svalbard ptarmigans have their feeding rhythms synchronized to food time (Reierth and Stokkan, 1998), but the data does not support the participation of separate food-entrainable and light-entrainable oscillators. Sheep have also been shown to synchronize their rhythms to feeding cycles in constant conditions (Piccione et al., 2010) and again results are not conclusive as to the involvement of an independent food-entrainable oscillator.

Within non-traditional rodents, there are reports in omnivorous species. FAA is observed in the golden spiny mouse exposed to 50% caloric restriction in the active (dark) phase, but again this anticipatory activity is confounded with the regular activity of the animals, which prevents strong conclusions about the existence of a FEO (Gutman et al., 2007). Diurnal Sudanian grass rats have their free-running rhythms synchronized as a single activity component by restricted feeding schedules in DD, but only upon caloric restriction in very short (2-hour) feeding windows (Mendoza et al., 2012). In LD, both normocaloric and hypocaloric time-restricted feeding elicit dark-phase FAA separately from the usual light-phase activity, suggesting the existence of a separate FEO in that species. Likewise, FEO is probably functional in the nocturnal volcano mouse, which expresses a separate FAA when the food is restricted to the light phase of the LD cycle (Luna-Illades et al., 2014).

Within model laboratory rodents, results reported with hamsters may shed light onto possible explanations for our results. Hamsters express FAA after SCN-lesions (Mistlberger, 1992a) and the anticipatory activity can emerge in LD, separately from the regular dark-phase activity (Mistlberger, 1993), supporting the existence of a functional FEO. However, in hamsters, the FEO and SCN appear to be more strongly coupled than in rats, which may explain why some individuals do not express FAA separated from the dark-phase activity (Mistlberger, 1993; Rusak et al., 1988).

Interestingly, hamsters lack the ability to compensate their daily food consumption during restricted feeding, even if they are offered a daily feeding window of 12 hours (Silverman and Zucker, 1976). Therefore, restricted feeding experiments with hamsters require adjustments in the feeding protocol (Mistlberger, 1993; Rusak et al., 1988). On the other hand, rats adjust well to restricted feeding schedules, since they eat quantities close to the amounts consumed in *ad libitum* feeding (Silverman and Zucker, 1976). Our pilot studies reported here suggest that tuco-tucos may be somewhere in between these two cases. Tuco-tucos cannot eat enough food in 3 hours, but, when offered 9 hours of food per day, they can eat almost as much as in *ad libitum* feeding. Nevertheless, even the 9-hour feeding window seemed too short for some animals, which, on average, ate only 60-80% of their *ad libitum* feeding levels and lost 10-20% of their *ad libitum* feeding body mass.

It is proposed that the inability of hamsters to compensate for long intervals of fasting could be explained by their lack of food deprivation in nature (Silverman and Zucker, 1976). Hamsters collect food only at night, still, 40% of their food intake happens during the day in the laboratory (Silverman and Zucker, 1976). Feeding in the rest phase is possible, since food is hoarded in the active phase, thus the animal does not face long hours of food deprivation. This contrasts to rats, which do not hoard food and whose daily feeding rhythm probably imposes a natural feeding-fasting cycle. Tuco-tucos could be similar to hamsters in this respect; as reported here, 2/3 of the animals in the laboratory ate as much in the light phase as in the dark phase. On the other hand, we cannot define tuco-tucos as hoarders, since we never found a nest or food stock in their excavated burrows in the natural habitat. It would be instructive to verify whether tuco-tucos in nature also eat throughout the day.

If we assume that the feeding habits of tuco-tucos are similar to those of hamsters, we could speculate that their FEO has also evolved in a similar fashion. In this sense, the lack of FAA in some tuco-tucos in restricted feeding may be explained by the same reasoning

used for hamsters (Mistlberger, 1993). In these individuals, the FEO and the SCN might be more strongly coupled to each other, preventing the emergence of a separate FAA component. A stronger feeding signal or complete SCN lesions could possibly reveal FAA components in 100% of the individuals. The tuco-tucos that expressed FAA were also the ones that responded more emphatically to restricted feeding, with reduced food consumption and body mass loss. In hamsters (Mistlberger, 1993), similarly, the animals whose rhythms synchronized to the feeding schedule in constant light lost more body mass than the animals whose rhythms were not synchronized. A greater metabolic stress in response to restricted feeding may boost the strength of the synchronizing signal to the FEO, possibly increasing the chances of observing a separate FAA in LD and/or food entrainment in constant lighting.

A boost in the feeding signal has been suggested previously, in rats under metabolic stress. Usually FEO's influence on the SCN is small in rats, such that physiological rhythms are synchronized by feeding cycles, but the SCN remains fairly undisturbed (Stokkan et al., 2001). However, in malnourished individuals (Salazar-Juárez et al., 2003) or in animals exposed to hypocaloric time-restricted feeding (Challet et al., 1996), the phase of the SCN is affected by the timed food, probably because the strength of the food-FEO pathway is increased in the circadian system.

In the volcano mouse (Luna-Illades et al., 2014), lean individuals express stronger FAA than obese ones, but it seems that FAA is delayed rather than suppressed in the obese animals, since fasting after restricted feeding reveals FAA even in the obese group. Possibly, if we could fast tuco-tucos for a couple of days after the restricted feeding protocol, we might uncover a delayed FAA during fasting, in the animals that do not express FAA during restricted feeding. This procedure would be, however, risky, because we cannot guarantee that tuco-tucos would resist long fasting episodes.

In conclusion, the study of FAA and FEO in tuco-tucos is marked by great interindividual variability. We predict however, that strategies to boost the feeding signal can enhance the chances of observing, and thus studying, FAA in this wild herbivorous species. Ecological studies on the feeding habits of these animals could shed light into the meaning of food entrainment and help explain the different patterns we observed here.

Acknowledgements

This research was funded by FAPESP (Processes 2013/50482-1, 2012/15767-2), FONCyT (PICT 2011/1979) and CONICET (PIP-11420090100252). DEFLF received PhD scholarships from CNPq (161438/2011-3) and FAPESP (2011/24120-0). We wish to thank Jose D. Paliza, Patricia Tachinardi and Vinicus Dokkedal for technical assistance, animal care and help with the restricted feeding schedules.

Supplemental Material

Pilot studies

Two pilot studies were performed to help decide the length of the daily feeding window to be used in restricted feeding. In a first pilot, animals (2 males and 2 females) originally with *ad libitum* feeding were transferred to a restricted feeding protocol with 3 hours of food per day, from 12:00 to 15:00 (Figure S3.1A). Food was given in excess, based on their *ad libitum* food consumption. Food ingestion was measured for 1 day in *ad libitum* feeding and in the 6 days of restricted feeding. During restricted feeding, the consumption was much lower than the ingestion observed during *ad libitum* feeding (Figure S3.2A). This was accompanied by acute body mass loss and two animals did not resist the protocol, reaching 60% of their *ad libitum* feeding body mass at the end of the feeding schedule.

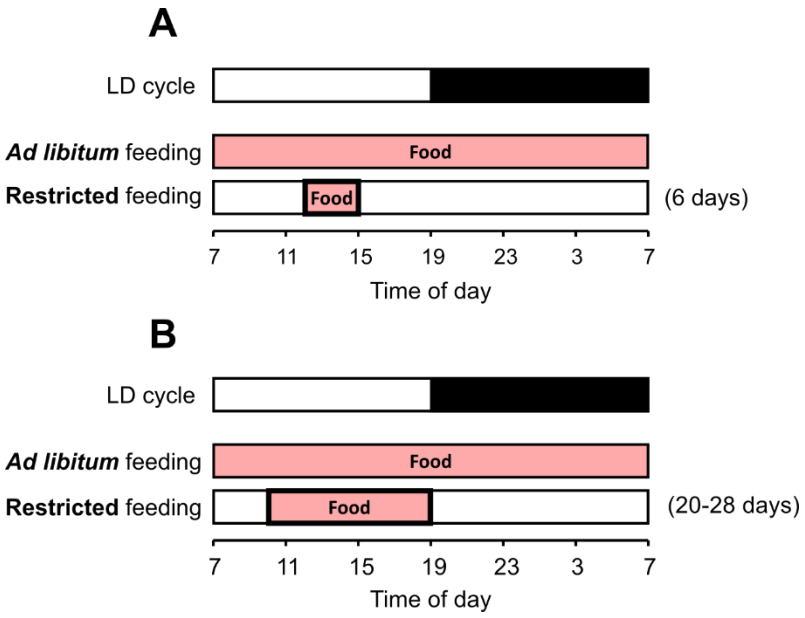

Figure S3.1. Schematic protocols of the pilot studies. **A**: In the first pilot study, animals were kept initially in *ad libitum* feeding, and then in time-restricted feeding with a daily feeding window of 3 hours, from 12:00 to 15:00. **B**: In a second pilot study, animals were transferred from *ad libitum* feeding to time-restricted feeding, with a daily feeding window of 9 hours, from 10:00 to 19:00. In both cases pilots, animals were kept in a light/dark cycle (white-black bars). Food times are painted in pink.

In the second pilot study, we tested a daily feeding window of 9 hours. Tuco-tucos (2 males and 1 female) that had been in *ad libitum* feeding were subjected to a restricted

feeding protocol with food available from 10:00 to 19:00, in excess (Figure S3.1B). Daily food consumption was measured for 5 days during *ad libitum* feeding and for 20 days during restricted feeding. Food consumption in restricted feeding with this longer feeding window was closer to the values registered during *ad libitum* feeding (Figure S3.2B). The body masses did not fall to the levels observed in the first pilot study.

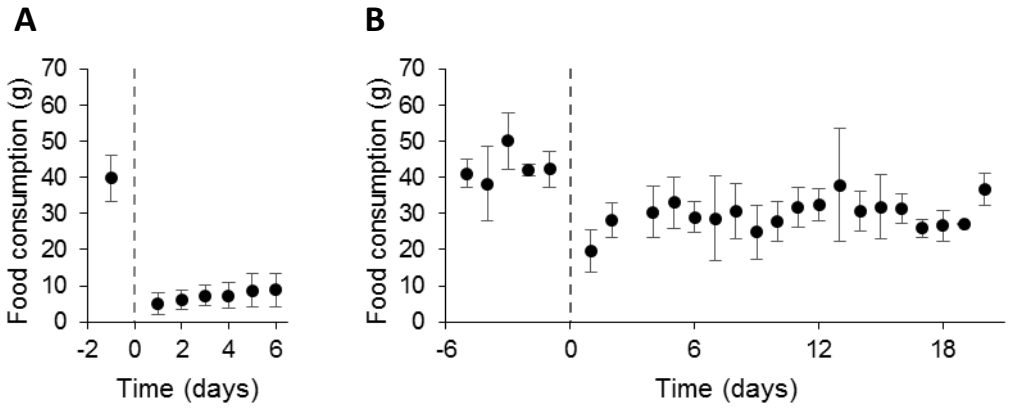

Figure S3.2. Food consumption in the pilot studies. **A**: Consumption during 1 *ad libitum* feeding day (before the dashed line) and on the 6 days of 3-hour time-restricted feeding starting at day 1 (after dashed line). Values **B**: Consumption during 5 days of *ad libitum* feeding (before the dashed line) and during the days of 9-hour restricted feeding starting at day 1 (after dashed line). Values (black dots) express the average food consumption per day ± the standard deviation among the animals.

Chapter 4. Period-independent novel circadian oscillators revealed by timed exercise and palatable meals

4.1. BACKGROUND

In this fourth chapter, I will approach the non-photic synchronization of circadian rhythms in a model species, the laboratory mouse. Synchronization to feeding and rewarding signals was tested in wild-type and mutant mice with genetic disruption of the circadian clock. The work reported here is one of the projects I performed in Dr. Shin Yamazaki's laboratory, from march 2014 to march 2015 at the University of Texas Southwestern Medical Center, within the BEPE-FAPESP program. Dr. Yamazaki has experience on photic and non-photic entrainment in wild-type and mutant mice, with focus on the SCN, FEO and the reward aspects of the circadian system. The paper published in Scientific Reports with this data (Flôres et al., 2016b) is presented here. But before the manuscript, I will introduce some important background concepts.

The generation of circadian rhythms within the cells of many organisms depends on cyclic molecular mechanisms (Dunlap, 1999). In mammals, this molecular machinery operates within the neuronal cells of the SCN, via transcriptional and translational feedback loops (Ko and Takahashi, 2006). The core mechanism involves the transcription factors CLOCK and BMAL1, which bind to the promoters of the genes *Period* (*Per1*, *Per2*, *Per3)* and *Cryptochrome* (*Cry1* and *Cry2*) and induce their expression. The PER and CRY proteins form dimers in the cytoplasm and come back to the nucleus to suppress the activity of CLOCK and BMAL1, thus feeding back into the expression of their own genes (Figure 4.1.1). The molecular feedback loop also connects to output genes (clock controlled genes) and thus transmits the rhythm to the rest of the cell and eventually to other parts of the organism. The genes that play a role in the generation of circadian rhythms are known as **clock genes**.

Clockgene expression is, however, not restricted to the SCN. Self-sustaining oscillations in the expression of clockgenes have been found in different body tissues in vitro (Balsalobre et al., 1998; Yamazaki et al., 2000), revealing peripheral circadian

oscillators in virtually all tissues of the body. Nevertheless, the SCN has the role of a central oscillator, at the top of the hierarchy, coordinating the rhythms of peripheral oscillators and mediating photic entrainment of the circadian system (Dibner et al., 2010; Yoo et al., 2004).

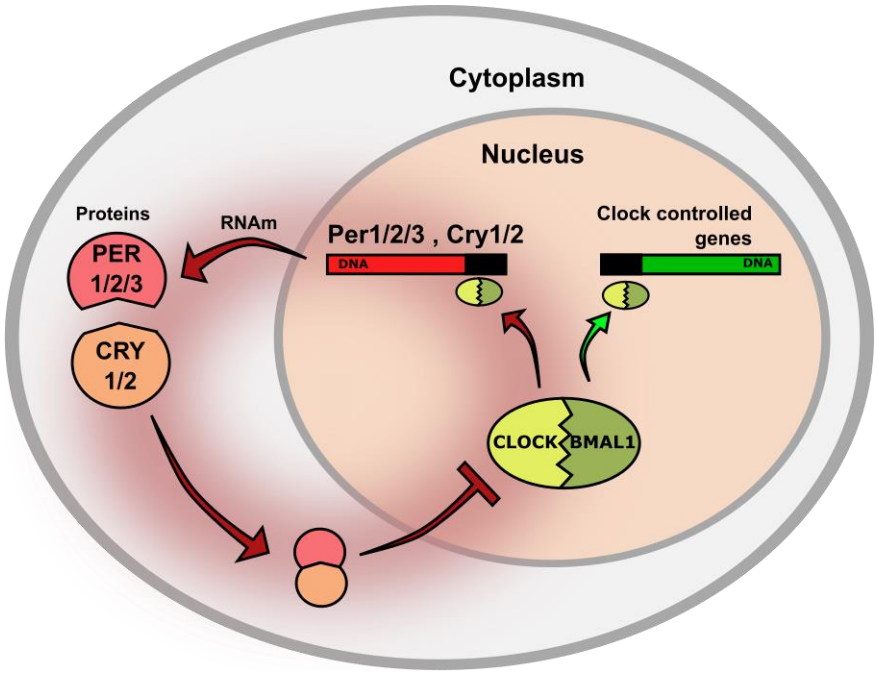

Figure 4.1.1. Simplified representation of the molecular mechanism for circadian rhythm generation within mammalian cells. CLOCK and BMAL1 proteins bind to and induce expression of the genes *Per* and *Cry* genes, whose protein products form dimers in the cytoplasm and come back to the nucleus to suppress CLOCK and BMAL1. The process takes approximately 24 hours to complete. Arrowheads indicate induction and flat ends indicate repression. The molecular feedback loop also connects to output genes (clock controlled genes) and thus transmits the rhythm to the rest of the cell and eventually to other parts of the organism.

In the previous chapter, we introduced the food entrainable oscillator (FEO) as an extra-SCN clock that responds to feeding signals. The wide distribution of clockgene expression in body tissues brought new possibilities for the locus of FEO, and different brain and peripheral structures have been hypothesized as the potential identity of the oscillator (Davidson 2009; Mistlberger 2011; Patton e Mistlberger 2013). Nevertheless, the expression of food anticipatory activity (FAA), the output of FEO, was confirmed in many mutant mice with deficiencies in clockgenes, some of which completely impaired the functionality of the molecular clock mechanism (Iijima et al., 2005; Pitts et al., 2003;

Pendergast et al., 2009; Storch et al., 2009; Pendergast et al., 2012). This indicates that the generation of rhythmicity in the FEO relies on an alternative molecular mechanism.

Another phenomenon that does not depend on the SCN has brought attention to circadian researchers. Rats in LD or DD exposed to low dose **methamphetamine (MA)** in the drinking water express rhythms with two simultaneous periodicities, 1 close to 24 hours and another greater than 24 hours (Honma et al., 1986). After SCN lesions, rats that were originally arrhythmic develop a single long-period rhythm after exposure to a MA solution and this does not dependent on rhythmic drinking input (Honma et al., 1987). Similar results have been observed in mice (Tataroglu et al., 2006). Together, these results suggest the existence of an SCN-independent **methamphetamine-sensitive circadian oscillator** (**MASCO**). Just like FEO, the anatomical locus of MASCO is still under debate, although one paper indicates that the oscillator may be a dopaminergic brain structure (Blum et al., 2014). There is a hypothesis that FEO and MASCO may be the same entity revealed by different input stimuli. One argument in favor of this hypothesis is the maintenance of both oscillators in clockgene mutant mice (e.g. Pendergast et al. 2012).

FEO studies are challenging because FAA immediately disappears when the animal is released to *ad libitum* feeding (Figure 3.2), as we demonstrated in the previous chapter on tuco-tucos. FAA re-appears if the animal is subsequently food-deprived for a few days (Clarke and Coleman, 1986; Coleman et al., 1982). The persistence (or resumption) of FAA during fasting demonstrates the endogenous (self-sustaining) characteristic of the FEO. However, because mice can only be fasted for ~48 h, the free-running rhythm of the FEO cannot be easily observed in this species. The long-sought identification of the FEO would be facilitated if the free-running FAA/FEO could be observed more easily in mice, since mutant mice can be used as tools to help identify the genetic an anatomical bases of FEO.

In the experiments reported below, we devised two non-photic entrainment protocols that reveal novel rhythms in mutant mice that do not express the *Period* genes. The known molecular mechanism for circadian rhythm generation (Figure 4.1.1) is disrupted in the SCN of these mutant mice, as well as in the peripheral tissues. We wished to verify whether persisting anticipatory rhythms could be generated in this mutant mice, in protocols that did not involve fasting. Different from the regular FAA induced by feeding cycles, the rhythms reported here persist for several cycles in constant conditions with no

need to fast the animals. The methodologies we applied in the present study could be used in future research to help finding the anatomical locus of extra-SCN oscillators.

4.2. MANUSCRIPT

Period-independent novel circadian oscillators revealed by timed exercise and palatable meals

Published in Scientific Reports (Flôres et al., 2016b).

Authors: Danilo E. F. L. Flôres[1,2], Crystal N. Bettilyon[1] and Shin Yamazaki[1,*]

Addresses:

1. Department of Neuroscience, University of Texas Southwestern Medical Center, 5323 Harry Hines Blvd., Dallas, TX, 75390-9111 USA

2. Institute of Biosciences, University of São Paulo, Rua do Matao – Travessa 14, 321, São Paulo, SP, Brazil, 05508-900.

*: corresponding author: Shin Yamazaki.

Affiliation: University of Texas Southwestern Medical Center.

FAX: 214-648-1801

E-mail: shin.yamazaki@utsouthwestern.edu

Abstract

The mammalian circadian system is a hierarchical network of oscillators organized to optimally coordinate behavior and physiology with daily environmental cycles. The suprachiasmatic nucleus (SCN) of the hypothalamus is at the top of this hierarchy, synchronizing to the environmental light/dark cycle, and coordinates the phases of peripheral clocks. The *Period* genes are critical components of the molecular timekeeping mechanism of these clocks. Circadian clocks are disabled in *Period1/2/3* triple mutant mice, resulting in arrhythmic behavior in constant conditions. We uncovered rhythmic behavior in this mutant by simply exposing the mice to timed access to a palatable meal or running wheel. The emergent circadian behavior rhythms free-ran for many cycles under constant conditions without cyclic environmental cues. Together, these data demonstrate that the palatable meal-inducible circadian oscillator (PICO) and wheel-inducible circadian oscillator (WICO) are generated by non-canonical circadian clocks. Entrainment of these novel oscillators by palatable snacks and timed exercise could

become novel therapeutics for human conditions caused by disruptions of the circadian clocks.

Introduction

Anticipation of daily changes in the environment is believed to improve the fitness of living organisms (DeCoursey, 2014). This anticipation is conferred by circadian clocks that control ~24-h rhythms of physiology and behavior. The mammalian circadian system has a hierarchical chrono-architecture (Yamazaki et al., 2000; Yoo et al., 2004). At the top of this hierarchy is the master circadian pacemaker, located in the suprachiasmatic nucleus (SCN) of the brain. The SCN entrains to the light/dark cycle, which is often the dominant environmental factor, and orchestrates the ensemble of peripheral clocks. These peripheral clocks then regulate local physiological processes.

The molecular circadian machinery has been extensively studied (Dunlap, 1999). In mammals, a self-sustaining, cell-autonomous circadian rhythm is generated by interconnected molecular feedback loops of gene transcription and translation (Ko and Takahashi, 2006). CLOCK and BMAL1 are positive regulators that activate transcription of *Period (Per), Cryptochrome (Cry)* and other genes. PERIOD and CRYPTOCHROME, in turn, form a complex with other proteins and negatively regulate their own transcription (Tamayo et al., 2015). This molecular circadian feedback loop is universal among all known clocks in the brain and peripheral tissues (Liu et al., 2007).

Although the light/dark cycle is often the dominant environmental signal, food availability is also critical for the survival of organisms (Mistlberger, 1994; Stephan, 2002). Animals anticipate the timing of food availability via the food-entrainable oscillator (FEO). In rodents, locomotor activity increases several hours before food availability (food anticipatory activity, FAA) when a single meal is provided daily at a fixed time (restricted feeding) (Richter, 1922). It is also well demonstrated that restricted feeding entrains clocks in peripheral tissues (Damiola et al., 2000; Hara et al., 2001; Stokkan et al., 2001); however, a recent study suggests that this may be a mechanism independent from the appearance of FAA (Hamaguchi et al., 2015). This food anticipatory activity (the output of the FEO) observed during restricted feeding immediately disappears when the animal is released to *ad libitum* feeding, but re-appears when the animal is subsequently food-deprived. The persistence of FAA during fasting

demonstrates the endogenous (self-sustaining) characteristic of the FEO. However, because mice can only be fasted for ~48 h, the free-running rhythm of the FEO cannot be observed. Notably, food-anticipatory activity appears even when the SCN is lesioned, but the anatomical location of the FEO remains unknown (despite exhaustive searches) (Davidson, 2009). The identification of the FEO would be facilitated if the free-running rhythm of the FEO could be observed.

Rodents anticipate rewarding stimuli, including scheduled access to water, stimulants, and palatable meals (Ángeles-Castellanos et al., 2008; Hsu et al., 2010; Iijima et al., 2002; Keith et al., 2013; Mendoza et al., 2005; Mistlberger, 1992b; Mistlberger and Rusak, 1987; Mohawk et al., 2013). In the current study, we sought to develop an approach to expose the free-running rhythm of the FEO by providing scheduled access to a high-fat/high-sugar palatable meal in the presence of *ad libitum* chow. Instead, using this approach we discovered a novel non-canonical circadian clock, the palatable meal-inducible circadian oscillator (PICO). Similarly, we found that entrainment to timed access to a running wheel was dependent on a non-canonical circadian clock, the wheel-inducible circadian oscillator (WICO). Entrainment of these novel oscillators by palatable snacks and timed exercise could become novel therapeutics for human conditions caused by disruptions of the circadian clocks.

Results

Wild-type mice anticipate palatable meals

We first used a training protocol that combined restricted feeding of both chow and a palatable meal (peanut butter) to establish palatable meal anticipatory activity (PAA) in wild-type mice in the light/dark cycle (see Supplementary Fig. S4.2.1 online; the protocol was slightly modified from Keith et al. (2013)). After training, mice were provided with *ad libitum* chow and given peanut butter (for 1 h) at either ZT4 or ZT10 (Supplementary Fig. S4.2.2). Consistent with Keith et al. (2013), the robustness of PAA was phase-dependent; all mice fed peanut butter at ZT4 (6 of 6) exhibited PAA, but only 4 out of 7 mice displayed PAA when fed at ZT10. We next tested whether PAA persisted in constant conditions by removing the daily palatable meal. After termination of daily palatable meal access, mice in both the ZT4 (5 of 6) and ZT10 (3 of 7) groups had sustained PAA when provided only with *ad libitum* chow (Supplementary Fig. S4.2.2, S4.2.3). These data

suggest that there is an endogenous, self-sustained oscillator entrained by palatable food. There was no correlation between the amount of peanut butter consumed and robustness of anticipatory activity (Supplementary Fig. S4.2.4).

It is possible that the PAA we observed resulted from entrainment of the FEO by the scheduled restricted feeding of chow during the training portion of the protocol. To address this potential caveat, we asked whether mice would entrain to a daily palatable meal without the training step (i.e. with no chow restricted feeding). For this, mice were maintained with *ad libitum* chow and peanut butter was provided for 1 h at ZT4 or ZT10. For ZT4, we found that 4 out of 6 mice expressed PAA starting 1-2 h before peanut butter was placed in the cage (Fig. 4.2.1 and Supplementary Fig. S4.2.5). PAA persisted for 2 days after termination of daily peanut butter feeding (Supplementary Fig. S4.2.6). In contrast, none of the mice (0 of 6) fed peanut butter at ZT10 developed PAA. There was no correlation between the amount of peanut butter consumed and robustness of anticipatory activity (Supplementary Fig. S4.2.7). These data demonstrate that mice developed PAA to scheduled peanut butter during *ad libitum* chow and PAA persisted when the palatable meal was removed. Moreover, training the mice with coincident restricted chow and scheduled peanut butter was not necessary for the development of palatable meal anticipatory activity.

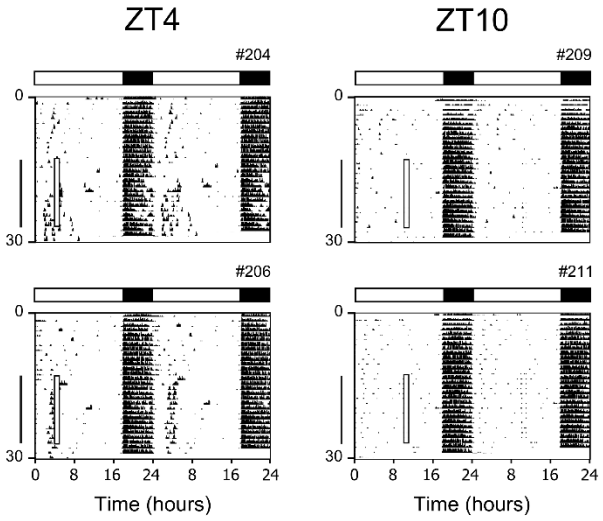

Figure 4.2.1. Wild-type mice display anticipatory activity to a daily palatable meal. Representative double-plotted actograms of wheel-running activity of wild-type male C57BL/6J mice singly housed in 18L:6D (indicated by white and black bars) with *ad libitum* chow for the entire experiment. From days 14 to 27 (indicated by vertical line), peanut butter was placed in the cage for 1 h (indicated by the open square box on the left of each actogram) at either ZT4 (4h after lights-on) or ZT10 (10h after lights-on). Mice were then maintained in *ad libitum* feeding conditions for 3 days (days 28-30; no peanut butter feeding). Individual actograms from all mice are shown in Supplementary Fig. S4.2.5.

The palatable meal-inducible circadian oscillator is a novel non-canonical oscillator

In our initial experiment, we could not rule out the possibility that PAA was driven by the SCN. Thus, we next tested whether timed palatable meal could reveal PICO in arrhythmic *Period* mutant mice, in which the molecular clocks in the SCN and peripheral organs are disabled. In constant conditions (*ad libitum* chow and constant darkness) *Per1/2/3* triple mutant mice did not have circadian rhythms of wheel-running activity, demonstrating that the SCN was disabled in these mice (Fig. 4.2.2, Supplementary Fig. S4.2.8; they displayed ultradian behavior rhythms typical of circadian mutant mice).

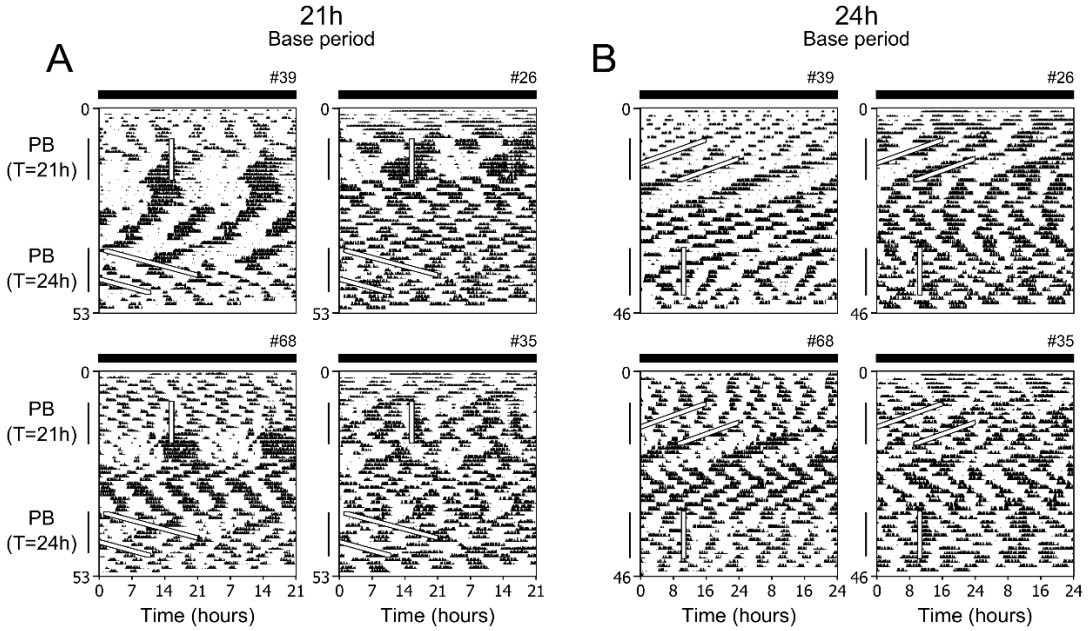

Figure 4.2.2. The PICO in *Per1/2/3* triple mutant mice has a 21-h period that persists in constant conditions. Representative double-plotted actograms of wheel-running activity of *Per1/2/3* triple mutant mice kept in constant darkness (indicated by black bars) with *ad libitum* chow throughout the experiment. Actograms are plotted with either a 21-h period (**A**) or 24-h period (**B**). Mice were fed peanut butter for 1 h each cycle on a 21-h cycle (PB: T=21h) and then released into constant conditions (no peanut butter). Then mice were given peanut butter for 1 h each cycle on a 24-h cycle (PB: T=24h) and then released into constant conditions. All individual actograms are shown in Supplementary Fig. S4.2.8. Male: #39 and 68. Female: #26 and 35.

We gave periodic 1-h peanut butter access to *Per1/2/3* triple mutant mice in constant darkness with *ad libitum* chow (Fig. 4.2.2, Supplementary Fig. S4.2.8). When peanut butter was given at a 21-h interval (T21), half of the mice (4 of 8) showed consolidated

PAA with a 21-h period (Fig. 4.2.2, Supplementary Fig. S4.2.8; mice #39, 26, 68 and 02). Another mouse developed a ~ 17-h period PAA rhythm (Supplementary Fig. S4.2.8; #27). The remaining 3 mice did not develop consolidated activity prior to peanut butter feeding (Fig. 4.2.2 and Supplementary Fig. S4.2.8; #29, 30 and 35); however, the ultradian rhythmicity in these mice was affected by the treatment. There was no correlation between the development of consolidated activity and peanut butter consumption (Supplementary Fig. S4.2.9).

Surprisingly, the palatable meal-induced rhythm continued for up to 7 cycles after the termination of peanut butter feeding. The free-running periods of these rhythms were ~21-h (Supplementary Table S4.2.1). We then fed the mice peanut butter for 1 h each day on a 24-h cycle (T24). None of the *Per1/2/3* triple mutant mice developed PAA to the 24-h palatable meal schedule (Fig. 4.2.2, Supplementary Fig. S4.2.8 and S4.2.9). In addition, the T24 peanut butter feeding did not alter the ultradian activity rhythm. Thus, the PAA rhythm has two fundamental properties of a circadian oscillator: it has a range of entrainment (e.g. entrains to T21 but not T24) and it persists in constant conditions. Together, these data suggest that the PAA rhythm is generated by a circadian oscillator. We named this novel circadian oscillator the palatable meal-inducible circadian oscillator (PICO). Moreover, because PICO persists in the absence of functional PERIOD 1, 2, and 3, it is a non-canonical circadian clock.

The period of the methamphetamine sensitive circadian oscillator is equivalent to PICO

The methamphetamine sensitive circadian oscillator (MASCO or methamphetamine-induced oscillator, MAO) is a non-SCN circadian oscillator. The rhythmic output of MASCO can only be observed when low dose methamphetamine is chronically administered (Honma and Honma, 2009; Honma et al., 1986, 1987; Tataroglu et al., 2006). We measured the MASCO period from the same mutant mice used in the timed palatable meal experiments. After the palatable meal-induced behavior rhythms (PICO outputs) were extinguished (evidenced by the presence of ultradian, but no circadian rhythms), mice were administered low-dose methamphetamine (0.005%) in their drinking water. Consistent with our previous study, all *Per1/2/3* mutant mice exhibited consolidated activity (Pendergast et al., 2012). Mice initially had a ~18-h period of wheel-running activity rhythm that persisted for several days and then switched to a stable 22-h period (Fig. 4.2.3, Supplementary Fig. S4.2.10 and Table S4.2.1).

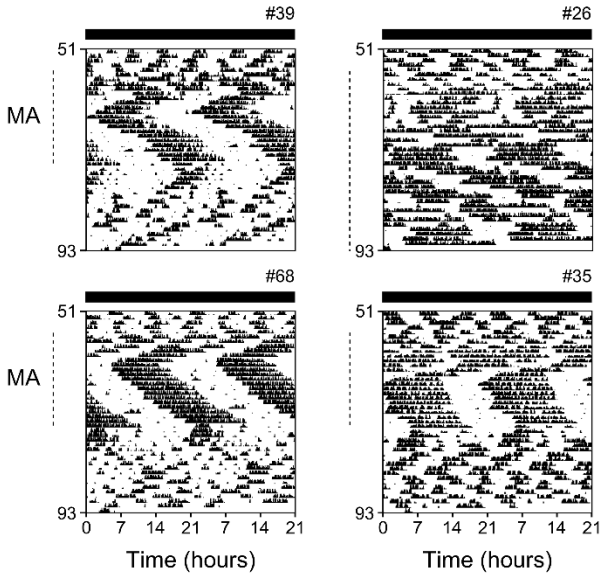

Figure 4.2.3. MASCO driven behavior rhythms in *Per1/2/3* triple mutant mice. Representative double-plotted actograms (the same mice shown in Fig. 4.2.2) of wheel-running activity of *Per1/2/3* triple mutant mice given methamphetamine (MA; indicated by dotted lines to the left of the actograms) in their drinking water (0.005%) in constant darkness. Actograms are plotted with a 21-h period. All individual actograms are shown in Supplementary Fig. S4.2.10.

Timed access to a running wheel reveals the wheel-induced circadian oscillator

Mice develop anticipatory activity to scheduled palatable meals, and low doses of methamphetamine reveal rhythmic behavior. Both of these stimuli are potent rewarding stimuli that activate the dopaminergic system (Ángeles-Castellanos et al., 2008; Blum et al., 2014; Mohawk et al., 2013; Steele and Mistlberger, 2015). Likewise, voluntary running wheel activity elevates dopamine in the rodent brain (Morgan et al., 2015; Novak et al., 2012). Therefore, we tested if timed access to a running wheel would also elicit a circadian rhythm in *Per1/2/3* mutant mice. Six of the *Per1/2/3* triple mutant mice used in the palatable meal experiments were kept in constant darkness and housed with a locked running wheel. The wheel was unlocked for 1 h each cycle on a 21-h interval (T21). When the wheel was unlocked, 5 of the 6 mice ran on the wheels (Fig. 4.2.4, Supplementary Fig. S4.2.11 and S4.2.12). Unlike the PAA during scheduled peanut butter access, mice did not anticipate the recurrent unlocking of the wheel. Instead, general activity, measured by passive infrared sensors, increased shortly after the wheel was unlocked and remained elevated for 1-2 h after the wheel was relocked. The consolidated wheel-induced activity

developed in 3 of the 6 mice (Fig. 4.2.4 and Supplementary Fig. S4.2.11; mice #68, 29 and 30). The 3 mice that exhibited rhythmic behavior had the most wheel-running revolutions during the 1 h of wheel access (Supplementary Fig. S4.2.12).

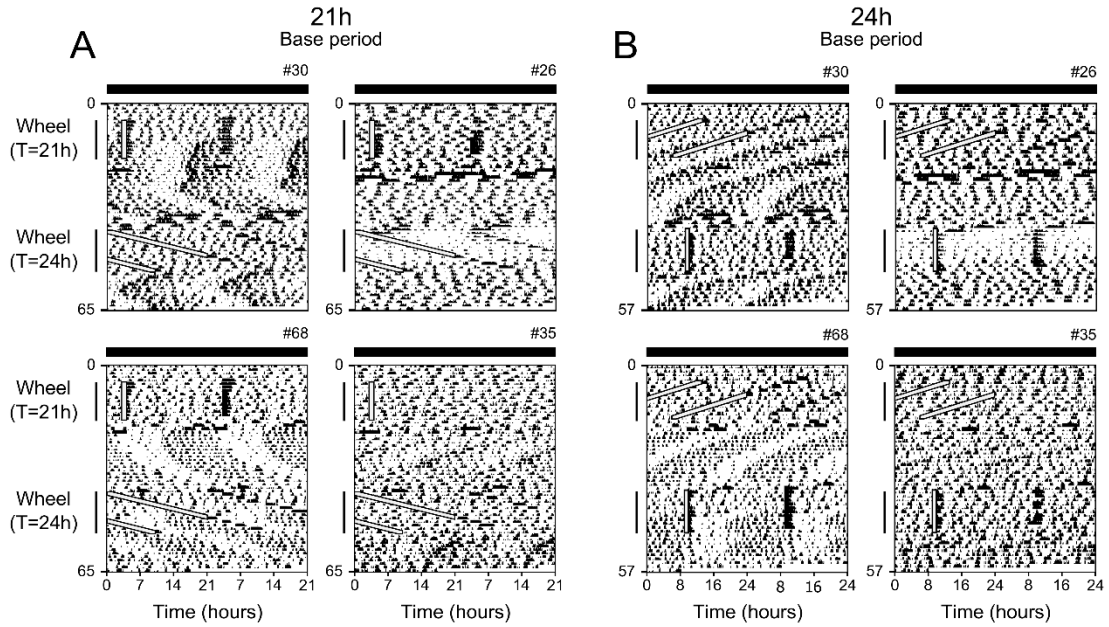

Figure 4.2.4. Timed voluntary wheel activity reveals an endogenous circadian activity rhythm in *Per1/2/3* triple mutant mice. Representative double-plotted actograms of general activity of *Per1/2/3* triple mutant mice recorded by passive infrared motion detectors in constant darkness with *ad libitum* chow and a locked running wheel. Actograms are plotted with either a 21-h period (**A**) or 24-h period (**B**). The wheel was unlocked for 1 h each cycle on a 21-h interval (Wheel: T=21h) and then released into constant conditions (continuously locked wheel). Then the wheel was unlocked for 1 h each cycle on a 24-h cycle (Wheel: T=24h) and then released into constant conditions. All individual actograms of general activity and wheel revolutions are shown in Supplementary Fig. S4.2.11. Male: #30 and 68. Female: #26 and 35.

When the mice were released into constant conditions (the wheel remained locked), the wheel-induced rhythm free-ran for many days with a ~21-h period (Supplementary Table S4.2.1). Interestingly, in one of the cages the wheel-locking mechanism failed during constant conditions and the wheel was unlocked for a day. The consolidated 21-h activity rhythm of the mouse in this cage quickly changed to an ultradian rhythm (Supplementary Fig. S4.2.11; #29).

We then gave the same *Per1/2/3* mutant mice 1 h of wheel access on a 24-h interval (T24). Two (out of 6) mice developed consolidated activity. When the wheel was permanently locked, their rhythms free-ran with periods of 21-h and 23-h, respectively.

Throughout the course of our experiments, only one mouse (#68) exhibited consolidated activity in all three treatments (peanut butter, methamphetamine, running wheel). With the exception of this mouse, the mice that displayed PAA (#39, 26, 27, 02) did not display wheel-induced consolidated rhythms. Similarly, the mice that showed wheel-induced rhythms (#29, 30) did not display PAA.

Discussion

In this study we discovered 2 stimuli, scheduled palatable meals and timed voluntary exercise, that reveal free-running circadian rhythms that do not rely on the canonical molecular timekeeping mechanism. Because scheduled palatable meals and wheel access induced circadian behavior rhythms that persisted in constant conditions, we believe these rhythms are the output of non-canonical circadian oscillators, PICO and WICO, respectively.

It is unclear whether PAA and wheel-induced activity are controlled by a single circadian oscillator (i.e. PICO and WICO are the same oscillator). However, it should be noted that 2 different behavioral outputs were measured – wheel-running activity for PICO and general activity for WICO. This could account for differences in the phases of the induced rhythms.

It is tempting to speculate that either PICO or WICO (or both) are the same circadian oscillator as the FEO and MASCO. Indeed, PICO and WICO share characteristics with the FEO and MASCO. First, all of these oscillators require treatment in order to express their behavioral outputs (unlike the SCN that controls numerous behavior rhythms without requiring a stimulus). Second, all of these oscillators are present in *Per1/2/3* triple mutant mice, demonstrating that they use a non-canonical molecular timekeeping mechanism. Finally, the periods of the output rhythms of all four oscillators are ~21-h in *Per1/2/3* triple mutant mice.

Despite these similarities, PICO and WICO also express characteristics that are distinct from the FEO and MASCO. Unlike the FEO, both PICO and WICO have persistent self-sustained rhythms that continue in the absence of cyclic signals. Unlike MASCO, WICO requires timed wheel access to reveal its rhythm, as evidenced by the finding that *Per1/2/3* mutant mice with *ad libitum* wheel access do not express a ~21-h behavior rhythm. Likewise, PICO differs from MASCO because the output of PICO is observed only when

the rhythmic input is close to the endogenous PICO period. This cyclic external input is not necessary to reveal MASCO (constant infusion of methamphetamine can reveal MASCO (Honma et al., 1987)). We chose a standard procedure to reveal MASCO (methamphetamine was administered in the drinking water). However, it has been shown that mice exhibit anticipatory activity to daily injections of methamphetamine (Mohawk et al., 2013). It will be interesting to see if T21 methamphetamine injection reveals a PICO/WICO like behavior rhythm.

The mysteries of these reward-related oscillators can only be solved by discovering the anatomical loci of these clocks. To this end, we have established 2 new experimental tools for identifying the underlying neural substrates of PICO and WICO (and perhaps the FEO and MASCO). Several studies have shown that it is difficult to produce even weak anticipatory activity to scheduled palatable meals in mice (Hsu et al., 2010; van der Vinne et al., 2015). In contrast, Keith et al reported robust anticipatory activity to a daily offering of peanut butter in mice using a training protocol that combined scheduled chow and palatable meal training (Keith et al., 2013). In the current study we established a new simplified protocol (that does not require training) to establish PAA in mice during *ad libitum* chow access. Moreover, using this method, we can measure the free-running period of PAA in wild-type and circadian mutant mice.

Scheduled access to a wheel also induces robust wheel-induced activity. To perform these experiments, we designed an automated wheel lock-and-release system that is controlled by the computer. Unlike restricted feeding of chow to entrain the FEO or scheduled feeding of palatable meals to entrain PICO, this new automated method requires very little investigator effort to reveal a robust wheel-induced rhythm that free-runs when the wheel is permanently locked.

Beyond the relevance to the basic understanding of the mammalian circadian system and regulation of complex behavior, our findings also have translational impact. In this study we showed that timed exercise and palatable snack (at the proper timing) are potent entraining stimuli. Thus, these highly accessible methods may be used to treat human disorders caused by disruptions of circadian rhythms.

Methods

Animals

Wild-type male C57BL/6J mice were obtained from the E. K. Wakeland Mouse Breeding Core (UT Southwestern, Dallas, TX USA) or from our breeding colony at UT Southwestern. *Per1/2/3* triple mutant mice were generated by intercrossing *Per1*$^{+/-}$/*Per2*$^{-/-}$/*Per3*$^{-/-}$ mice (C57BL/6J N15) for 4 to 6 generations in our breeding colony (Pendergast et al., 2012). All mice were bred and maintained in 12L:12D illuminated by fluorescent bulbs (Ecolux, 32W). Weaned mice were group-housed in cages without running wheels with *ad libitum* chow and water (20-23 ^{o}C and 18-68 % relative humidity). Male wild-type C57BL/6J (7-18 weeks old) and male and female *Per1/2/3* triple mutant mice (10-55 weeks old) were used for experiments. All experiments were conducted in accordance with the guidelines of the National Institutes of Health Guide for the Care and Use of Laboratory Animals. All procedures were approved by the Institutional Animal Care and Use Committee at UT Southwestern Medical Center (Protocol#: 2013-0035).

Activity recordings

Circadian behavior recordings were conducted in light-tight ventilated boxes (22-23 ^{o}C, 19-54 % relative humidity). Light (7 μW/cm^2/s, 55 lux inside the cage) was generated by green LEDs controlled by Chamber Controller (Phenome Technologies, Inc Chicago, IL USA). Mice were singly housed in plastic cages (length × width x height: 29.5 × 11.5 × 12.0 cm) with running wheels (diameter 11 cm). Wheel revolutions were continuously recorded every minute by the ClockLab system (Actimetrics, Wilmette, IL USA). A passive infrared sensor (product ID 189, Adafruit, NYC, NY USA) located 10 cm above the cage lid was used to monitor general activity in the timed wheel access experiment. Cages and water bottles were changed once every 3 weeks. An infrared viewer (FIND-R-SCOPE Infrared Viewer; FJW Optical Systems, Inc. Palatine, IL USA) was used to perform maintenance and feeding in the dark without exposing mice to visible light.

Restricted feeding and timed palatable meal feeding

Restricted feeding of chow was done manually by placing and removing chow (Teklad Global 18% Protein Rodent Diet 2918; Harlan, Madison WI USA) on the bottom of the cage. Peanut butter (Jif® Creamy Peanut Butter, 50% fat, 25% carbs and 22% protein; The J.M. Smucker Company, Orrville, OH USA) was added and removed manually in a

35 mm plastic petri-dish lid on the bottom of cage. The protocols are detailed in Supplementary Fig. S4.2.1 and the time of each treatment is indicated on each actogram.

Methamphetamine

During methamphetamine treatment, a bottle containing regular water was replaced with a bottle containing 0.005% methamphetamine (Sigma-Aldrich, Inc. St. Louis, MO USA). The time when methamphetamine water was available is indicated on each actogram.

Timed access to running wheel

A large push-pull solenoid (product ID 413, Adafruit, NYC, NY USA) was placed on the cage lid and blocked the rotation of the running wheel. The wheel was unlocked or locked via the Pick and Hold Solenoid Driver Module (PH-ET-01, Optimal Engineering Systems, Inc, Van Nuys, CA, USA) controlled by ClockLab. The pickup voltage (24V) was set for 1.2 sec and followed by a hold voltage (3V). The schedule for wheel-unlocking is indicted on each actogram.

Data analysis

Each actogram was generated using 6-min bins and the percentile option in the ClockLab analysis software. Twenty-four hour group average activity profiles were generated from 6-min bin activity files using ClockLab. For each activity profile, either 3 days of *ad libitum* chow, all days during 1-h peanut butter access, or the first 3 days of *ad libitum* chow after peanut butter treatment were averaged for individual mice. Then group average profiles were generated by averaging individual activity profiles. PAA was defined as the total number of wheel revolutions during the 2 h prior to peanut butter access. The individual daily average of anticipatory activity during peanut butter feeding was used for PAA analysis. Mean peanut butter consumption was compared between groups by the Wilcoxon-Mann-Whitney unpaired two-tailed test. Spearman's correlation test was used for correlation analysis. For both statistical tests, alpha level was set to 0.05. The free-running period was calculated by fitting a regression line to the onset of activity detected by ClockLab (default criteria settings). The days used for period analysis (at least 5 cycles) are indicated on each individual actogram in the supplemental figures.

Acknowledgements

This research was supported by a National Science Foundation grant IOS-1419477 to S.Y. D.E.F.L.F was supported by FAPESP process 2013/24740-3. The authors thank Julie S. Pendergast for extensive discussion of the work and Vivek Kumar for comments on the manuscript.

Author contributions

S.Y. conceived the experiments; D.E.F.L.F., C.N.B. and S.Y. designed the experiments; S.Y. designed and made wheel lock-and-release apparatus; D.E.F.L.F., C.N.B. and S.Y. performed the experiments; D.E.F.L.F. and S.Y. analyzed the results; D.E.F.L.F., C.N.B. and S.Y. wrote the manuscript.

Competing financial interests

The authors declare no competing financial interests.

Supplementary information

Table S4.2.1. Periods of emergent rhythms in *Per1/2/3* triple mutant mice under different conditions. NT: Not tested (mouse was removed from the study). UR: Ultradian rhythm (no consolidated circadian rhythm). Days used for period determination are indicated by brackets on the right side of the actograms in Figure S4.2.8, S4.2.10, S4.2.11. *: Bimodal rhythm. **: Stable rhythm induced by methamphetamine.

	Period of consolidated rhythm (h)			
Mouse ID	T21 peanut butter	Methamphetamine	T21 wheel	T24 wheel
#68 (male)	21.16	18.86 | 22.29**	21.71	23.45
#29 (male)	UR	22.69	20.86	UR
#30 (male)	UR	21.19 | 19.55 | 21.34	20.69 | 22.86	20.96
#39 (male)	20.78	18.95 | 22.62**	NT	NT
#26 (female)	19.81	25.27	UR	UR
#27 (female)	17.19	19.24	NT	NT
#02 (female)	21.05*	20.51 | 24.77 | 18.37	UR	UR
#35 (female)	UR	17.61 | 21.88**	UR	UR

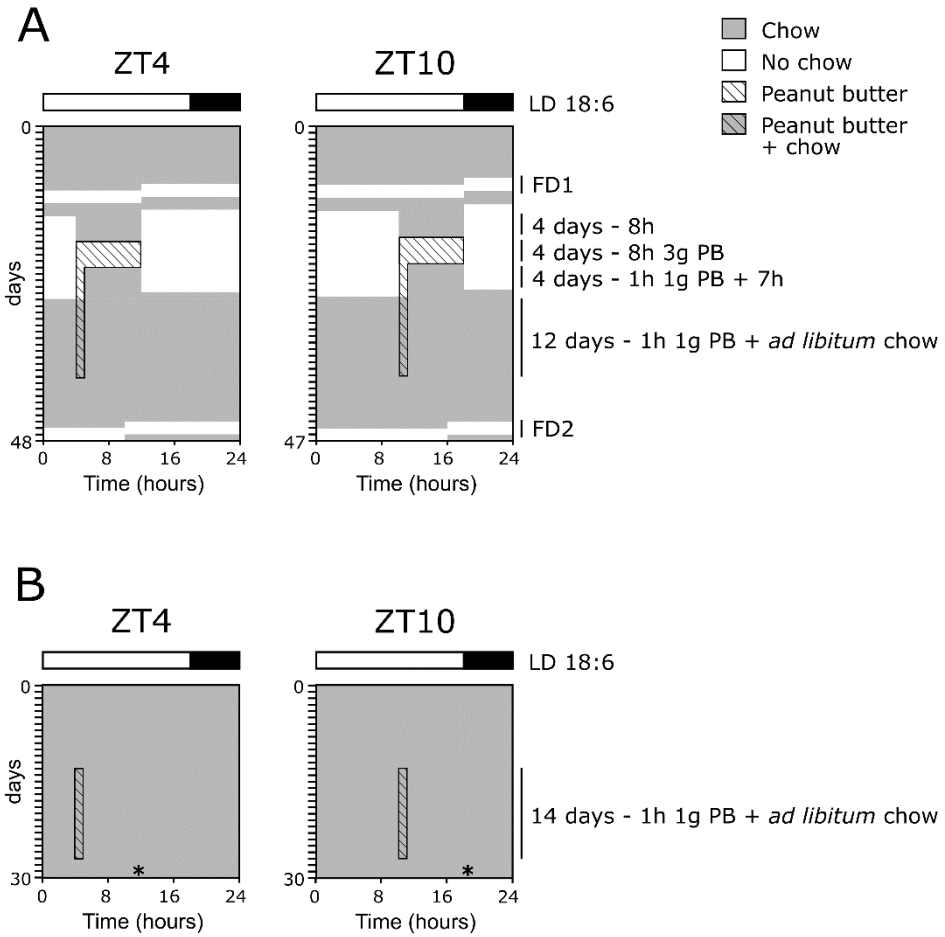

Figure S4.2.1. Protocols for observing palatable meal anticipatory activity. Two protocols with (**A**) or without (**B**) training steps are shown. Gray areas represent the times of regular chow availability. White areas indicate the absence of chow. The time when peanut butter was given is depicted by the areas filled with diagonal lines. The experimental conditions are indicated on the right side of each panel. RF: restricted feeding. PB: peanut butter treatment. FD: food deprivation. The white and black bar on top of each panel indicates the light/dark cycle. *: light and dark cycle was shifted for another experiment.

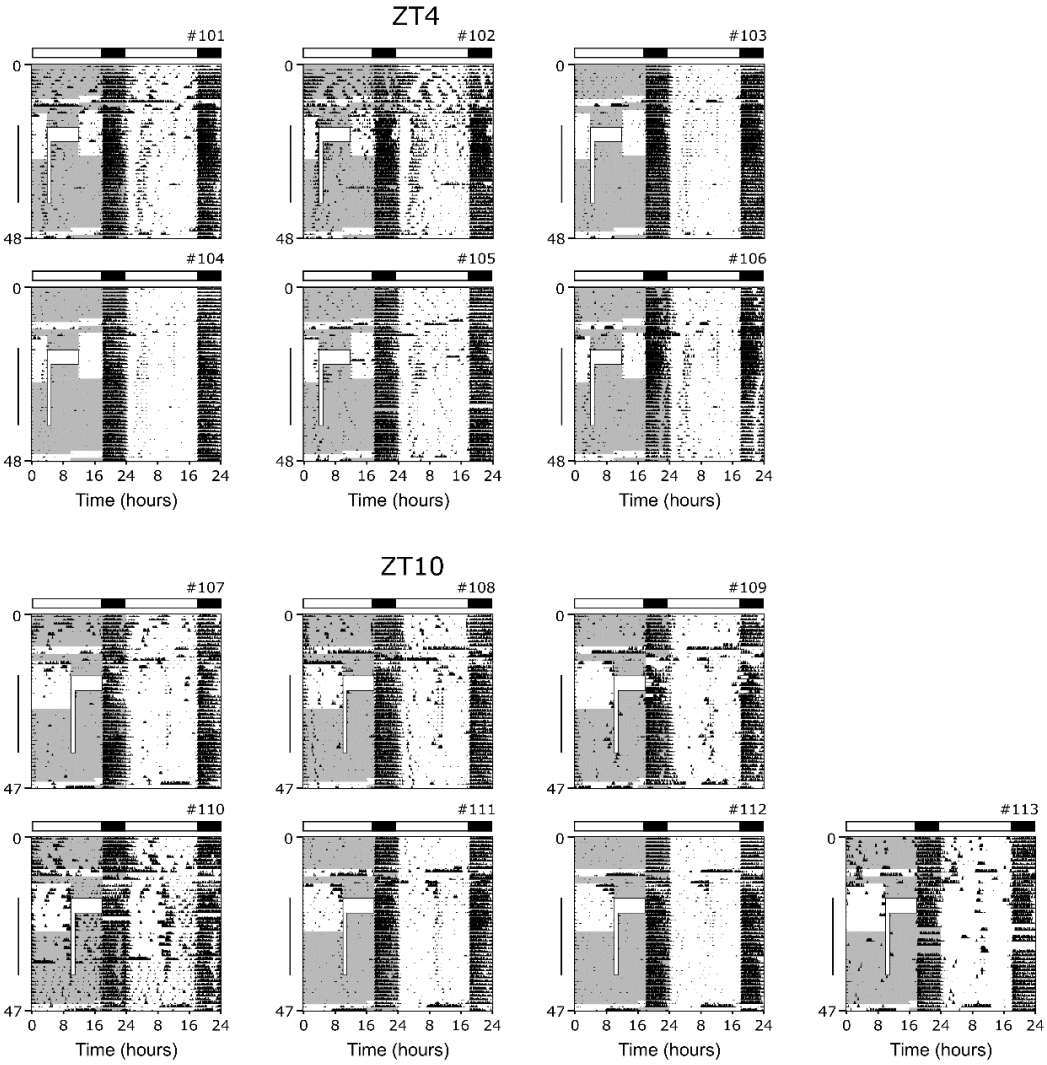

Figure S4.2.2. Wild-type mice display anticipatory activity to a daily palatable meal. Double-plotted actograms of wheel-running activity of wild-type male C57BL/6J mice singly housed in 18L:6D (indicated by white and black bars). Scheduled restricted feeding of chow was paired with scheduled palatable meal access (days 15-27) to develop palatable meal anticipatory activity (training protocol in Figure S4.2.1A). From days 28-39, mice received only daily palatable meals with *ad libitum* chow. On the left panel of each actogram, the time when chow was available is indicated by gray shading and the time when peanut butter was available is indicated by a white box. Peanut butter was given at either ZT4 (top panel) or ZT10 (bottom panel). A vertical line to the left of each actogram shows days of peanut butter presentation.

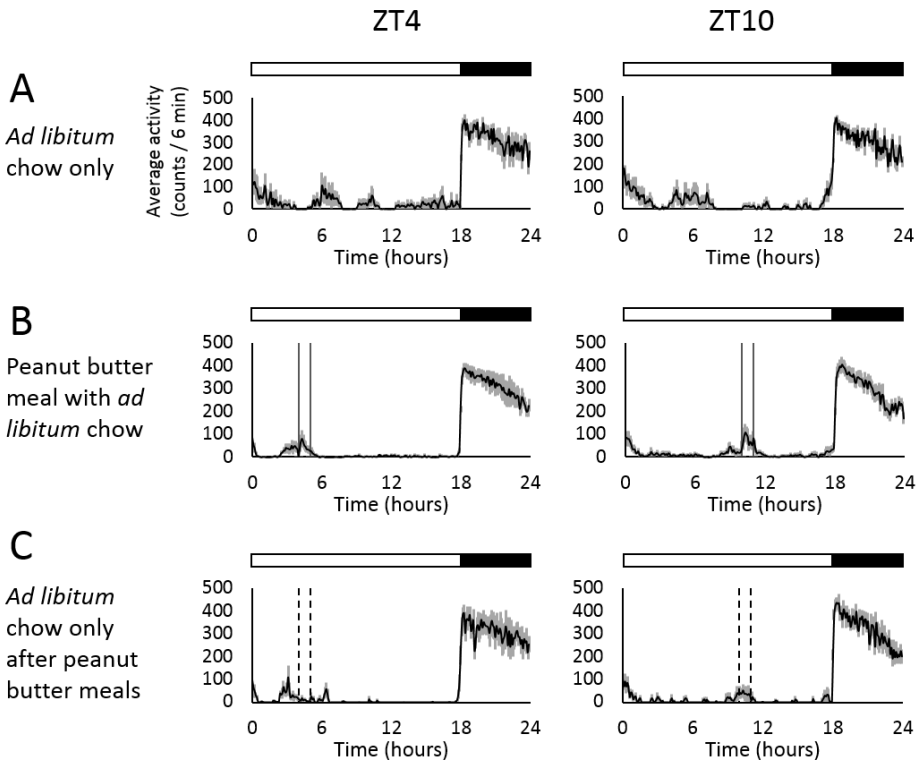

Figure S4.2.3. Group average activity profiles of data presented in Figure S4.2.2. Group average activity profiles (6-min bins) showing; **A**: the last 3 days of *ad libitum* chow, **B**: all days of 1-h peanut butter access (indicated by two vertical lines), and **C**: the first 3 days after termination of peanut butter feeding (previous peanut butter time indicated by dotted lines). Peanut butter was given at ZT4 (left column) or ZT10 (right column). White and black bars above each graph represent the light/dark cycle.

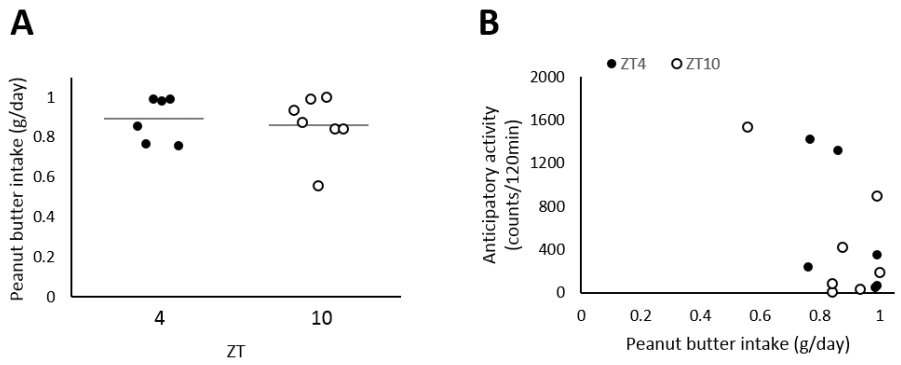

Figure S4.2.4. Peanut butter consumption is not correlated with the robustness of palatable meal anticipatory activity (from the experiment in Figure S4.2.2). Peanut butter consumption was calculated as an average of daily peanut butter intake for the last 12 days of peanut butter access. Anticipatory activity was calculated as the total number of wheel revolutions during the 2 h before peanut butter access (average of the last 12 days of peanut butter access). **A**: There was no difference in peanut butter consumption between mice fed peanut butter at ZT4 vs. ZT10 ($p=0.94$ Mann-Whitney). Horizontal lines indicate the group average. **B**: There was no correlation between robustness of palatable meal anticipatory activity and peanut butter intake ($p=0.31$ Spearman's correlation coefficient).

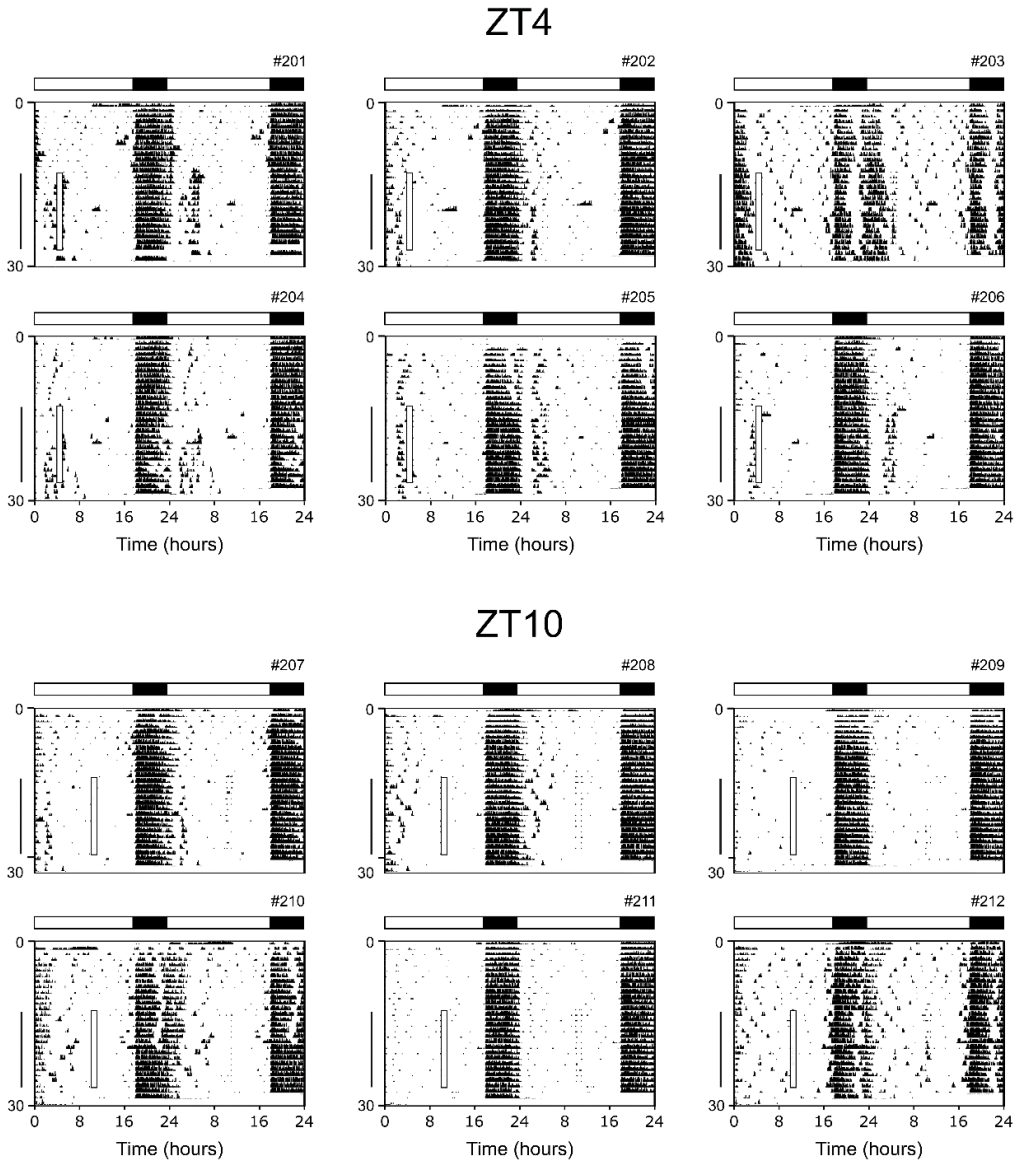

Figure S4.2.5. Palatable food anticipatory activity in naïve wild-type mice without food restriction. Double-plotted actograms of wheel-running activity of wild-type male C57BL/6J mice singly housed in 18L:6D (indicated by white and black bars) with *ad libitum* chow for the entire experiment. From days 14 to 27 (indicated by vertical line), peanut butter was placed in the cage for 1 h (indicated by the open square box on the left side of each actogram) at either ZT4 or ZT10 (protocol shown in Figure S4.2.1B). Mice were then maintained in *ad libitum* feeding conditions for 3 days (days 28-30; no peanut butter).

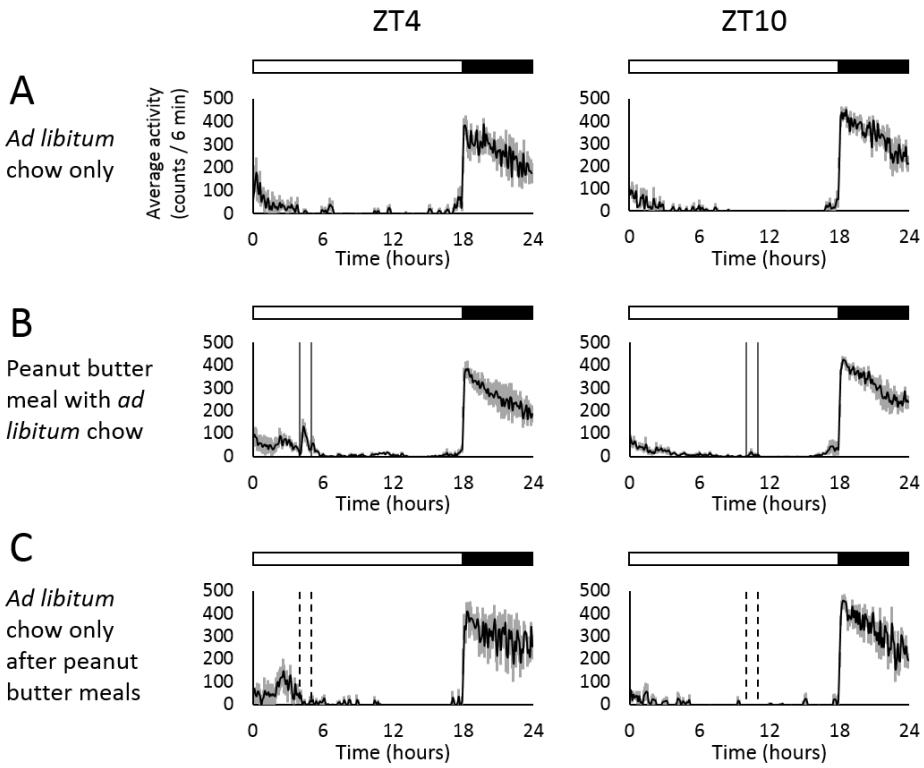

Figure S4.2.6. Group average activity profiles of the experiment presented in Figure 4.2.1 and S4.2.5). For graph specifications, see figure S4.2.3.

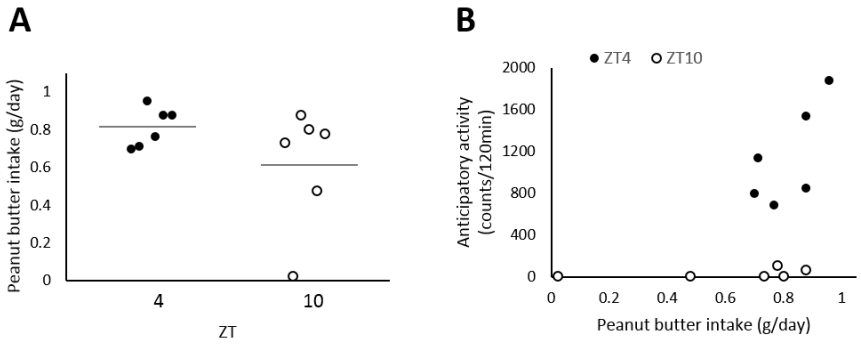

Figure S4.2.7. Peanut butter consumption is not correlated with the robustness of palatable meal anticipatory activity (from the experiment presented in Figure 4.2.1 and Figure S4.2.5). **A**: There is no difference in peanut butter consumption between the ZT4 and ZT10 groups (p=0.38 Mann-Whitney). **B**: There is no correlation between robustness of palatable meal anticipatory activity and peanut butter consumption (p=0.06, Spearman's correlation coefficient). See details in Figure S4.2.4, except that the last 9 days of peanut butter treatment were used to calculate peanut butter consumption, and all 14 days of peanut butter treatment were used to calculate anticipatory activity.

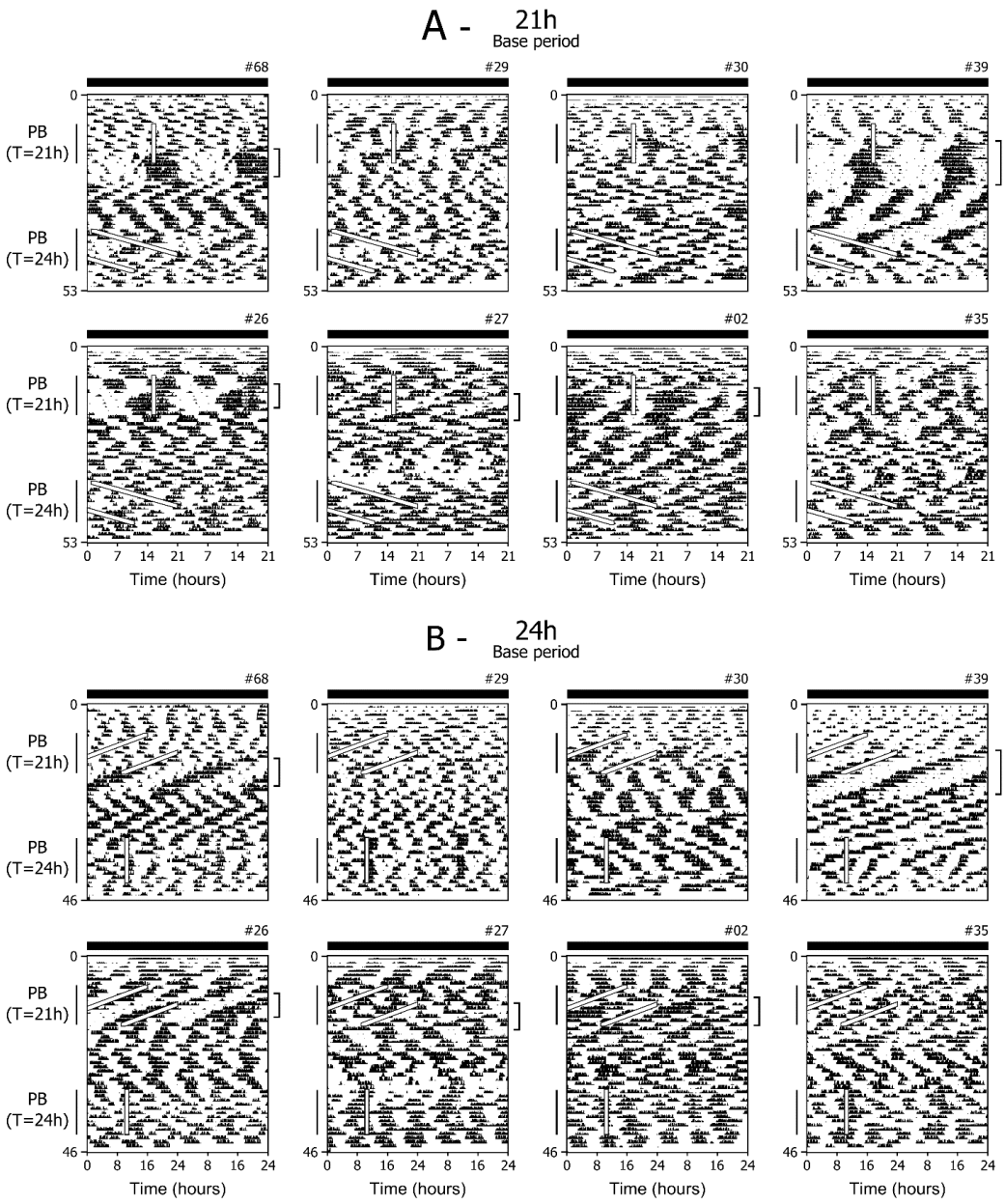
A - 21h
Base period
#68
#29
#30
#39
#26
#27
#02
#35
PB
(T=21h)
PB
(T=24h)
0
53
0 7 14 21 7 14 21
Time (hours)
B - 24h
Base period
46
0 8 16 24 8 16 24

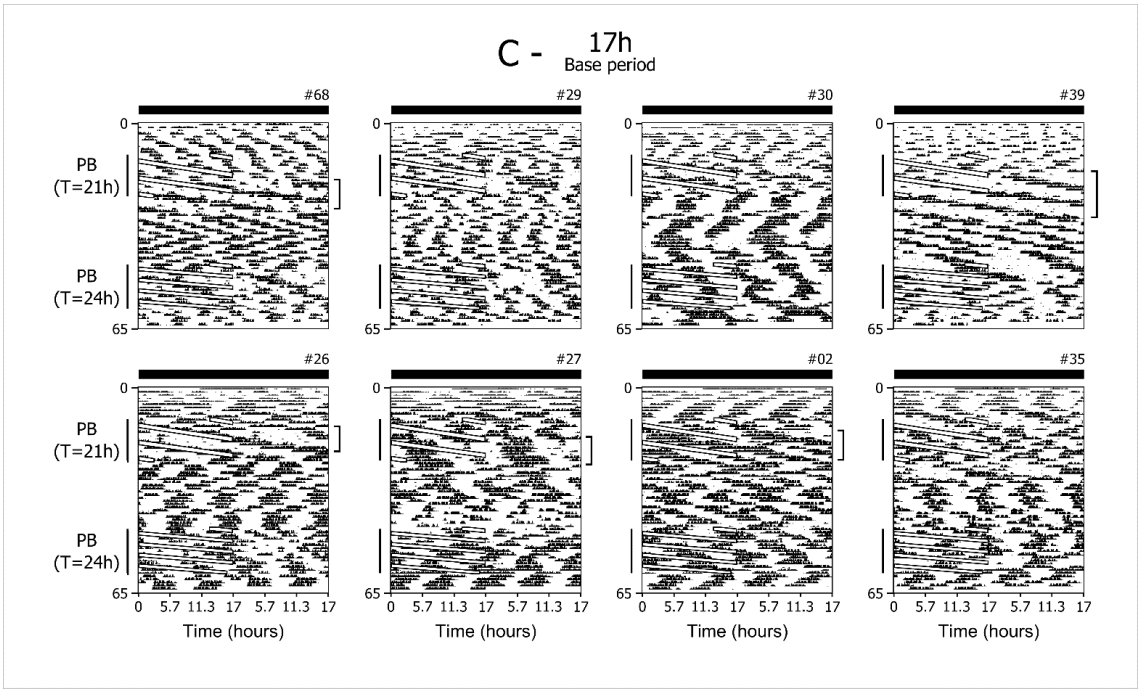

Figure S4.2.8. PICO in *Per1/2/3* triple mutant mice has a 21-h period and persists in constant conditions. Double-plotted actograms of wheel-running activity of *Per1/2/3* triple mutant mice kept in constant darkness with *ad libitum* chow throughout the experiment. Actograms are plotted with either a 21-h period (**A**), 24-h period (**B**), or 17-h period (**C**). Mice were fed peanut butter for 1 h each cycle on a 21-h cycle (T=21h) and then released into constant conditions (no peanut butter). Then mice were given peanut butter for 1 h each cycle on a 24-h cycle (T=24h). Brackets on the right of the graphs indicate the days used for period analysis (Table S4.2.1). Male: #68, 29, 30, 39. Female: #26, 27, 02, 35. Representative actograms were presented in Figure 4.2.2.

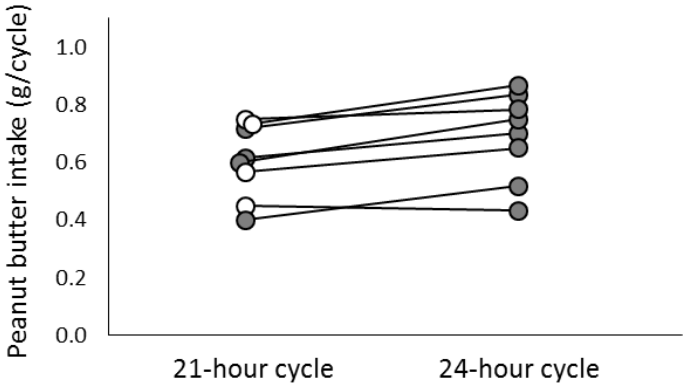

Figure S4.2.9. Peanut butter consumption of triple *Per1/2/3 triple* mutant mice. Average peanut butter consumption was calculated using the last 5 palatable meals in each treatment (21-hour cycle and 24-hour cycle). Each circle represents the average value for a single animal and the black lines connect the data for the same individual in the two treatments. Open circle: mouse developed consolidated activity rhythms. Closed circle: no consolidated activity rhythms developed.

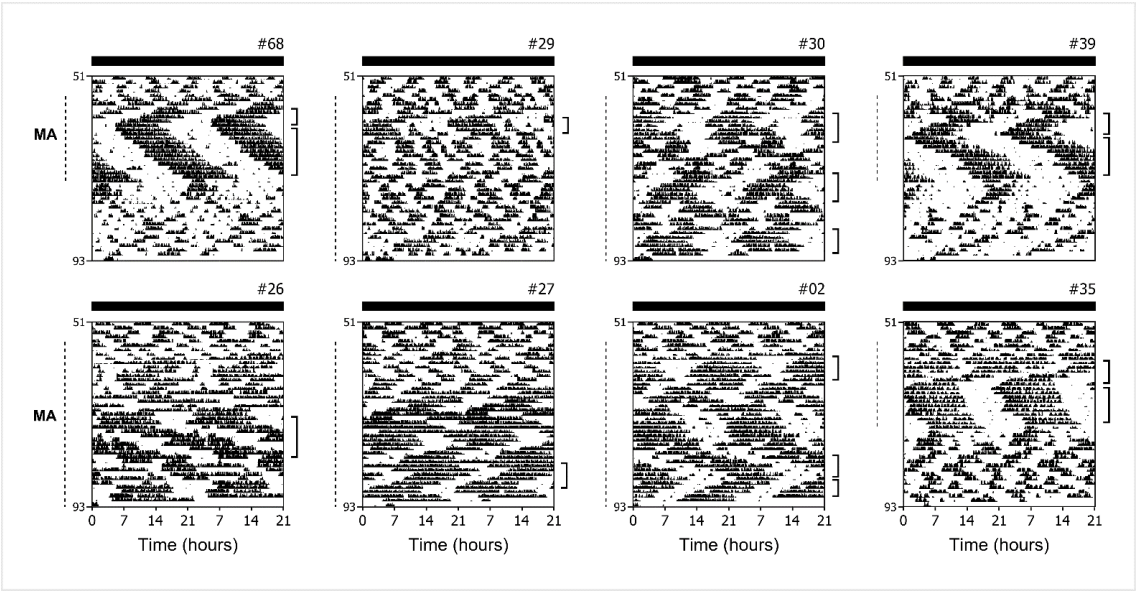

Figure S4.2.10. MASCO rhythm in *Per1/2/3* triple mutant mice. Double-plotted actograms (same mice are shown in Fig. S4.2.8) of the wheel-running activity of *Per1/2/3* mutant mice given methamphetamine (MA) in their drinking water (0.005%) in constant darkness. Actograms are plotted with a 21-h period (T21). Representative actograms were shown in Figure 4.2.3. Brackets on the right of the graphs indicate the days used for period analysis (Table S4.2.1)

.

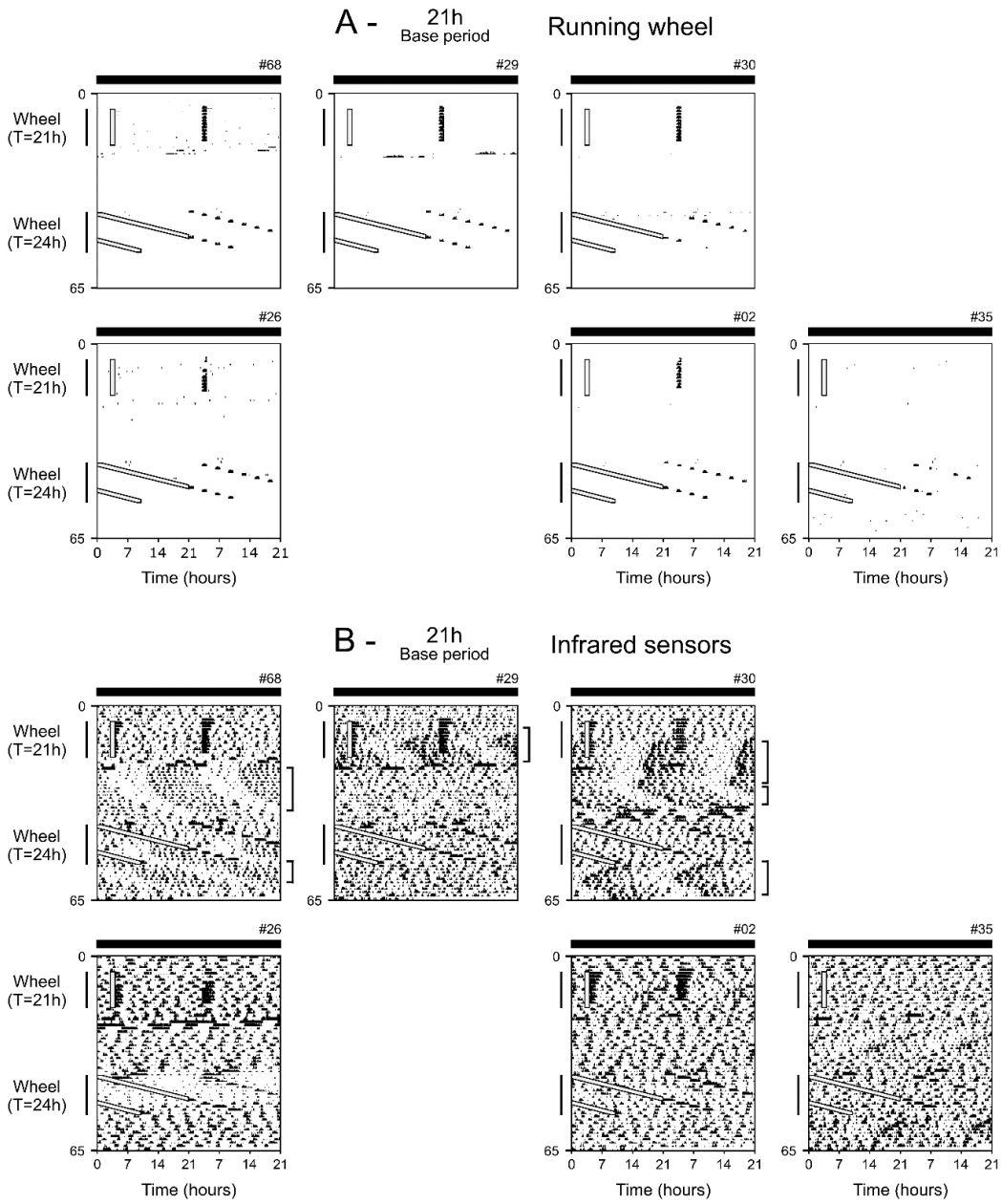
A - 21h Base period
Running wheel
#68
#29
#30
#26
#02
#35
Wheel (T=21h)
Wheel (T=24h)
0
65
0 7 14 21 7 14 21
Time (hours)
B - 21h Base period
Infrared sensors

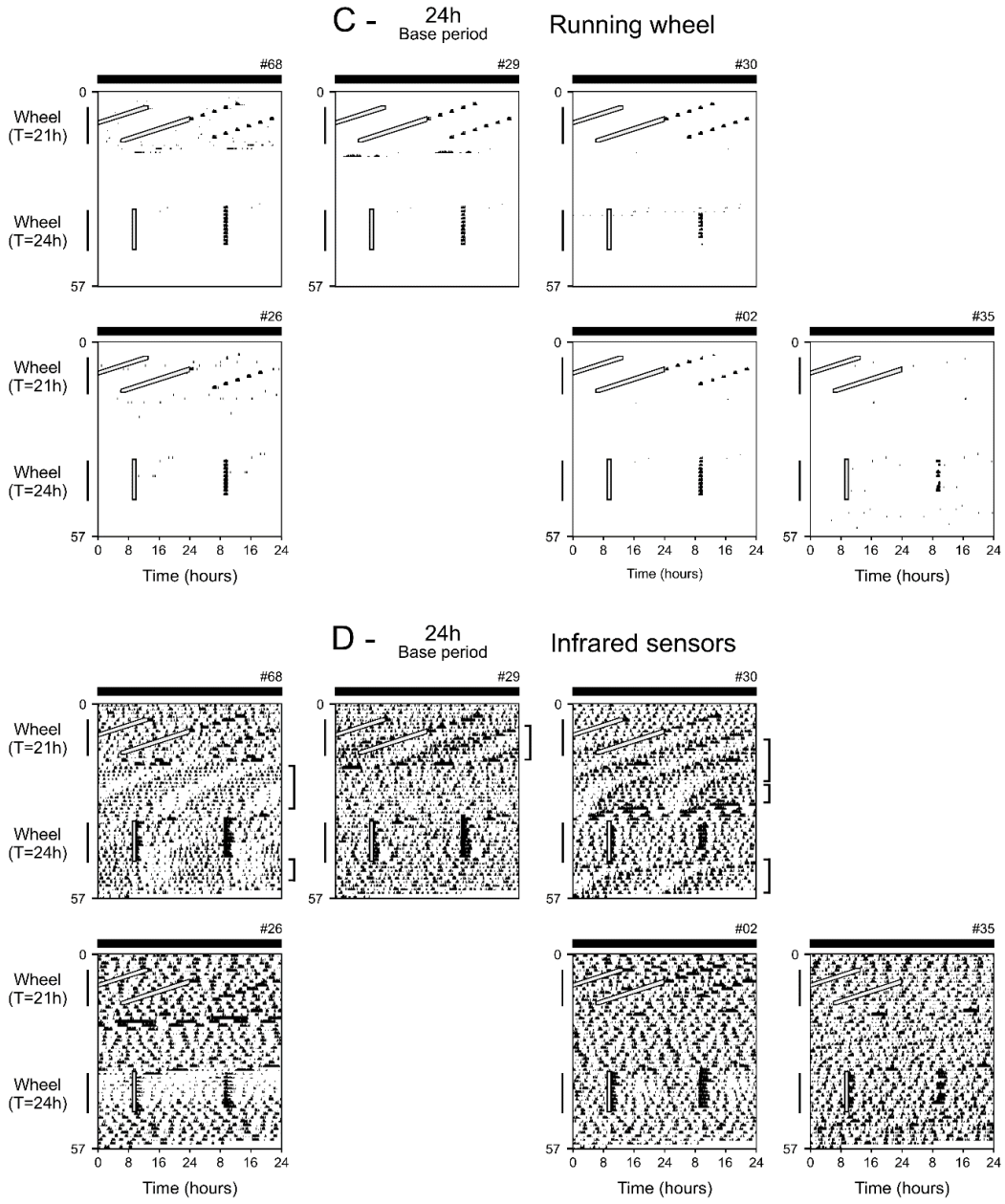

Figure S4.2.11. WICO rhythm is revealed in *Per1/2/3* triple mutant mice by periodic voluntary activity. Double-plotted actograms of wheel-running activity (**A**, **C**) and general activity (**B**, **D**, passive IR sensors) of *Per1/2/3* triple mutant mice in constant darkness with *ad libitum* chow. The wheel was automatically unlocked for 1 h each cycle on a 21-h interval (Wheel: T=21h; indicated by white box on left half of actograms) and then mice were released into constant conditions (continuously locked wheel). Then the wheel was unlocked for 1 h each cycle on a 24-h cycle (Wheel: T=24h) and then released into constant conditions. Actograms are plotted with either a 21-h period (**A**, **B**) or 24-h period (**C**, **D**). Representative actograms were presented in Figure 4.2.4. Brackets on the right of the actograms indicate the days used for period analysis (Table S4.2.1). Mice #39 and #27 did not undergo this study because of a limited number of channels in the wheel locking system and a health-related concern.

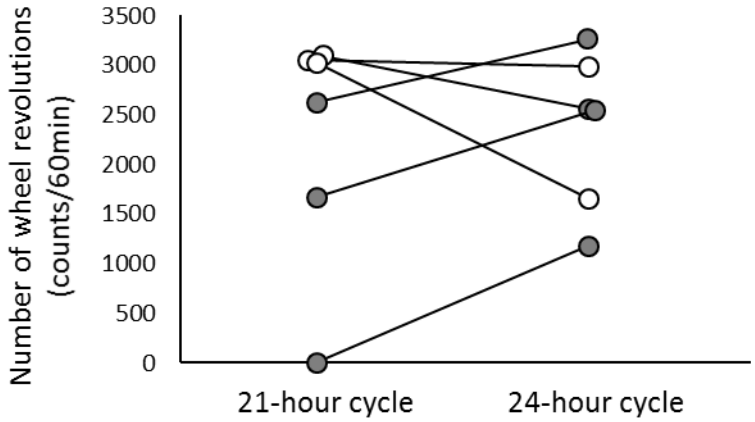

Figure S4.2.12. Wheel-running revolutions during 1 h of unlocked wheel. The number of wheel revolutions during 1 h of wheel unlocking in each mouse was obtained for each of the 11 cycles. Each circle represents the average wheel revolutions during the 11 cycles of wheel access for an individual mouse. Open circle: mouse exhibited activity consolidation (rhythmic). Closed circle: mouse did not show consolidated activity.

Chapter 5. Conclusions and final considerations

Abstract

In this last chapter I will make a summary of our main findings. The results on photic entrainment in tuco-tucos will be discussed in perspective to other natural light exposure studies in the literature. Data on non-photic synchronization in tuco-tucos and in laboratory mice will be reviewed in light of the metabolic and reward aspects of food entrainment.

Photic synchronization: the robustness of entrainment

The importance of being in phase with the environment has been increasingly recognized, since relationships have been found between circadian rhythm disruption and health problems such as metabolic diseases (Bass and Takahashi, 2010) and cancer (Fu and Lee, 2003). Field and laboratory studies also stress the adaptive advantage of having circadian rhythms synchronized to the environmental day and night (DeCoursey, 2014; Ouyang et al., 1998; Spoelstra et al., 2016), even though in some specific cases, the lack of a precise rhythm might be adaptive (Bloch et al., 2013). In this thesis, we have shown that the rhythms of the subterranean tuco-tucos are also timed to their environment, even tough they spend most of the day isolated in dark tunnels.

In chapter 1, we checked the natural light exposure pattern of tuco-tucos and the potential of this light/dark regimen as a zeitgeber. The current field data confirms our previous records based on visual observations of behavior (Tomotani et al., 2012). Frequent exposures to the surface are also in line with anatomical studies in congenerous tuco-tuco species. While the eyes of some subterranean rodents are reduced or even internalized (Nemec et al., 2007), tuco-tucos have externalized eyes of regular size and normally developed retinas (Schleich et al., 2010), which suggests a role for the visual system in their natural habitat.

As expected from their subterranean nature, tuco-tucos are not exposed to the complete LD cycle (Figure 5.1A). Previous works in the literature have reported incomplete light exposure, especially in den-dwelling nocturnal animals. Bats (DeCoursey and DeCoursey, 1964; Twente, 1955; Voute et al., 1974) and scorpions (Fleissner and Fleissner, 1998), for instance, sleep in dark dens during the day and only expose to light at the end of the day, upon the start of their nocturnal activity (Figure 5.1B). This particular light/dark regimen is equivalent to laboratory experiments with nocturnal rodents that have long demonstrated that circadian rhythms can be synchronized to short daily light pulses, which occur once a day at a regular time (DeCoursey, 1972; Pittendrigh and Daan, 1976a, 1976b).

Interestingly, a laboratory study with the flying-squirrel *Glaucomys volans* revealed an even more extreme light exposure pattern, when they are kept in a semi-natural cage with a light-tight darkened next boxes. This nocturnal species also sees the light mainly at lights-off time (Figure 5.1C top), but the days of light exposure are intervened with several days without any light information (Figure 5.1C bottom) (DeCoursey, 1986; Menon et al., 1988). The sporadic light exposure of the flying squirrel is nonetheless enough to keep its rhythm in synchrony with the environmental light/dark cycle.

Tuco-tucos, on the other hand, do expose to light every day in short episodes (Figure 5.1D top), but the times of exposure vary from day to day, which makes their light/dark regimen less regular than those of bats and scorpions. In terms of timing within the 24 hours, the temporal pattern of light exposure of tuco-tucos is even less regular than that of the flying squirrel. Therefore, we questioned whether the natural light exposure pattern could synchronize the circadian rhythms of tuco-tucos.

We then applied a model of this light exposure regimen to tuco-tucos in the laboratory. The model had already been shown to synchronize the rhythms of a mathematical oscillator in computer simulations (Flôres, 2011; Flôres et al., 2013). Our experimental data confirmed the predictions from the simulations: light pulses applied once a day at varying random times (Figure 5.1D bottom) can still act as a zeitgeber. To our knowledge, this is the first time that entrainment is verified in this extreme condition of light stimuli carrying minimal timing information. Of note, two studies on photoperiodism in hamster reproduction (Elliott et al., 1972; Stetson et al., 1975) preluded our results. The unusual light/dark regimens used in those works were able to keep the hamsters' circadian activity rhythms within a 24-hour period, even though the times of the photophases happened with a 12-hour difference among consecutive days.

The minimal timing provided by our light/dark regimens indicate that the process of entrainment is indeed very robust, even in face of day-to-day temporal variability of the zeitgeber, as predicted by our computer simulations (Flôres et al., 2013). It would be interesting to test the effectiveness of our random pulse paradigm as a zeitgeber in animal models with modifications in the SCN (Yamaguchi et al., 2013).

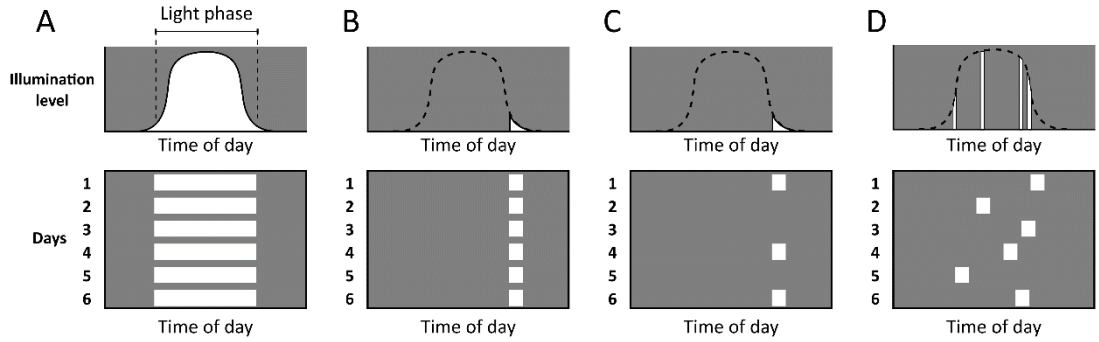

Figure 5.1. Schematic representations of different light exposure patterns. Upper graphs: Variation of the light level perceived. Lower graphs: Actograms representing the light/dark cycle day after day. **A**: Idealized light exposure pattern from an aboveground animal that sees the whole transition of the light/dark cycle. **B**: Light exposure from a burrowing animal that leaves its refuge at the end of the day, like scorpions and bats. **C**: Sporadic light exposure at the end of the day, based on the pattern observed in flying squirrels. **D**: Upper graph: a conceptual representation of the light exposure of tuco-tucos, composed of brief exposure episodes along the day. Lower graph: simplified model of the tuco-tuco's light exposure, used in the laboratory and in previous computer simulations.

Non-photic synchronization: food and reward

In the second part of the thesis, chapters 3 and 4, we explored another facet of the circadian system: synchronization by food availability cycles. Non-photic synchronizers regulate the system through alternative input pathways to the SCN (Mistlberger 2011), but in the extreme case of food synchronization, the entrainment process is mediated by a completely separate oscillator (Mistlberger, 1994; Stephan, 2002). When subjected to cyclic feeding signals, the food entrainable oscillator (FEO) induces and regulates a food anticipatory activity (FAA), independent of the activity dictated by the SCN.

The anatomical locus of FEO has not been elucidated, despite the long history of anatomical lesion and gene knockout studies (Davidson, 2009; Pendergast et al., 2012). Still, many factors have been identified, which either inhibit or stimulate the expression of FAA (Flôres et al., 2016c). It is evident now that at least two aspects revolve around the expression of FAA: metabolism and reward.

In chapter 3, the metabolic aspect is evidenced in our food synchronization study with tuco-tucos. These herbivorous animals do not experience great variations in food availability along the 24 hours of the day; still, we demonstrate that they can develop FAA in response to artificial food availability cycles. The FAA expression was, however, restricted to a few animals and they were the ones that ate less and lost more body mass during the food availability cycles. We hypothesize that food entrainment is strengthened when the animals are exposed to a greater metabolic stress. This is supported by data on other rodent species (Challet et al., 1996; Salazar-Juárez et al., 2003).

Despite the clear effect of metabolic stress on the expression of FAA, chapter 4 illustrates that animals exposed to cyclic rewarding stimuli can still develop anticipatory activities even in the absence of food shortage. This study investigated entrainment to rewarding stimuli in wild-type and clock-mutant laboratory mice. Both wild-type and triple *Period* mutant mice anticipated the cyclic availability of palatable food and the cyclic opportunity to use a running-wheel. Moreover, the originally arrhythmic mutant mice developed a self-sustaining rhythmicity that persisted for some days after removal of the synchronizing stimuli. These evidences indicate that synchronization to rewarding stimuli is mediated by extra-SCN non-canonical mechanisms, here named palatable meal-inducible circadian oscillator (PICO) and wheel-inducible circadian oscillator (WICO). Future studies will hopefully resolve whether these oscillators are equivalent to the FEO and to another extra-SCN oscillator, the methamphetamine-sensitive circadian oscillator (MASCO).

In our pilot protocols of food entrainment in tuco-tucos, the animals presented signs of poor health when exposed to time-restricted feeding schedules of 3 hours of food per day, a feeding regimen normally used in rats. Even with the final protocol with 9 hours of food per day, one animal lost much body mass and another one died at the very end of the experiment. The severity of the response to time-restricted feeding limits the experimental interventions that could be used to further explore food entrainment in tuco-tucos. Nevertheless, our results with palatable meal entrainment in mice open a new venue. A feeding schedule with daily palatable food could be used to try inducing FAA

expression in tuco-tucos with *ad libitum* regular food in the background, thus solving the issues of time-restricted feeding in these animals.

Concluding remarks

While model laboratory species such as the mouse can bring valuable information on mechanisms, due to the variety of mutant lineages in different clock and non-clock genes, wild species like the tuco-tuco can give us insights into the ecological meaning of circadian phenomena, as well as invite reevaluations of our basic concepts on circadian oscillators and entrainment.

References

Abe, H., Kida, M., Tsuji, K., and Mano, T. (1989). Feeding cycles entrain circadian rhythms of locomotor activity in CS mice but not in C57BL/6J mice. Physiol. Behav. *45*, 397–401.

Abraham, E., del Valle, H.F., Roig, F., Torres, L., Ares, J.O., Coronato, F., and Godagnone, R. (2009). Overview of the geography of the Monte Desert biome (Argentina). J. Arid Environ. *73*, 144–153.

Abraham, U., Granada, A.E., Westermark, P.O., Heine, M., Kramer, A., and Herzel, H. (2010). Coupling governs entrainment range of circadian clocks. Mol. Syst. Biol. *6*, 438.

Ángeles-Castellanos, M., Salgado-Delgado, R., Rodríguez, K., Buijs, R.M., and Escobar, C. (2008). Expectancy for food or expectancy for chocolate reveals timing systems for metabolism and reward. Neuroscience *155*, 297–307.

Aschoff, J. (1979). Circadian rhythms: influences of internal and external factors on the period measured in constant conditions. Zeitschrift Für Tierpsychologie *49*, 225–249.

Aton, S.J., Block, G.D., Tei, H., Yamazaki, S., and Herzog, E.D. (2004). Plasticity of circadian behavior and the suprachiasmatic nucleus following exposure to non-24-hour light cycles. J. Biol. Rhythms *19*, 198–207.

Balsalobre, A., Damiola, F., and Schibler, U. (1998). A serum shock induces circadian gene expression in mammalian tissue culture cells. Cell *93*, 929–937.

Bartness, T.J., Song, C.K., and Demas, G.E. (2001). SCN Efferents to Peripheral Tissues: Implications for Biological Rhythms. J. Biol. Rhythms *16*, 196–204.

Bass, J., and Takahashi, J.S. (2010). Circadian integration of metabolism and energetics. Science *330*, 1349–1354.

Beersma, D.G.M., Daan, S., and Hut, R.A. (1999). Accuracy of circadian entrainment under fluctuating light conditions: contributions of phase and period responses. J. Biol. Rhythms *14*, 320–329.

Begall, S., Daan, S., Burda, H., and Overkamp, G.J.F. (2002). Activity Patterns in a Subterranean Social Rodent, Spalacopus cyanus (Octodontidae). J. Mammal. *83*, 153–158.

Ben-Shlomo, R., Ritte, U., and Nevo, E. (1995). Activity Pattern and Rhythm in the Subterranean Mole Rat Superspecies Spalax ehrenbergi. Behav. Genet. *25*, 239–245.

Berson, D.M., Dunn, F.A., and Takao, M. (2002). Phototransduction by retinal ganglion cells that set the circadian clock. Science (80-.). *295*, 1070–1073.

Bloch, G., Barnes, B.M., Gerkema, M.P., and Helm, B. (2013). Animal activity around the clock with no overt circadian rhythms: patterns, mechanisms and adaptive value. Proc. R. Soc. BThe R. Soc. *280*, 20130019.

Blum, I.D., Zhu, L., Moquin, L., Kokoeva, M. V, Gratton, A., Giros, B., and Storch, K.-F. (2014). A highly-tunable dopaminergic oscillator generates ultradian rhythms of

behavioral arousal. Elife *3*, e05105.

Bolles, R.C., and Lorge, J. (1962). The rat's adjustment to a-diurnal feeding cycles. *55*, 760–762.

Boulos, Z., and Rusak, B. (1982). Circadian phase response curves for dark pulses in the hamster. J. Comp. Physiol. ? A *146*, 411–417.

Boulos, Z., Rosenwasser, A.M., and Terman, M. (1980). Feeding schedules and the circadian organisation of behavior in the rat. Behav. Brain Res. *1*, 39–65.

Buhr, E.D., Yoo, S.-H., and Takahashi, J.S. (2010). Temperature as a universal resetting cue for mammalian circadian oscillators. Science *330*, 379–385.

Campbell, A., Gonzalez, A., Gonzalez, D.L., Piro, O., and Larrondo, H.A. (1989). Isochrones and the dynamics of kicked oscillators. Physica A *155*, 565–584.

Casiraghi, L.P., Oda, G. a, Chiesa, J.J., Friesen, W.O., and Golombek, D. a (2012). Forced desynchronization of activity rhythms in a model of chronic jet lag in mice. J. Biol. Rhythms *27*, 59–69.

Challet, E., Malan, A., and Pévet, P. (1996). Daily hypocaloric feeding entrains circadian rhythms of wheel-running and body temperature in rats kept in constant darkness. Neurosci. Lett. *211*, 1–4.

Chandrashekaran, M.K., Johnsson, A., and Engelmann, W. (1973). Possible "dawn" and "dusk" roles of light pulses shifting the phase of a circadian rhythm. J. Comp. Physiol. *82*, 347–356.

Clarke, J.D., and Coleman, G.J. (1986). Persistent meal-associated rhythms in SCN-lesioned rats. Physiol. Behav. *36*, 105–113.

Coleman, G.J., Harper, S., Clarke, J.D., and Armstrong, S. (1982). Evidence for a separate meal-associated oscillator in the rat. Physiol. Behav. *29*, 107–115.

Comas, M., Beersma, D.G.M., Hut, R.A., and Daan, S. (2008). Circadian Phase Resetting in Response to Light-Dark and Dark-Light Transitions. J. Biol. Rhythms *23*, 425–434.

Comparatore, V.M., Cid, M.S., and Busch, C. (1995). Dietary preferences of two sympatric subterranean rodent populations in Argentina. Rev. Chil. Hist. Nat. *68*, 197–206.

Cook, J.A., and Lessa, E.P. (1998). Are Rates of Diversification in Subterranean South American Tuco-Tucos (Genus Ctenomys, Rodentia: Octodontidae) Unusually High ? Evolution (N. Y). *52*, 1521–1527.

Cutrera, A.P., Antinuchi, C.D., Mora, M.S., and Vassallo, A.I. (2006). Home-range and activity patterns of the South American subterranean rodent Ctenomys talarum. J. Mammal. *87*, 1183–1191.

Daan, S. (2000). Colin Pittendrigh , Jürgen Aschoff , and the Natural Entrainment of Circadian Systems. J. Biol. Rhythms *15*, 195–207.

Daan, S., and Pittendrigh, C.S. (1976a). A Functional Analysis of Circadian Pacemakers in Nocturnal Rodents: II. The Variability of Phase Response Curves. J. Comp. Physiol. A *106*, 253–266.

Daan, S., and Pittendrigh, C.S. (1976b). A Functional Analysis of Circadian Pacemakers in Nocturnal Rodents: III. Heavy Water and Constant Light: Homeostasis of Frequency? J. Comp. Physiol. A *106*, 267–290.

Damiola, F., Le Minli, N., Preitner, N., Kornmann, B., Fleury-Olela, F., and Schibler, U. (2000). Restricted feeding uncouples circadian oscillators in peripheral tissues from the central pacemaker in the suprachiasmatic nucleus. Genes Dev. *14*, 2950–2961.

Davidson, A.J. (2009). Lesion studies targeting food-anticipatory activity. Eur. J. Neurosci. *30*, 1658–1664.

Davidson, A.J., and Menaker, M. (2003). Birds of a feather clock together - Sometimes: Social synchronization of circadian rhythms. Curr. Opin. Neurobiol. *13*, 765–769.

DeCoursey, P.J. (1960). Phase control of activity in a rodent. In Cold Spring Harbor Symposia on Quantitative Biology XXV: Biological Clocks, (Long Island: Long Island Biological Association), pp. 49–55.

DeCoursey, P.J. (1972). LD Ratios and the Entrainment of Circadian Activity in a Nocturnal and a Diurnal Rodent. J. Comp. Physiol. *78*, 221–235.

DeCoursey, P.J. (1986). Light-sampling behavior in photoentrainment of a rodent circadian rhythm. J. Comp. Physiol. A. *159*, 161–169.

DeCoursey, P.J. (2014). Survival value of suprachiasmatic nuclei (SCN) in four wild sciurid rodents. Behav. Neurosci. *128*, 240–249.

DeCoursey, G., and DeCoursey, P.J. (1964). Adaptive aspects of activity rhythms in bats. Biol. Bull. *126*, 14–27.

Dibner, C., Schibler, U., and Albrecht, U. (2010). The mammalian circadian timing system: organization and coordination of central and peripheral clocks.

Dunlap, J.C. (1999). Molecular Bases for Circadian Clocks. Cell *96*, 271–290.

Elliot, J.A. (1976). Cicadian rhythms and photoperiodic time measurement in mammals. Fed. Proc. *35*, 2339–2346.

Elliott, J.A., Stetson, M.H., and Menaker, M. (1972). Regulation of Testis Function in Golden Hamsters: A Circadian Clock Measures Photoperiodic Time. Science (80-.). *178*, 771–773.

Fleissner, G., and Fleissner, G. (1998). Natural photic Zeitgeber signals and underlying neuronal mechanisms in scorpions. In Biological Clocks: Mechanisms and Adaptations, Y. Touitou, ed. (Amsterdan: Elsevier Science), pp. 171–180.

Flôres, D.E.F.L. (2011). Sincronização fótica de um roedor subterrâneo: um estudo cronobiológico de campo e de laboratório do tuco-tuco (Ctenomys cf. knighti). University of São Paulo.

Flôres, D.E.F.L., Tomotani, B.M., Tachinardi, P., Oda, G.A., and Valentinuzzi, V.S. (2013). Modeling natural photic entrainment in a subterranean rodent (Ctenomys aff. knighti), the tuco-tuco. PLoS One *8*, e68243.

Flôres, D.E.F.L., Jannetti, M.G., Valentinuzzi, V.S., and Oda, G.A. (2016a). Entrainment of circadian rhythms to irregular light/dark cycles: a subterranean perspective. Sci. Rep. *6*, 34264.

Flôres, D.E.F.L., Bettilyon, C.N., and Yamazaki, S. (2016b). Period-independent novel circadian oscillators revealed by timed exercise and palatable meals. Sci. Rep. *6*, 21945.

Flôres, D.E.F.L., Bettilyon, C.N., Jia, L., and Yamazaki, S. (2016c). The Running Wheel Enhances Food Anticipatory Activity: An Exploratory Study. Front. Behav. Neurosci. *10*.

Fu, L., and Lee, C.C. (2003). The circadian clock: pacemaker and tumour suppressor. Nat. Rev. Cancer *3*, 350–361.

Gallardo, C.M., Darvas, M., Oviatt, M., Chang, C.H., Michalik, M., Huddy, T.F., Meyer, E.E., Shuster, S. a, Aguayo, A., Hill, E.M., et al. (2014). Dopamine receptor 1 neurons in the dorsal striatum regulate food anticipatory circadian activity rhythms in mice. Elife *3*, e03781.

Golombek, D.A., and Rosenstein, R.E. (2010). Physiology of Circadian Entrainment. Physiol. Rev. *90*, 1063–1102.

Granada, A.E., Cambras, T., Diez-Noguera, A., and Herzel, H. (2011). Circadian desynchronization. Interface Focus *1*, 153–166.

Gutman, R., Yosha, D., Choshniak, I., and Kronfeld-Schor, N. (2007). Two strategies for coping with food shortage in desert golden spiny mice. Physiol. Behav. *90*, 95–102.

Hamaguchi, Y., Tahara, Y., Kuroda, H., Haraguchi, A., and Shibata, S. (2015). Entrainment of mouse peripheral circadian clocks to <24 h feeding/fasting cycles under 24 h light/dark conditions. Sci. Rep. *5*, 14207.

Hannibal, J., Hindersson, P., Knudsen, S.M., Georg, B., and Fahrenkrug, J. (2002). The photopigment melanopsin is exclusively present in pituitary adenylate cyclase-activating polypeptide-containing retinal ganglion cells of the retinohypothalamic tract. J. Neurosci. *22*, RC191.

Hara, R., Wan, K., Wakamatsu, H., Aida, R., Moriya, T., Akiyama, M., and Shibata, S. (2001). Restricted feeding entrains liver clock without participation of the suprachiasmatic nucleus. Genes to Cells *6*, 269–278.

Hattar, S., Liao, H.-W., Takao, M., Berson, D.M., and Yau, K.-W. (2002). Melanopsin-Containing Retinal Ganglion Cells: Architecture, Projections, and Intrinsic Photosensitivity. Science (80-.). *295*, 1065–1070.

Honma, K., and Honma, S. (2009). The SCN-independent clocks, methamphetamine and food restriction. Eur. J. Neurosci. *30*, 1707–1717.

Honma, K., Honma, S., and Hiroshige, T. (1986). Disorganization of the rat activity rhythm by chronic treatment with methamphetamine. Physiol. Behav. *38*, 687–695.

Honma, K., Honma, S., and Hiroshige, T. (1987). Activity rhythms in the circadian domain appear in suprachiasmatic nuclei lesioned rats given methamphetamine. Physiol. Behav. *40*, 767–774.

Hsu, C.T., Patton, D.F., Mistlberger, R.E., and Steele, A.D. (2010). Palatable meal anticipation in mice. PLoS One *5*, e12903.

Hut, R.A., van Oort, B.E.H., and Daan, S. (1999). Natural Entrainment without Dawn and Dusk: The Case of the European Ground Squirrel (Spermophilus citellus). J. Biol. Rhythms *14*, 290–299.

Iijima, M., Nikaido, T., Akiyama, M., Moriya, T., and Shibata, S. (2002). Methamphetamine-induced, suprachiasmatic nucleus-independent circadian rhythms of activity and mPer gene expression in the striatum of the mouse. Eur. J. Neurosci. *16*, 921–929.

Indic, P., Forger, D.B., St. Hilaire, M.A., Dean II, D.A., Brown, E.N., Kronauer, R.E., Klerman, E.B., and Jewett, M.E. (2005). Comparison of Amplitude Recovery Dynamics of Two Limit Cycle Oscillator Models of the Human Circadian Pacemaker. Chronobiol. Int. *22*, 613–629.

Jarvis, J.U.M., O'Riain, M.J., Bennett, N.C., and Sherman, P.W. (1994). Mammalian eusociality: a family affair. Trends Ecol. Evol. *9*, 47–51.

Johnson, C.H. (1999). Forty Years of PRCs- What Have We Learned? Chronobiol. Int. *16*, 711–743.

Johnson, C.H., Elliott, J.A., and Foster, R. (2003). Entrainment of circadian programs. Chronobiol. Int. *20*, 741–774.

Keith, D.R., Hart, C.L., Robotham, M., Tariq, M., Le Sauter, J., and Silver, R. (2013). Time of day influences the voluntary intake and behavioral response to methamphetamine and food reward. Pharmacol. Biochem. Behav. *110*, 117–126.

Kenagy, G.J. (1980). Center-of-gravity of circadian activity and its relation to free-running period in two rodent species. J. Interdiscipl. Cycle Res. *11*, 1–8.

Ko, C.H., and Takahashi, J.S. (2006). Molecular components of the mammalian circadian clock. Hum. Mol. Genet. *15*, R271–R277.

de la Iglesia, H.O., Fernandez-Duque, E., Golombek, D.A., Lanza, N., Duffy, J.F., Czeisler, C.A., and Valeggia, C.R. (2015). Access to Electric Light Is Associated with Shorter Sleep Duration in a Traditionally Hunter-Gatherer Community. J. Biol. Rhythms *30*, 342–350.

Lacey, E.A., Patton, J.L., and Cameron, G.N. (2000). Life underground: The biology of subterranean rodents (Chicago: The University of Chicago Press).

Liu, A.C., Welsh, D.K., Ko, C.H., Tran, H.G., Zhang, E.E., Priest, A.A., Buhr, E.D., Singer, O., Meeker, K., Verma, I.M., et al. (2007). Intercellular Coupling Confers Robustness against Mutations in the SCN Circadian Clock Network. Cell *129*, 605–616.

Luna-Illades, C., Carmona-Castro, A., and Miranda-Anaya, M. (2014). Differences in locomotor activity before and during the access to food in a restricted feeding protocol between obese and lean female mice Neotomodon alstoni. Biol. Rhythm Res. *45*, 915–923.

Marchant, E.G., and Mistlberger, R.E. (1997). Anticipation and entrainment to feeding time in intact and SCN-ablated C57BL/6j mice. Brain Res. *765*, 273–282.

Mendoza, J., Angeles-Castellanos, M., and Escobar, C. (2005). Entrainment by a palatable meal induces food-anticipatory activity and c-Fos expression in reward-related areas of the brain. Neuroscience *133*, 293–303.

Mendoza, J., Gourmelen, S., Dumont, S., Sage-Ciocca, D., Pévet, P., and Challet, E. (2012). Setting the main circadian clock of a diurnal mammal by hypocaloric feeding. J. Physiol. *590*, 3155–3168.

Menon, S.A., Decoursey, P.J., and Bruce, D.R. (1988). Frequency Modulation of a Circadian Pacemaker during Photoentrainment. Physiol. Zool. *61*, 186–196.

Michalik, M., Steele, A.D., and Mistlberger, R.E. (2015). A sex difference in circadian food-anticipatory rhythms in mice: Interaction with dopamine D1 receptor knockout. Behav. Neurosci. *129*, 351–360.

Mistlberger, R.E. (1992a). Nonphotic entrainment of circadian activity rhythms in suprachiasmatic nuclei-ablated hamsters. Behav. Neurosci. *106*, 192–202.

Mistlberger, R.E. (1992b). Anticipatory Activity Rhythms under Daily Schedules of Water Access in the Rat. J. Biol. Rhythms *7*, 149–160.

Mistlberger, R.E. (1993). Effects of scheduled food and water access on circadian rhythms of hamsters in constant light, dark, and light:dark. Physiol. Behav. *53*, 509–516.

Mistlberger, R.E. (1994). Circadian food-anticipatory activity: formal models and physiological mechanisms. Neurosci. Biobehav. Rev. *18*, 171–195.

Mistlberger, R.E. (2011). Neurobiology of food anticipatory circadian rhythms. Physiol. Behav. *104*, 535–545.

Mistlberger, R., and Rusak, B. (1987). Palatable daily meals entrain anticipatory activity rhythms in free-feeding rats: Dependence on meal size and nutrient content. Physiol. Behav. *41*, 219–226.

Mistlberger, R.E., and Antle, M.C. (2011). Entrainment of circadian clocks in mammals by arousal and food. Essays Biochem. *49*, 119–136.

Mohawk, J.A., Pezuk, P., and Menaker, M. (2013). Methamphetamine and Dopamine Receptor D1 Regulate Entrainment of Murine Circadian Oscillators. PLoS One *8*, e62463.

Moore, R.Y. (1983). Organization and function of a central nervous system circadian oscillator: the suprachiasmatic nucleus. Fed. Proc. *42*, 2783–2789.

Moore, R.Y., and Eichler, V.B. (1972). Loss of a circadian adrenal corticosterone rhythm following suprachiasmatic lesions in the rat. Brain Res. *42*, 201–206.

Moore-Ede, M.C., Sulzman, F.M., and Fuller, C.A. (1982). The clocks that time us (Cambridge: Harvard University Press).

Moreno, C.R.C., Vasconcelos, S., Marqueze, E.C., Lowden, A., Middleton, B., Fischer, F.M., Louzada, F.M., and Skene, D.J. (2015). Sleep patterns in Amazon rubber tappers with and without electric light at home. Sci. Rep. *5*, 14074.

Morgan, J.A., Corrigan, F., and Baune, B.T. (2015). Effects of physical exercise on central nervous system functions: a review of brain region specific adaptations. J. Mol. Psychiatry *3*, 1–13.

Mrosovsky, N. (1988). Phase response curves for social entrainment. J. Comp. Physiol. A *162*, 35–46.

Mrosovsky, N. (1994). In Praise of Masking: Behavioral Responses of Retinally Degenerate Mice To Dim Light. Chronobiol. Int. *11*, 343–348.

Mrosovsky, N., Reebs, S.G., Honrado, G.I., and Salmon, P.A. (1989). Behavioral entrainment of circadian rhythms. Experientia *45*, 696–702.

Nemec, P., Cveková, P., Burda, H., Benada, O., and Peichl, L. (2007). Visual systems and the role of vision in subterranean rodents: diversity of retinal properties and visual system designs. In Subterranean Rodents: News from Underground, S. Begall, H. Burda, and C.E. Schleich, eds. (Berlin: Springer), pp. 129–160.

Nevo, E. (1979). Adaptive Convergence and Divergence of Subterranean Mammals. Annu. Rev. Ecol. Syst. *10*, 269–308.

Novak, C.M., Burghardt, P.R., and Levine, J.A. (2012). The use of a running wheel to measure activity in rodents: Relationship to energy balance, general activity, and reward. Neurosci. Biobehav. Rev. *36*, 1001–1014.

Okudaira, N., Kripke, D., and Webster, J. (1983). Naturalistic studies of human light exposure. Am. J. Physiol. *245*, R613–R615.

van Oort, B.E.H., Tyler, N.J.C., Gerkema, M.P., Folkow, L., Blix, A.S., and Stokkan, K.-A. (2005). Circadian organization in reindeer. Nature *438*, 1095–1096.

Oosthuizen, M.K., Cooper, H.M., and Bennett, N.C. (2003). Circadian rhythms of locomotor activity in solitary and social species of African mole-rats (family: Bathyergidae). J. Biol. Rhythms *18*, 481–490.

Ouyang, Y., Andersson, C.R., Kondo, T., Golden, S.S., and Johnson, C.H. (1998). Resonating circadian clocks enhance fitness in cyanobacteria. Proc. Natl. Acad. Sci. U. S. A. *95*, 8660–8664.

Panda, S., Provencio, I., Tu, D.C., Pires, S.S., Rollag, M.D., Castrucci, A.M., Pletcher, M.T., Sato, T.K., Wiltshire, T., Andahazy, M., et al. (2003). Melanopsin Is Required for Non-Image-Forming Photic Responses in Blind Mice. Science (80-.). *301*, 525–527.

Patton, D.F., and Mistlberger, R.E. (2013). Circadian adaptations to meal timing: Neuroendocrine mechanisms. Front. Neurosci. *7*, 1–14.

Pendergast, J.S., and Yamazaki, S. (2014). Effects of light, food, and methamphetamine on the circadian activity rhythm in mice. Physiol. Behav. *128*, 92–98.

Pendergast, J.S., Oda, G.A., Niswender, K.D., and Yamazaki, S. (2012). Period determination in the food-entrainable and methamphetamine-sensitive circadian oscillator(s). PNAS *109*, 14218–14223.

Petersen, C.C., Patton, D.F., Parfyonov, M., and Mistlberger, R.E. (2014). Circadian food anticipatory activity: Entrainment limits and scalar properties re-examined. Behav. Neurosci. *128*, 689–702.

Peterson, E.L. (1980). A limit cycle interpretation of a mosquito circadian oscillator. J. Theor. Biol. *84*, 281–310.

Phillips, J.L.M., and Mikulka, P.J. (1979). The effects of restricted food access upon locomotor activity in rats with suprachiasmatic nucleus lesions. Physiol. Behav. *23*, 257–262.

Piccione, G., Giannetto, C., Marafioti, S., Casella, S., and Caola, G. (2010). The effect of photic entrainment and restricted feeding on food anticipatory activity in Ovis aries. Small Rumin. Res. *94*, 190–195.

Pittendrigh, C.S. (1954). On Temperature Independence in the Clock System Controlling Emergence Time in Drosophila. Proc. Natl. Acad. Sci. U. S. A. *40*, 1018–1029.

Pittendrigh, C.S., and Daan, S. (1976a). A Functional Analysis of Circadian Pacemakers in Nocturnal Rodents: I. The stability and lability of spontaneous frequency. J. Comp. Physiol. A *106*, 223–252.

Pittendrigh, C.S., and Daan, S. (1976b). A Functional Analysis of Circadian Pacemakers in Nocturnal Rodents: IV. Entrainment: Pacemaker as Clock. J. Comp. Physiol. A *106*, 291–331.

Pittendrigh, C.S., and Daan, S. (1976c). A Functional Analysis of Circadian Pacemakers in Nocturnal Rodents: V. Pacemaker Structure: A Clock for All Seasons. J. Comp. Physiol. A *106*, 333–335.

Pittendrigh, C.S., Kyner, W.T., and Takamura, T. (1991). The amplitude of circadian oscillations: temperature dependence, latitudinal clines, and the photoperiodic time measurement. J. Biol. Rhythms *6*, 299–313.

Pratt, B.L., and Goldman, B.D. (1986). Activity rhythms and photoperiodism of syrian hamsters in a simulated burrow system. Physiol. Behav. *36*, 83–89.

Rado, R., Shanas, U., Zuri, I., and Terkel, J. (1993). Seasonal activity in the blind mole rat (Spalax ehrenbergi). Can. J. Zool. *71*, 1733–1737.

Ralph, M.R., Foster, R.G., Davis, F.C., and Menaker, M. (1990). Transplanted suprachiasmatic nucleus determines circadian period. Science *247*, 975–978.

Refinetti, R. (2010). Entrainment of circadian rhythm by ambient temperature cycles in mice. J. Biol. Rhythms *25*, 247–256.

Reierth, E., and Stokkan, K.-A. (1998). Dual Entrainment by Light and Food in the Svalbard Ptarmigan (Lagopus mutus hyperboreus). J. Biol. Rhythms *13*, 393–402.

Riccio, A.P., and Goldman, B.D. (2000). Circadian rhythms of locomotor activity in naked mole-rats (Heterocephalus glaber). Physiol. Behav. *71*, 1–13.

Richter, C.P. (1922). A behavioristic study of the activity of the rat. Comp. Psychol. Monogr. *1*, 1–54.

Roenneberg, T., and Foster, R.G. (1997). Twilight Times: Light and the Circadian System. Photochem. Photobiol. *66*, 549–561.

Roenneberg, T., Daan, S., and Merrow, M. (2003). The Art of Entrainment. J. Biol. Rhythms *18*, 183–194.

Rosi, M.I., Cona, M.I., Videla, F., Puig, S., Monge, S.A., and Roig, V.G. (2003). Diet selection by the fossorial rodent Ctenomys mendocinus Inhabiting an environment with low food availability (Mendoza, Argentina). Stud. Neotrop. Fauna Environ. *38*, 159–166.

Rusak, B., Mistlberger, R.E., Losier, B., and Jones, C.H. (1988). Daily hoarding opportunity entrains the pacemaker for hamster activity rhythms. J. Comp. Physiol. A *164*, 165–171.

Salazar-Juárez, A., Aguilar-Roblero, R., Parra, L., and Escobar, C. (2003). Restricted Feeding Schedules Modulate Free-running Drinking Activity in Malnourished Rats.

Biol. Rhythm Res. *34*, 459–474.

Sargeant, A.B. (1966). A live trap for pocket gophers. J. Mammal. *47*, 729–731.

Schleich, C.E., Vielma, A., Glösmann, M., Palacios, A.G., and Peichl, L. (2010). Retinal photoreceptors of two subterranean tuco-tuco species (Rodentia, Ctenomys): morphology, topography, and spectral sensitivity. J. Comp. Neurol. *518*, 4001–4015.

Sikes, R.S., and Gannon, W.L. (2011). Guidelines of the American Society of Mammalogists for the use of wild mammals in research. J. Mammal. *92*, 235–253.

Silver, R., LeSauter, J., Tresco, P.A., and Lehman, M.N. (1996). A diffusible coupling signal from the transplanted suprachiasmatic nucleus controlling circadian locomotor rhythms. Nature *382*, 810–813.

Silverman, H.J., and Zucker, I. (1976). Absence of post-fast food compensation in the golden hamster (Mesocricetus auratus). Physiol. Behav. *17*, 271–285.

Sokolove, P.G., and Bushell, W.N. (1978). The chi square periodogram: its utility for analysis of circadian rhythms. J. Theor. Biol. *72*, 131–160.

Spoelstra, K., Wikelski, M., Daan, S., Loudon, A.S.I., and Hau, M. (2016). Natural selection against a circadian clock gene mutation in mice. Proc. Natl. Acad. Sci. *113*, 686–691.

Steele, A.D., and Mistlberger, R.E. (2015). Activity is a slave to many masters. Elife *4*, e06351.

Stephan, F.K. (1981). Limits of entrainment to periodic feeding in rats with suprachiasmatic lesions. J. Comp. Physiol. A *143*, 401–410.

Stephan, F.K. (1986a). Coupling between feeding- and light-entrainable circadian pacemakers in the rat. Physiol. Behav. *38*, 537–544.

Stephan, F.K. (1986b). Interaction between light- and feeding-entrainable circadian rhythms in the rat. Physiol. Behav. *38*, 127–133.

Stephan, F.K. (2002). The "Other" Circadian System: Food as a Zeitgeber. J. Biol. Rhythms *17*, 284–292.

Stephan, F.K., and Zucker, I. (1972). Circadian Rhythms in Drinking Behavior and Locomotor Activity of Rats Are Eliminated by Hypothalamic Lesions. Proc. Natl. Acad. Sci. U. S. A. *69*, 1583–1586.

Stephan, F.K., Swann, J.M., and Sisk, C.L. (1979). Anticipation of 24-hr feeding schedules in rats with lesions of the suprachiasmatic nucleus. Behav. Neural Biol. *25*, 346–363.

Stetson, M.H., Elliott, J.A., and Menaker, M. (1975). Photoperiodic regulation of hamster testis: circadian sensitivity to the effects of light. Biol. Reprod. *13*, 329–339.

Stokkan, K.-A., Mortensen, A., and Blix, A.S. (1986). Food intake, feeding rhythm, and body mass regulation in Svalbard rock ptarmigan. Am. J. Physiol. *251*, R264-7.

Stokkan, K.-A., Yamazaki, S., Tei, H., Sakaki, Y., and Menaker, M. (2001). Entrainment of the circadian clock in the liver by feeding. Science *291*, 490–493.

Takahashi, J.S., Shimomura, K., and Kumar, V. (2008). Searching for genes underlying

behavior: lessons from circadian rhythms. Science *322*, 909–912.

Tamayo, A.G., Duong, H.A., Robles, M.S., Mann, M., and Weitz, C.J. (2015). Histone monoubiquitination by Clock-Bmal1 complex marks Per1 and Per2 genes for circadian feedback. Nat. Struct. Mol. Biol. *22*, 759–766.

Tataroglu, Ö., Davidson, A.J., Benvenuto, L.J., and Menaker, M. (2006). The methamphetamine-sensitive circadian oscillator (MASCO) in mice. J. Biol. Rhythms *21*, 185–194.

Taylor, S.R., Webb, A.B., Smith, K.S., Petzold, L.R., and Doyle, F.J. (2010). Velocity Response Curves Support the Role of Continuous Entrainment in Circadian Clocks. J. Biol. Rhythms *25*, 138–149.

Tomita, K., Kai, T., and Hikami, F. (1977). Entrainment of a Limit Cycle by a Periodic External Excitation. Prog. Theor. Phys. *57*, 1159–1177.

Tomotani, B.M., Flores, D.E.F.L., Tachinardi, P., Paliza, J.D., Oda, G.A., and Valentinuzzi, V.S. (2012). Field and laboratory studies provide insights into the meaning of day-time activity in a subterranean rodent (Ctenomys aff. knighti), the tuco-tuco. PLoS One *7*, e37918.

Twente, J.W.J. (1955). Some Aspects of Habitat Selection and Other Behavior of Cavern-Dwelling Bats Ecological Society of America. Ecology *36*, 706–732.

Valentinuzzi, V.S., Oda, G.A., Araujo, J.F., and Ralph, M.R. (2009). Circadian pattern of wheel-running activity of a South American subterranean rodent (Ctenomys cf knightii). Chronobiol. Int. *26*, 14–27.

van der Vinne, V., Akkerman, J., Lanting, G.D., Riede, S.J., and Hut, R.A. (2015). Food reward without a timing component does not alter the timing of activity under positive energy balance. Neuroscience *304*, 260–265.

Voute, A.M., Sluiter, J.W., and Grimm, M.P. (1974). Influence of Natural Light-Dark Cycle on Activity Rhythm of Pond Bats (Myotis dasycneme Boie, 1825) During Summer. Oecologia *17*, 221–243.

Williams, C.T., Barnes, B.M., and Buck, C.L. (2012a). Daily body temperature rhythms persist under the midnight sun but are absent during hibernation in free-living arctic ground squirrels. Biol. Lett. *8*, 31–34.

Williams, C.T., Barnes, B.M., Richter, M., and Buck, C.L. (2012b). Hibernation and circadian rhythms of body temperature in free-living Arctic ground squirrels. Physiol. Biochem. Zool. *85*, 397–404.

Wright, K.P., McHill, A.W., Birks, B.R., Griffin, B.R., Rusterholz, T., and Chinoy, E.D. (2013). Entrainment of the human circadian clock to the natural light-dark cycle. Curr. Biol. *23*, 1554–1558.

Yamaguchi, Y., Suzuki, T., Mizoro, Y., Kori, H., Okada, K., Chen, Y., Fustin, J.-M., Yamazaki, F., Mizuguchi, N., Zhang, J., et al. (2013). Mice Genetically Deficient in Vasopressin V1a and V1b Receptors Are Resistant to Jet Lag. Science (80-.). *342*, 85–90.

Yamazaki, S., Numano, R., Abe, M., Hida, A., Takahashi, R., Ueda, M., Block, G.D., Sakaki, Y., Menaker, M., and Tei, H. (2000). Resetting Central and Peripheral Circadian

Oscillators in Transgenic Rats. Science (80-.). *288*, 682–685.

Yoo, S.-H., Yamazaki, S., Lowrey, P.L., Shimomura, K., Ko, C.H., Buhr, E.D., Siepka, S.M., Hong, H.-K., Oh, W.J., Yoo, O.J., et al. (2004). PERIOD2::LUCIFERASE real-time reporting of circadian dynamics reveals persistent circadian oscillations in mouse peripheral tissues. Proc. Natl. Acad. Sci. U. S. A. *101*, 5339–5346.

Attachment 1. Tests with the Ecotone light logger

The report describes tests performed with the Ecotone light loggers (Figure 2.1.1B,C) in the years of 2011 and 2012. It was sent to the company after problems had been identified:

This report describes the tests made with the light loggers that you sent to us. The loggers were developed to be put on a rodent and register continuously the light intensities to which this rodent is exposed. We present 4 sets of test, the first three in the laboratory and the last one in the field, and describe two main problems that we could identify. We hope this report helps the company to fix the sensors.

Introduction

Tests in the laboratory

We applied several tests to the light loggers.

- **Test 1** - two loggers were exposed to different light intensities, for different amounts of time.
- **Test 2** - we left the same two loggers next to a window, to see if they could record "natural" variations in sunlight for several days.

Based on these Tests, we found two problems with the sensors: one systematic data loss and a time scale that did not correspond with reality.

After that, we designed **Test 3**, trying to compensate the two problems.

Test on a tuco-tuco in the field

After the tests in the lab, we made a collar with the logger and put it on our research animal, the tuco-tuco, a subterranean rodent.

The animal was released in an enclosure in its natural habitat, where it lives in subterranean tunnels. So, the logger was exposed do sand, plant roots, and maybe some humidity.

The results obtained really appear to represent the light conditions that the tuco-tuco sees in its natural habitat.

One logger was broken when we tried to bend it around the tuco-tuco's neck. Another problem was that we did not know how to compensate the time scale in the right way.

Identification of the loggers and batteries

The loggers were identified with numbers 1 to 10, and the batteries were identified with letters A to I. When describing the tests, loggers and batteries will be referred to by these identification codes.

Test 1 – Different light intensities

In these first tests, we put 2 loggers in different light conditions to test their sensibility to changing light. The scale below shows the different treatments applied to the loggers and an arbitrary (relative) light intensity that was defined to each condition.

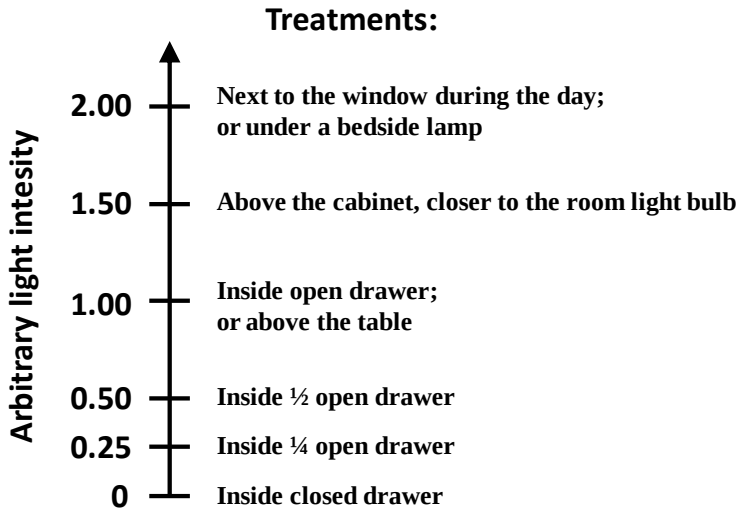

Figure 1.1A – Treatments applied to the loggers and the correspondent arbitrary light intensity designated.

Each logger was submitted to a different sequence of treatments. Based on the arbitrary light intensities designated for each treatment (Figure 1.1A), we were able to build graphics of **expected results** for all the tests, e.g., figure 1.1B. These expected graphics will always be shown in blue, together with the obtained results, to help the evaluation of the results.

Part 1

Logger 1 was connected to battery A without programming, at 10:23 in the morning. According to the manual, this should result in an automatic start 10 minutes later, with light intensities being recorded in an automatic interval of 10 seconds.

The data downloaded from the logger after the test confirmed that this was the case.

During the test, Logger 1 was submitted to a sequence of different light intensities. In the figure 1.1B, we show the expected results for the sequence of light conditions applied in this first test.

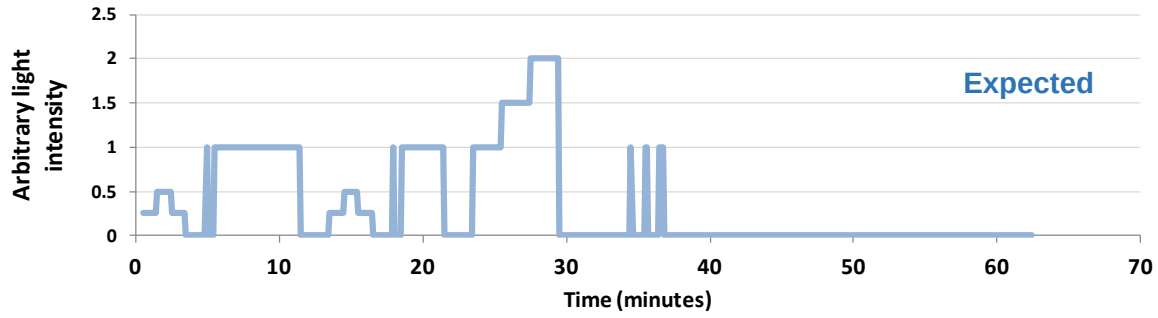

Figure 1.1B – Expected results from Test1 Part1.

The results downloaded from the logger are showed below in the figure 1.1C.

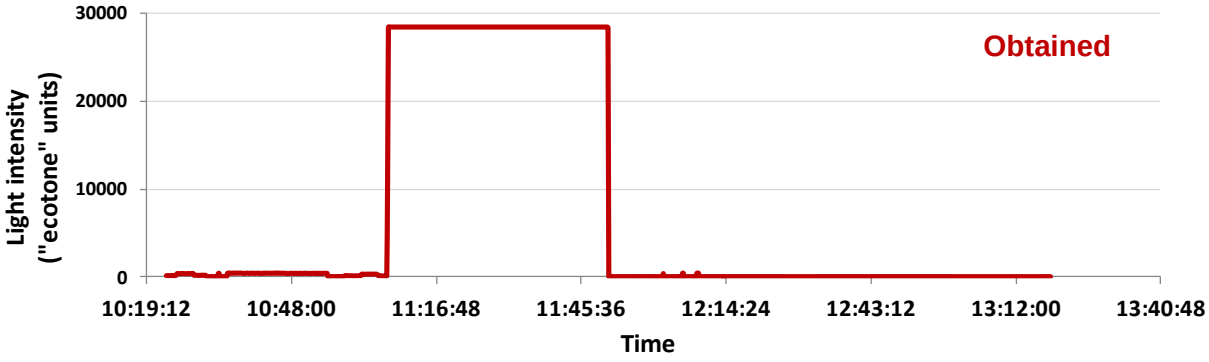

Figure 1.1C – Obtained results from Test1 Part1.

The figure with the obtained data does not correspond to the expected results (Fig. 1.1B). In the obtained data, we see a low light intensity in the beginning of the record, followed by a major block of high light intensity, and then a decrease to the previous low light level.

When we inspected the raw data (numeric txt file), we observed that this high light intensity in the middle of the record is a fixed super high value (almost 30000) that was maintained for several minutes. Another inspection of the figure 1.1C and the raw data indicated that this high level could be an error. Moreover, the super high values could prevent us from seeing the true light intensity changes, which were very low compared to this false high levels.

For that reason, we made a Zoom in the low light level region (limiting the y-axis to values between a minimum of 0 and a maximum of 800). This way we could have access to variations of light intensity in the lower level. The new graphic is shown in the following figue 1.1D (lower graphic), together with the expected results (upper graphic).

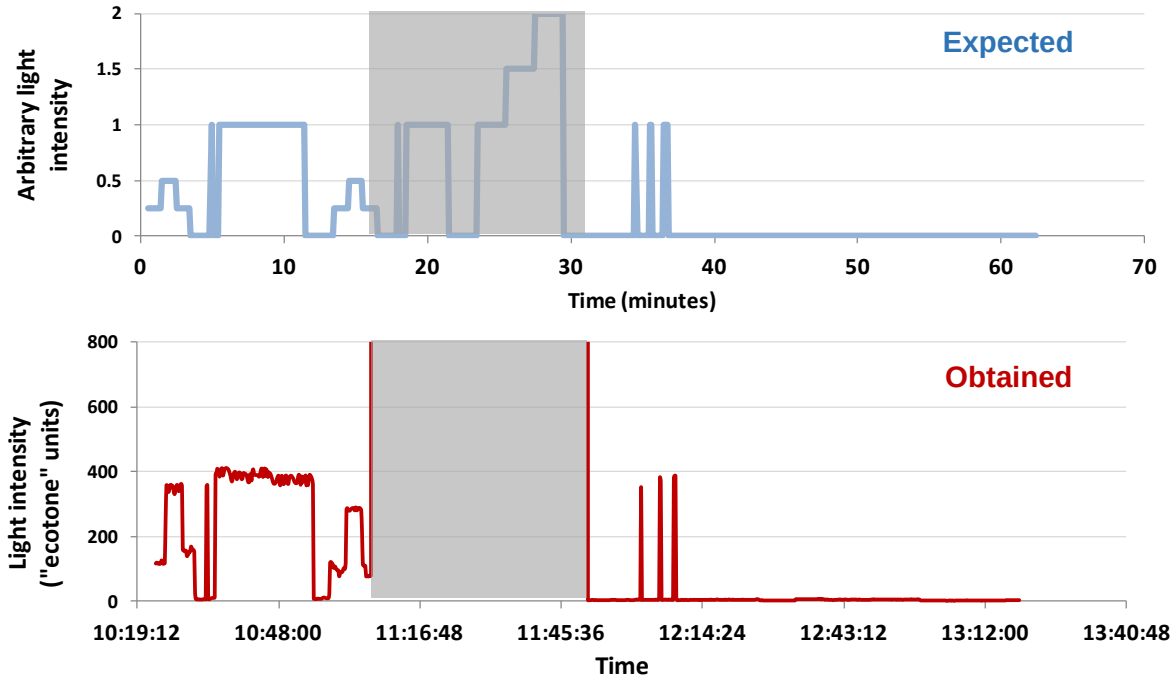

Figure 1.1D – Expected (upper graphic) and obtained (lower graphi) results from Test1 Part1. The y-axis of the obtained results is rescaled (between 0 and 800).

The general profile of this new graphic is much more similar to the expected data, except in the space occupied by the block of high light intensities (in gray). The true light intensities were never above 500 (much lower than the 30000 observed in the gray area of the graphic).

We concluded that this gray part of the data was an error, and did not correspond to real light intensities. So, for some reason, the constant high light intensity was recorded, substituting the real data in this part.

Part 2

This second part is a repetition of the previous test, but with another light logger. Moreover, the logger was programmed in the computer, so it was not an automatic start.

Logger 2 was connected to battery C. We then programmed it to start recording light intensities at 17:31, in an interval of 5 seconds. The protocol was similar to the one we used in Part1 and expected results are represented in the figure 1.2A below (upper graphic). Obtained results are shown in the lower graphic of the same figure.

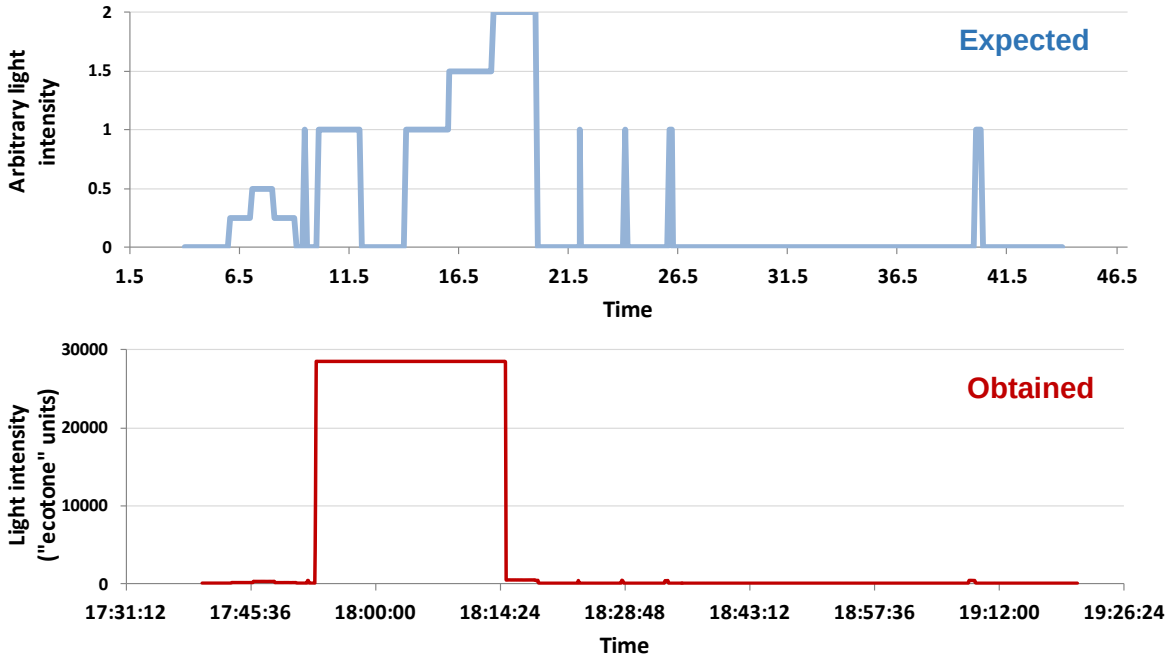

Figure 1.2A – Expected (upper graphic) and obtained (lower graphi) results from Test1 Part2.

In the obtained results (lower graphic), we observed the same problem as before. The data showed low light intensities in the beginning and in the end of the record, and a block of high light intensities in the middle.

Again, we changed the vertical axis to see better the changes in low light intensities (Fig. 1.2B lower graphic) and with this we could see that the obtained data was really similar to the expected results (Fig. 1.2B upper graphic), with the exception of the block of high light intensities (gray area).

Conclusions

From this Test1, we conclude that loggers can distinguish different light intensities, as expected. However, there is a systematic recording of a block of unreal high light intensities in the beginning of the record.

We looked again at the raw data (txt files) to try to understand the cause of these blocks of high light intensity, which do not correspond with real data. We discovered that, in both tests, this "fake" data was always between the data number 265 and the data number 528.

So, it appears that, in every test, the first 264 records of light intensity are real data, the second block of 264 records are occupied by a constant high light intensity, and the rest of the data is again real data.

The "light logger manual" that you sent to us informs that the light intensities measured by the device are recorded in the logger memory in blocks of 264 records. So, we believe that the problem happens only when the logger records the second block of 264 data in the memory. Instead of recording the real data, an unreal high light intensity is recorded.

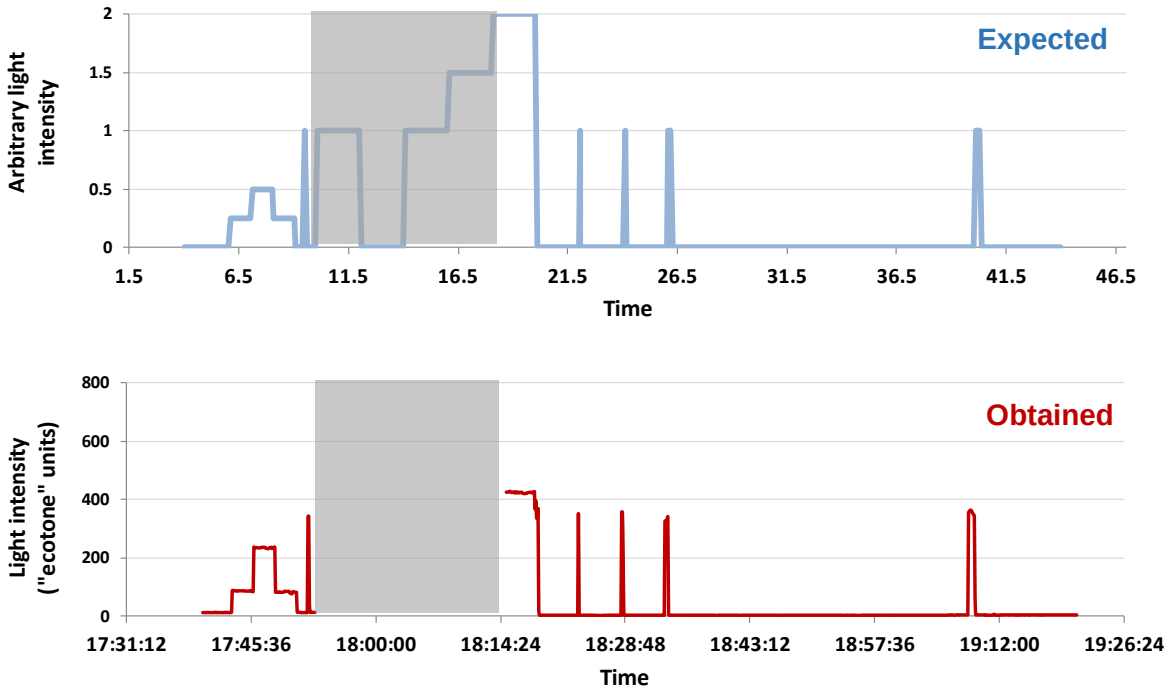

Figure 1.2B – Expected (upper graphic) and obtained (lower graphic) results from Test1 Part2. The y-axis of the obtained results is rescaled between 0 and 800.

For the next tests, we knew that the data from 265 to 528 would be lost, so we planned our tests knowing that we would have to discard this part of the data.

Test 2 – Recording for more than one day next to a window

The same two loggers tested before were left next to a window of the laboratory for some days, to record the light intensity from the outside (sky light). We expected the loggers to record the natural light/dark cycle of sun illumination, with some minor interference from our laboratory lights.

Part 1

Logger 1 with battery B was left next to the window for 2 days. Recording started around midday. We programmed the logger to record light intensities every 30 seconds. The expected results and obtained results from the test are shown in the figure 2.1 below.

The results from the logger show that the recording stopped before the end of the test, probably because the battery was not fully charged when we started measuring.

As expected, the light intensities recorded from data 265 to 528 were an unreal high value and were therefore excluded from the graphic (gray area).

Even though the recording stopped too early, this test indicated to us that the logger could have a second problem. We noted that the light intensities recorded were not expected for the correspondent time.

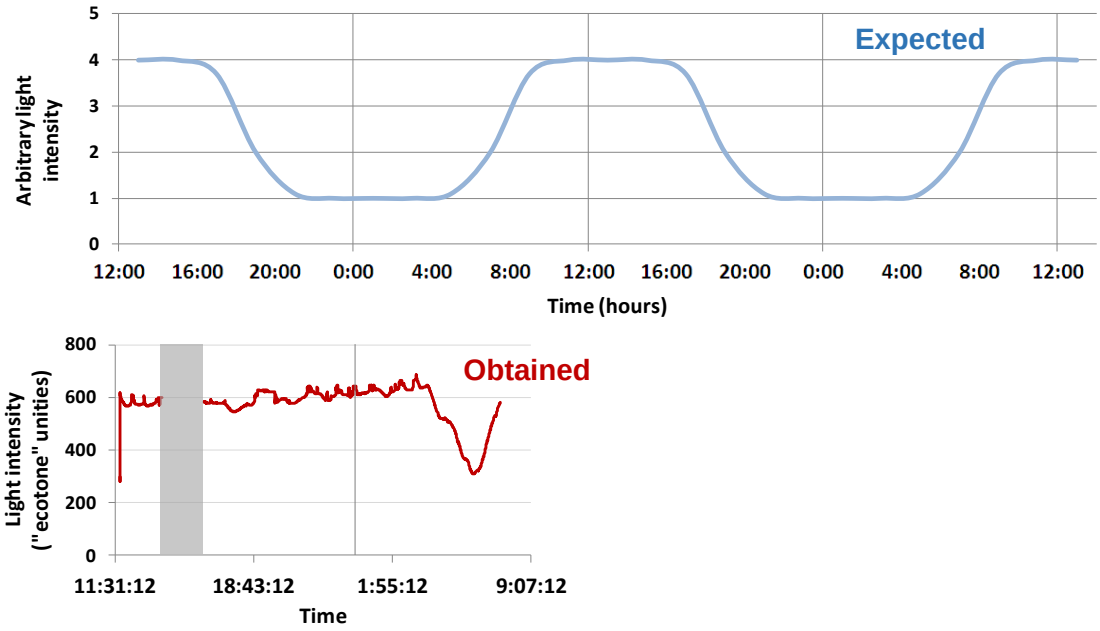

Figure 2.1 – Expected (upper graphic) and obtained (lower graphic) results from Test2 Part1. Vertical lines indicated the times 12:00 and 0:00. The gray rectangle in the obtained results delimits the data loss (block of high light intensities).

Light intensity remained high and rising until around 3:00, when it started to decline. It continued to decline until around 6 am, when it started rising again. We expected that the light intensity would decline in the beginning of the night and remain in a very low level for many hours in the night (Fig. 2.1 upper graphic). Only at the beginning of the day should the light intensity start rising again.

We could not conclude anything else, because we were afraid the unexpected light intensities could have something to do with the low charge of the battery.

Part 2

To avoid the same thing that happened in part 1 of this test, Logger 2 was connected with a completely new battery (D), that hadn't been used in any other test before. The recording started at around 18:00 and was downloaded three days later, at around 14:00 (almost 72 hours of recording). Logger was programmed to record every 30 seconds.

Expected results and obtained results are showed below (Fig. 2.2A).As in all the other tests before, we had to exclude the false data 265 to 528, for the reasons already pointed.

The general pattern of the obtained results corresponded to the expected results. There was a light/dark cycle corresponding to almost three days of recording. So we see that the logger could record for more than one day, and we could identify a difference between day-time data and night-time data. That is the minimum necessary for our purpose of measuring continuous light intensities in our research animals.

However, what was really unexpected was the length of the time scale in the obtained results. In the graphic (Fig. 2.2A lower graphic), vertical lines were put on the times recorded as midnight. So, according to what the logger recorded, there would be 9 days of measurement, not the real 3 days of test. The light/dark profile confirms that we only measured 3 days.

So, the total length of the time scale recorded in the memory of the logger was around three times greater than the real duration of the test. We concluded that this mistake was related to the sampling interval.

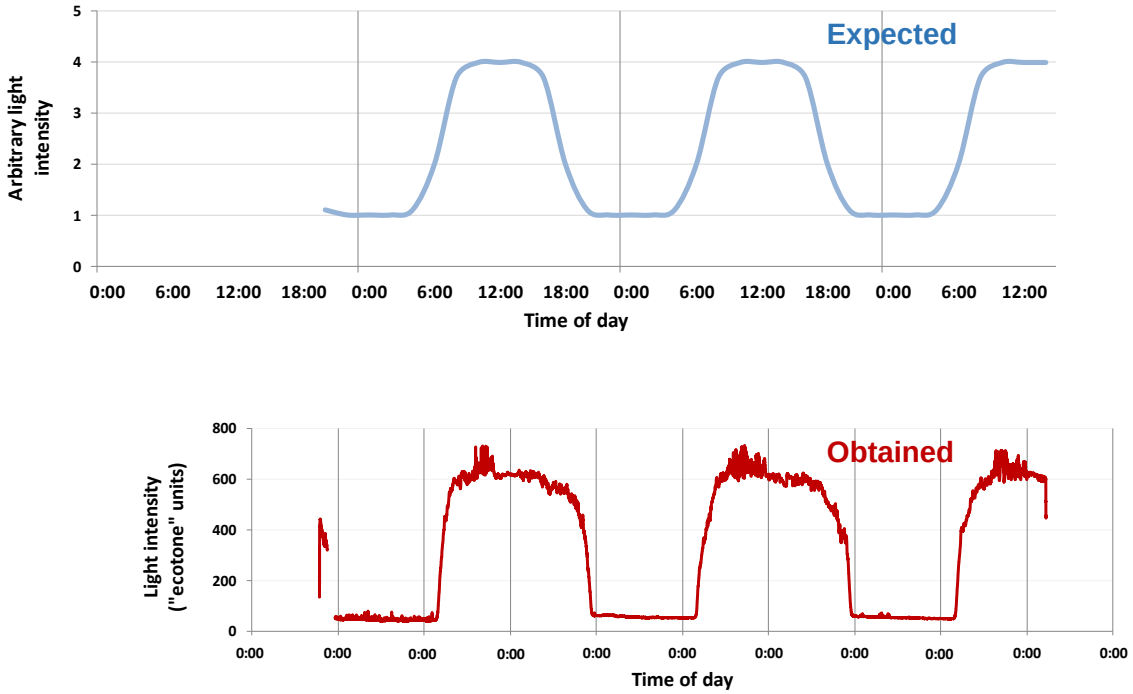

Figure 2.2A – Expected (upper graphic) and obtained (lower graphi) results from Test2 Part2. Gray vertical lines mark the times of midnight (0:00).

The reason for the discrepancy is that the real interval of measurement was shorter than the programmed interval (30 seconds). So, the logger assessed the light intensity more frequently than we asked it to do.

But, in the instructions that were recorded in the memory of the logger, the marked interval was the one we programmed, so, when we used the "light converter" program to build the txt file, the file was generated as if the data were recorded in the programmed interval of 30 seconds, not the real, non-programmed, interval.

For that reason, in the final txt file, the difference between the programmed and real interval were accumulated through all the data, resulting in a time scale much longer (9 days) than the expected one (3 days).

We tried to correct this problem by changing the final txt file. We changed all the times recorded, as if the sampling interval was 1/3 of the one we programmed initially: 10 seconds, instead of the original 30 seconds.

The final result is shown below (Fig. 2.2B). Note that now there are only 3 days of data in the obtained results. The vertical lines marking midnight time correspond to the expected results. And the light intensities measured at midnight are consistent with the expected light intensities for that time. So, apparently, we managed to correct the problem.

Coming back to part 1 of this Test2, the unexpected light intensities observed could be explained by this same problem. The time scale does not represent real time. So, each of those light intensities presented in figure 2.1 must have happened earlier than the times shown in the graphic.

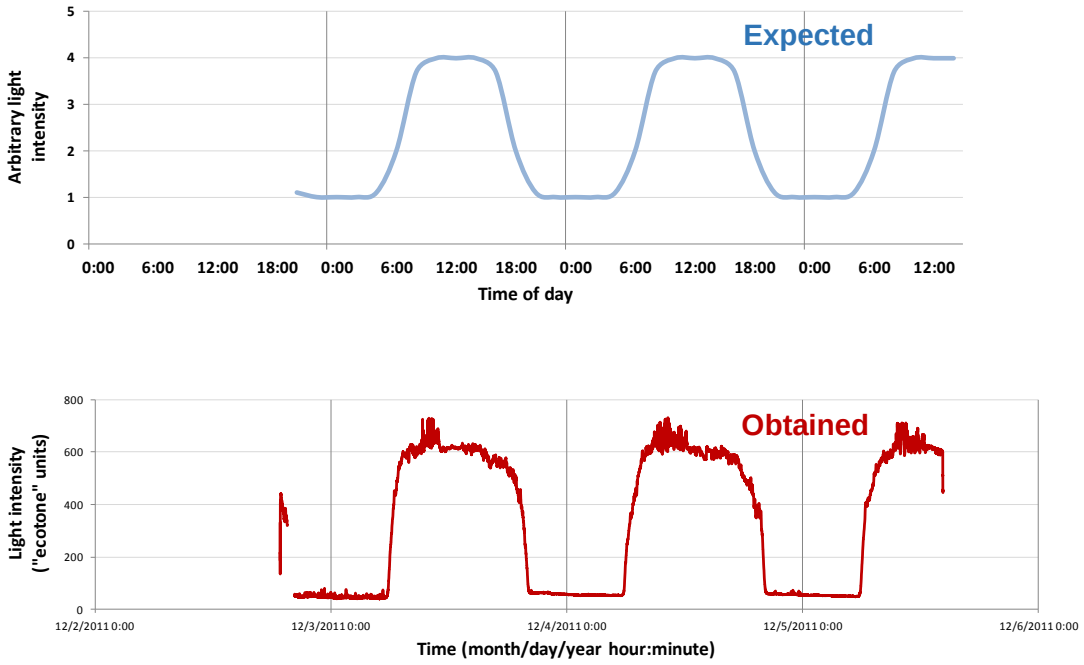

Figure 2.2B– Expected (upper graphic) and obtained (lower graphi) results from Test2 Part2. The time-scale was rebuilt to fix the wrong sampling interval.

Conclusions

1- Loggers can record for several days.
2- Data from 265 to 528 are recorded as unusually high light intensities. For now, we can conclude that this happens consistently, at least for loggers 1 and 2, regardless of the sampling interval chosen (5, 10 or 30 seconds).
3- There was a second problem with the sensors. They seem to use a sampling interval different from the one we program. But the txt file shows the data as if the interval was the same as programmed. For that reason, when we build a graphic using the txt file, the time scale is much longer than the expected. In the way the loggers work now, we have to change the txt files before analyzing the data.

Test 3 – New tests with different light intensities – How to manage the problems.

In this third set of tests, we applied a protocol similar to test 1, but trying to compensate for the problems with a) the block of high light intensities and b) the sampling interval that is different from what we program.

For this test we used all the loggers and batteries that were not used before, to verify if they were all working and also if the results would be consistent between all the loggers.

Part 1

Loggers 3 to 8 were connected with batteries C, E, F, G, H and I.

The start of the recording varied between the loggers, because of the time needed to solder each logger to its respective battery.

The sampling interval was programmed to 9 seconds. Based on test 2, we expected the real sampling interval to be three times shorter, so, 3 seconds.

All the loggers were submitted simultaneously to the controlled changes in light intensity.

We made calculations to start the important parts of the test only after the time predicted for the unreal data (block of high light intensities, from data 265 to 528, as predicted from results in Test1). And for that calculation, we had to take into consideration also the problem with the sampling interval.

The following table 1 indicates the time of the start of the test for each logger, and the expected time for the block of high light intensities (from data 265 to 528). We considered the sampling interval of 3 seconds (not the programmed 9 seconds).

Table 1. Start times and expected measurements in Test 3.

Logger-battery	Start of recording	data 265	data 528
3-C	17:36	17:49	18:02
4-E	17:38	17:51	18:04
5-F	17:42	17:55	18:08
6-G	17:45	17:58	18:11
7-H	17:48	18:01	18:14
8-I	17:51	18:04	18:17

We planned our protocol to start the light intensity changes only after the last logger had reached data 528, when we expected to be the end of the unreal data (high light intensities) in all loggers.

The expected results are shown in the upper graphic of figure 3.1 below. It is not shown in the expected results, but we predicted that the time of the fake data (between 265 and 528) is different for each logger, and dependent on the time of the start of the recording (as in table 1). On the other hand, the applied changes in light intensity (proper test) should happen at the same time for all the loggers, once they were all tested together and simultaneously.

The results (Fig. 3.1 from the second graphic to the last one) fit very well our expectations. We could predict the time of the unreal data (block of high light intensities) and could also compensate for the difference between programmed and real sampling intervals. So, it appears that all the loggers and batteries tested work well and the test also demonstrates that we are able to compensate for the problems found.

In the condition “uncontrolled light intensities” we did not take notes of the light intensities for each light-logger and therefore we could not predict the expected results. The test of light intensities itself is only the right part of each graphic.

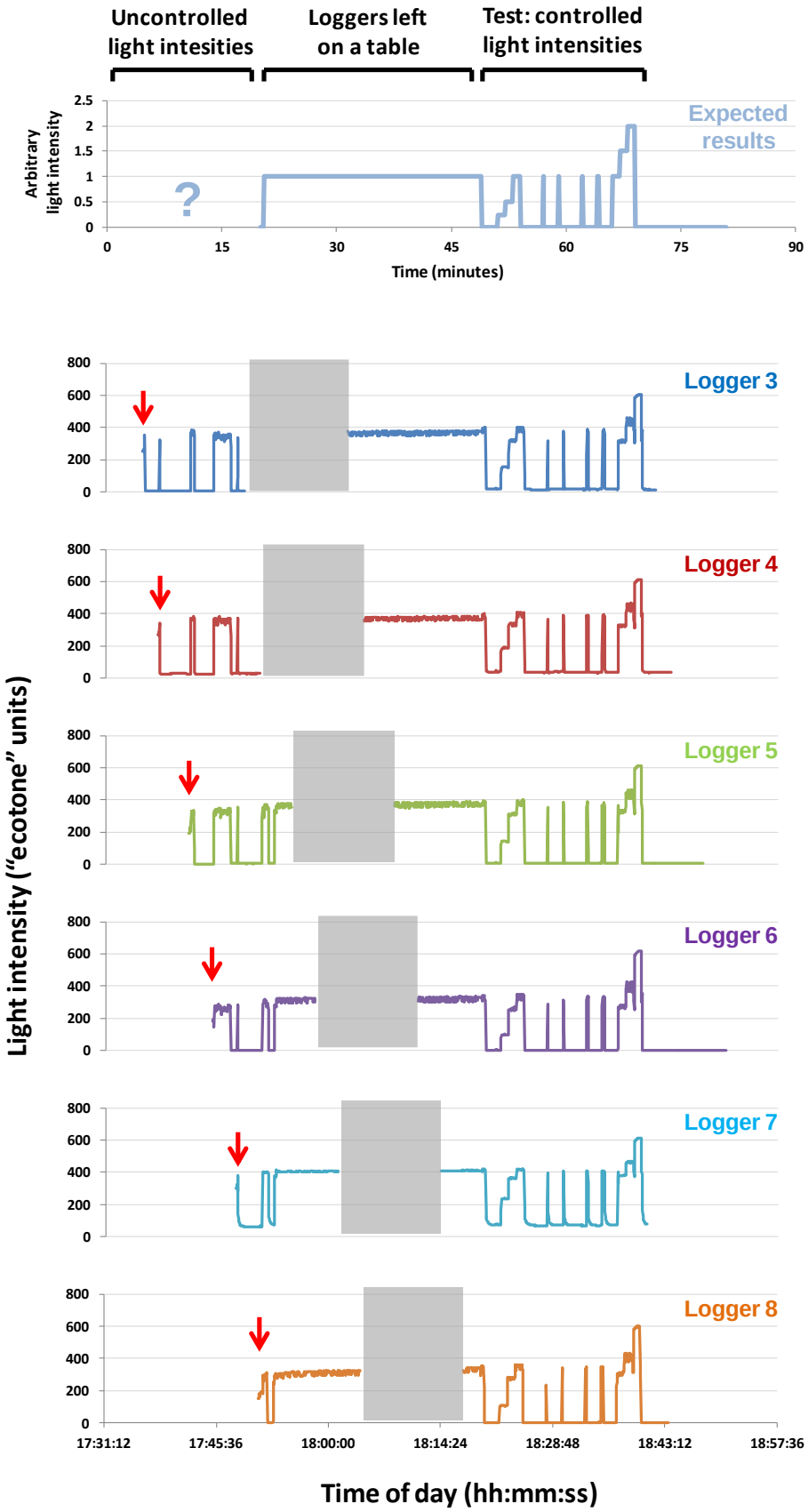

Figure 3.1 – Expected results (upper graphic) and obtained results (other graphics) from Test3 Part1. Experimental conditions are described above the first graphic. Red arrows indicate the time when each logger started recording and gray rectangles indicate the data loss correspondent to the deleted block of high light intensities.

Part 2

A similar protocol was applied to the remaining two loggers (9 and 10). Results are shown in figure 3.2. Again, we could predict the positions of the high light intensity data and start the proper test after that. And we could also compensate for the wrong sampling interval.

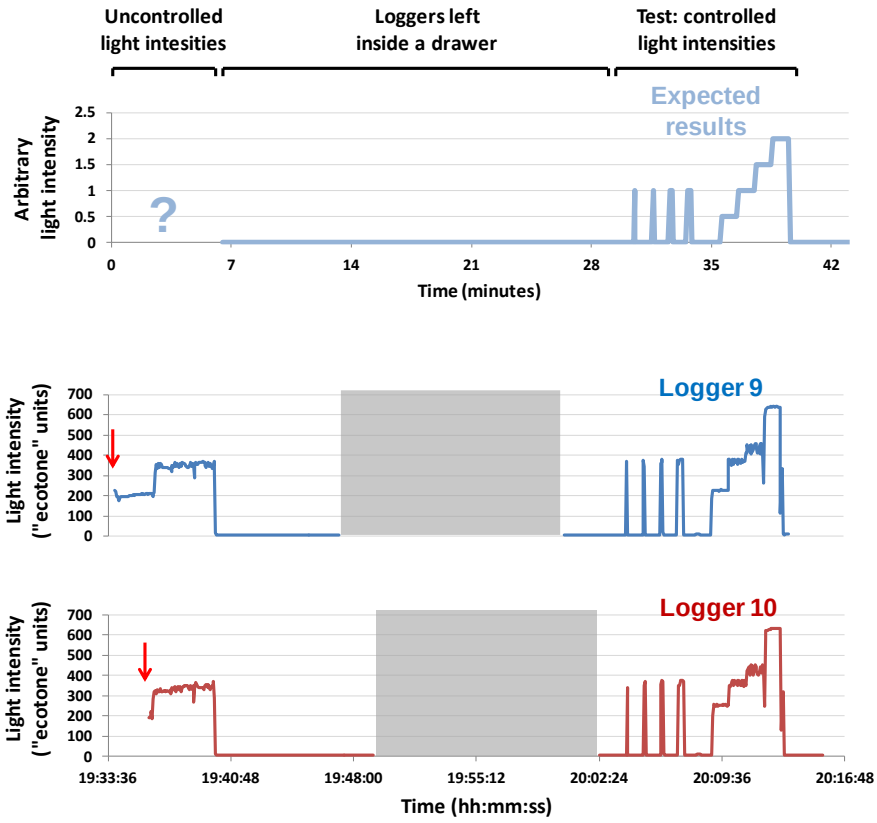

Figure 3.2 – Expected results (upper graphic) and obtained results (other graphics) from Test3 Part2. Experimental conditions are described above the first graphic. Red arrows indicate the time when each logger started recording and gray rectangles indicate the data loss correspondent to the deleted block of high light intensities.

Conclusions

It appears that we found a way to deal with the two detected problems of the light loggers.

General conclusions of the lab tests

The loggers can measure different light intensities, as we expected them to do.

We found two problems that can be controlled by manipulation of the data after the download.

The first one, "block of high light intensities", forces us to discard this part of the data.

The other problem, with the time scale, affects the data in an important way, making it useless if we do not know exactly what the real sampling interval used is. From the lab tests, it appeared we had found a way to compensate for this, because the real sampling interval always seemed to be 1/3 of the programmed sampling interval.

*<u>**However, the test on the animal, which is shown in the next session, revealed that this proportion may not always be the same 1/3.**</u>

Test 4 – Test on a tuco-tuco in the field

After having seen that the loggers could record well the changes in light intensity, for some days, and that the problems observed could be compensated, we were finally able to test the equipment on one of our animals (the tuco-tucos).

Unfortunately the "wristband" of the logger was still too wide to fold it around the neck of the animal, so we had to develop another way to attach the sensor. Figure 4.1 below demonstrates what we did:

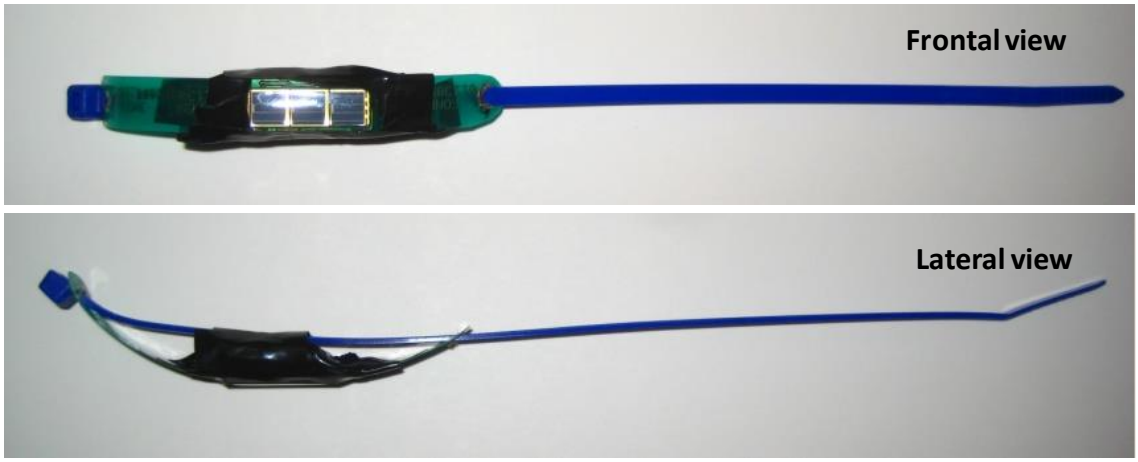

Figure 4.1 – Photos of the sensor and the changes made to use it on the animals.

We cut most of the "wristband", being careful not to damage any part of the circuitry of the sensor. Then, we made hole in each extremity of the remains of the "wristband", and passed a blue tie-wrap through these holes. So, we substituted most of the "wristband" for the tie-wrap. It is much more narrow, and easier to lock around the neck of the animal (Fig. 4.2).

Figure 4.2 – Photos of the sensor being attached to a model taxidermized specimen of tuco-tuco. For the test, we repeated this same process on the real animal.

As you can see in the figures, we also used electrical tape to cover the sensor and the battery, to protect them from the potential damages caused by sand and humidity in the field. The whole

equipment (logger + battery + tiewrap + electrical tape) weighed less than 5g (between 4 and 5g), so it is within the limits we wanted.

In our first attempt, with logger number 4, the process (Fig. 4.1) did not go well. As we bent the logger together with the tiewrap, it broke in two pieces. So, despite its flexibility, the logger was not projected to be folded as much as we need, to be put around the neck of the animal. Fortunately, we found a new way to use the sensor + the tiewrap, leaving some free space between them, so that the logger does not have to be strongly folded. The new method worked in this test and we hope it will work some more times, without the risk of breaking another logger.

In the new attempt, we used light logger 2 with battery E, and a programmed sampling interval of 180 seconds. We expected the real interval to be 3 times shorter, that means, 60 seconds.

The animal carrying the sensor was released in a fenced area in the field. We know that in the field these animals remain inside subterranean tunnels for most of the day, except for a few excursions to the aboveground environment.

Results

Logger number 2 worked well. It registered the light intensities through all the days on the tuco-tuco, until we removed the battery to stop the recording. As usually, there was a block of unreal light intensities between data 265 and 528 which was removed from the data.

There was however another unexpected problem with the sampling interval. From the tests 2 and 3 above, we concluded that the real sampling interval performed by the logger would be three times shorter than the interval chosen during the programming (180s). However, when we downloaded the data from logger 2 and built the graphic with the corrected sampling interval (60s), the data still made no sense. After analyzing the data for some time, we discovered that the true sampling interval was actually ¼ of the one programmed (45s).

After solving this last problem, we were finally able to build the right graphic and analyze the data. In the figure 4.3 below, the whole ten-day-record is shown.

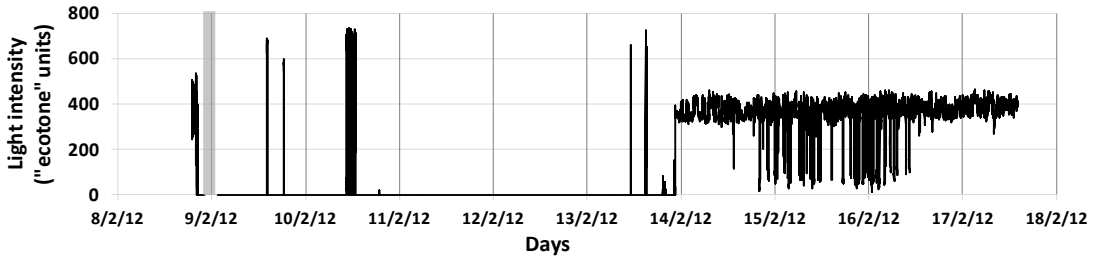

Figure 4.3 – Results from Test 4. Graphic presents the record for 10 consecutive days. Vertical lines mark the times of midnight, separating the days. The gray rectangle indicates the interval correspondent to the removed block of high light intensities.

To make the report easier to follow, we are going to describe the data in day-blocks.

Day 1 (08/02/2012)

In this day, the logger was started at 18:53 and put on the neck of the animal. Release of the animal in the field was performed at around 20:30 (see figure below). After that, the light intensity recorded for the rest of the day remained near zero.

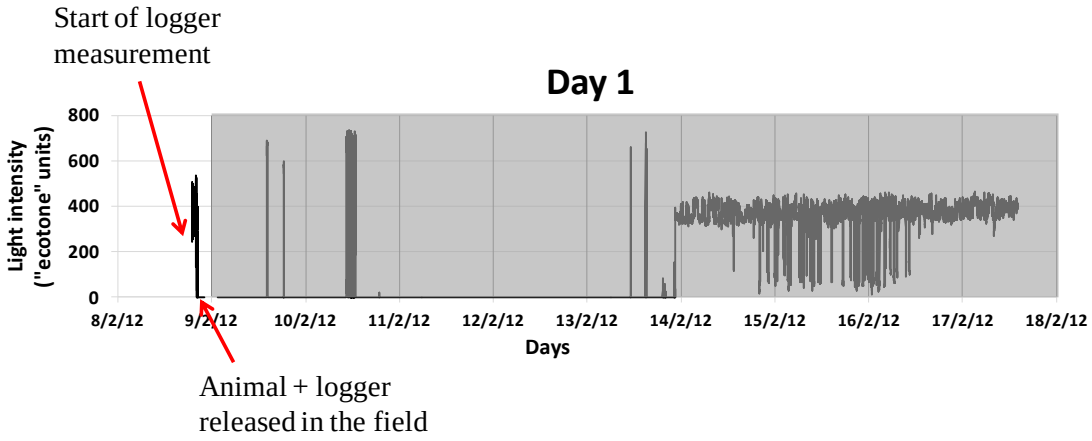

Days 2 to 6 (09 to 13/02/2012)

These were the days when the animal was in the field. We had no control over the light intensities to which the animal was exposed. For that reason, we can only speculate about the events that originated the recorded light intensities (graphic below).

We see that most of the time during these days, the light intensity remains in a baseline (zero). This is probably because the animal was mostly inside the dark subterranean tunnels, not exposed to light. If this is the case, then the times when the light intensity goes above zero baseline are probably times when the animal went out of the tunnel, to the aboveground, exposing itself to light.

These episodes of excursion to the aboveground are exactly the data that we need to register in our research. It appears that the sensor can truly give us the information we want.

On the sixth day, the animal was recaptured from the fenced area in the field and taken back to the laboratory.

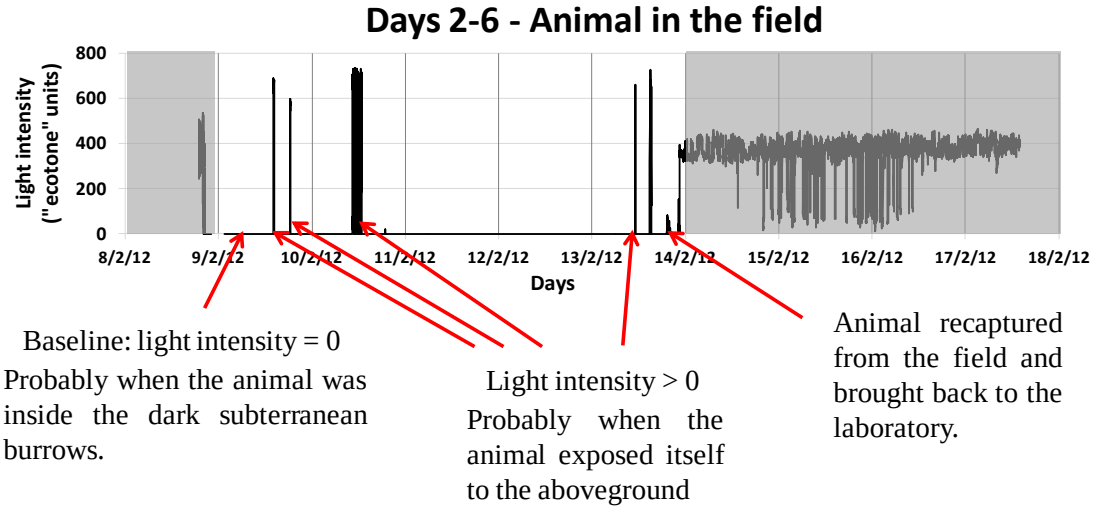

Days 7 to 10 (14 to 17/02/2012)

Until the end of the recording, the animal was kept in the lab, in a glass cage, under a constant dim red light. We can see in the graphic that there is a baseline of 400 (light intensity units) with some variation, when the light intensity falls to lower levels. Nevertheless it always comes back to 400. We believe this variation may be due to oscillations in the electricity of the building, which might cause instability of the light bulb; alternatively, it may be caused by movements of the animal, which change the position of the logger relative to the light source.

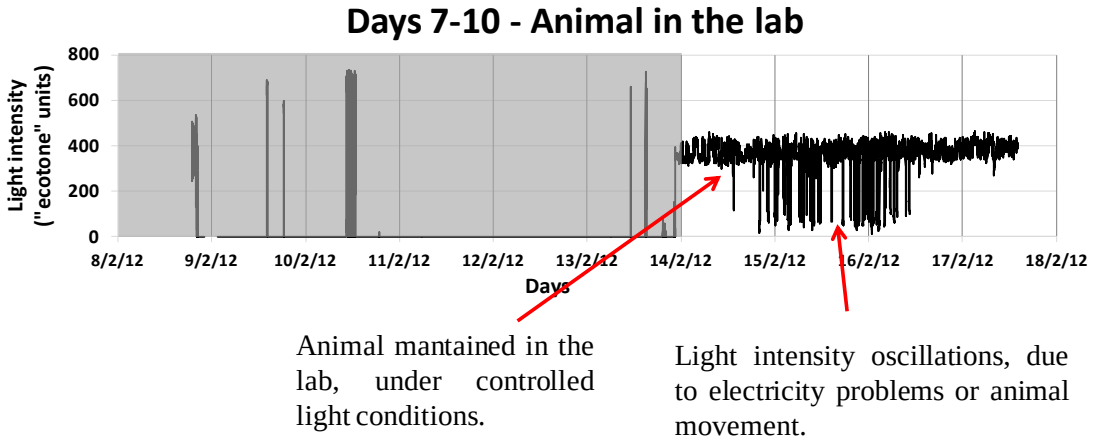

Animal mantained in the lab, under controlled light conditions.

Light intensity oscillations, due to electricity problems or animal movement.

Final conclusions

The light loggers can register for 10 days and the record can inform us the times when the animals leave the dark subterranean burrows and expose to light in the field. Therefore, the loggers are very good.

There are, however 2 problems. The first problem can be managed. Problem 2 needs fixing!!!

Problem 1: Data 265 to 528 is unreal. Solution: remove it.

Problem 2: Time scaling: Is it ¼ or 1/3? Sometimes is ¼, sometimes is 1/3. There should be 1/1. While the sensors work like this, we will have difficulties in analyzing our data, because we might not be sure what the real sampling interval is.